Electrophysiological monitoring of low frequency auditory thresholds in humans using the Auditory Nerve Overlapped Waveform

A thesis submitted in partial fulfilment
of the requirements for the Degree of
Master of Audiology
in the Department of Communication Disorders
at the university of Canterbury
by
Ashleigh Jayne Allsop

University of Canterbury, 2016

Acknowledgements

This thesis would not have been completed without the time, effort, and patience of my supervisors. Thank you so much Assoc. Prof. Greg O'Beirne for the amount of time and effort that you have put into helping me complete this thesis.

A special thank you needs to be given to Mr Phil Bird and Mr Jeremy Hornibrook, for allowing me into your practice and operating theatre, as well as your expertise. This also extends to the hospital staff of both Christchurch public hospital and St Georges Hospital who were involved with the many ins and outs of this project.

A huge thank you to the Christchurch Public Hospital audiology staff, for your support throughout the year and for your knowledge and patience. For the many times I popped into the department to ask for your time and assistance - thank you.

To all the participants who patiently allowed us to run our tests. Without them, this thesis and our findings would not have been possible. Future patients will forever have you to thank for what you contributed.

All the University of Canterbury Audiology staff and class mates who helped me through the past two years. For my supervisors who taught me, who made me the clinician I am today, I couldn't have asked for better clinicians to learn from. To all my classmates – we finally did it! All the best for your bright future careers.

And last, but certainly not least to all my family and friends who have helped me cope with the stresses through the whole of my university career. Yours has been the most important influence over the past two years. Without your support I would not be where I am today.

"Your profession is not what brings home your weekly pay check. Your profession is what you are put here on this earth to do, with such passion and such intensity that it becomes spiritual in calling"

Abstract

Current methods of objectively measuring hearing thresholds at frequencies below 1000 Hz are not as accurate, or effective as obtaining hearing thresholds from the higher frequencies. The auditory nerve overlapped waveform (ANOW) was developed to allow accurate assessment of frequencies below 1000 Hz from the production of the cochlear microphonic, to develop a method of objective measure of low frequency hearing threshold. In the current evidence base, no one has yet successfully measured the ANOW in humans. This study aimed to produce the ANOW in humans to develop it as an objective measure of hearing threshold.

We subjectively measured participant's thresholds using both pure tone audiometry and electrocochleography. The participants were all suspected of having Ménière's disease, and were undergoing transtympanic electrocochleography. We then used the electrocochleography needle to record our auditory responses. From these responses we derived the ANOW.

Comparing the data analysed to the audiograms of the participants, we cannot conclude at this stage that the ANOW that we measured was purely neural from the apex of the cochlea in origin. The sound levels at which testing took place generally exceeded those levels which guaranteed that the ANOW waveforms recorded were purely neural in origin. From this, future studies in this area will involve stacked derived band masking to show frequency specificity and neural origin of the recordings. As such, the current results were not able to accurately predict participant thresholds. However this study has further advanced the technique of utilising the ANOW as an objective measure of low frequency hearing, to the benefit of future studies.

Table of Contents

List of Abbreviations

ABR – Auditory brainstem response

AC – Alternating current

ANN – Auditory nerve neurophonic

ANOW – Auditory nerve overlapped waveform

ANSD – Auditory neuropathy spectrum disorder

AP – Action potential

CAP – Compound action potential

CM – Cochlear microphonic

CNAP – Cochlear nerve action potential

CON – Waveform from initial condensation stimulus

CPA – Cerebellopontine angle

dB – Decibels

dB HL – Decibels hearing level

dB nHL – Decibels normal hearing level

dB peSPL – Decibels peak equivalent sound pressure level

dB SL – Decibels sensation level

dB SPL – Decibels sound pressure level

DC – Direct current

DENM – Direct eighth nerve monitoring

DPOAE – Distortion product otoacoustic emission

ECochG / ECoG – Electrocochleography

ENT – Ear, nose, and throat specialist

IHCs – Inner hair cells

LOC – Lateral olivocochlear complex

MOC – Medial olivocochlear complex

MRI – Magnetic resonance imaging

OHCs – Outer hair cells

PAMR – Post auricular muscle response

PTA – Pure tone average

RAR – Waveform from initial rarefaction stimulus

SNR – Signal to noise ratio

SOAE – Spontaneous otoacoustic emission

SOC – Superior olivocochlear complex

SP – Summating potential

SPL – Sound pressure level

SRT - Speech recognition threshold

TEOAE – Transient otoacoustic emission

WRS – Word recognition score

List of Figures

List of Tables

Chapter One: Introduction and Literature Review

Hearing loss affects 15% or 1019 million of the world's population, with 360 million people having a debilitating (moderate or worse) hearing loss (World Health Organisation, 2015). Those with profound hearing loss (the greatest amount of hearing loss) make up approximately 0.3% of all those with a hearing loss, equating to approximately 20 million people (World Health Organisation, 2015). Hearing loss affects over 330,000 people within New Zealand, with that number set to double within the next 50 years (Statistics New Zealand; Exeter, Wu, Lee, & Searchfield, 2015). Of those with hearing loss, profound hearing loss affects approximately 0.01% of the total New Zealand population, or approximately 3000-4000 people (Sanders, Houghton, Dewes, McCool, & Thorne, 2015). There are 180 to 200 children born each year with a hearing impairment in New Zealand, and 5-11% of those are severely to profoundly deaf bilaterally (Digby, Purdy, & Kelly, 2014; Digby, Purdy, & Kelly, 2015). For those with severe to profound hearing loss, cochlear implantation is an option to help aid hearing, speech, and language, where other options such as hearing aids may not be able to. As of 2014, over 600 people throughout New Zealand had received cochlear implants (CIs) through the Southern Cochlear Implant Programme, with over 60 adults on the wait list (Heslop, 2014).

Formerly it was taken for granted that any residual acoustic hearing would be lost on implantation, due to cochlear damage incurred during the insertion of the electrode. However, due to improved surgical techniques it is now common for residual hearing to be preserved (Kiefer et al., 2004). There is plenty of evidence to suggest that monitoring hearing during surgery can alert the surgeon to early warning of any iatrogenic damage that may be occurring, allowing them to modify their procedure, and preserve residual hearing (Calloway et al., 2014; Radeloff et al., 2012). Electric hearing from the CI processors is optimised for

speech, but residual hearing (often aided with a hearing aid) helps with music and speech perception, localisation, articulation, and literacy (Gantz, Dunn, Walker, Van Voorst, Gogel, & Hansen, 2016; James et al., 2005; Marx et al., 2015).

The useful residual hearing that CI patients present with is usually in the very low-frequency range (Cosetti et al. 2013). It is these low frequencies that monitoring techniques have trouble with (Laureano, McGrady, & Campbell, 1995; Spoor & Eggermont, 1976). As will be explained in depth in later sections, a new method of recording low frequency neural activity has recently been published: the auditory nerve overlapped waveform or *ANOW*. This potential holds great promise for the intraoperative monitoring of CI surgeries, but so far the only published recordings have been those made in cats and guinea pigs (Lichtenhan, Cooper, & Guinan Jr, 2013; Lichtenhan, Hartsock, Gill, Guinan Jr, & Salt, 2014).

This project began in the pursuit of the intraoperative monitoring of auditory potentials in CI patients. Throughout the course of this project, multiple attempts were made to record potentials intraoperatively. New software for this task, called “Te Pihareinga” has been developed by O’Beirne (O’Beirne & Bird, 2015), and although the software is working well, technical issues with the common-mode rejection of the amplifiers used prevented usable potentials from being recorded in that setting, despite multiple attempts over several months, and low CI patient numbers meant there were few opportunities to resolve these technical issues in the operating theatre setting.

To pursue our goal of recording the ANOW in humans, we switched our focus to undertaking a pilot study in a patient population that underwent electrocochleographic assessment more frequently (four or five patients a month at Christchurch Public Hospital) using an established low-noise recording set-up, and a population which could also benefit

from examination of their low-frequency neural activity: patients with Ménière's Disease. The patients that are examined using ECochG at Christchurch Hospital usually have recordings made in both ears, which would give us the opportunity to compare ANOW thresholds with audiometric thresholds in both normal and Ménière's ears.

This thesis details a pilot study that has resulted in the first published recordings of the ANOW waveform in five humans, improvements made to the signal processing techniques that halved the acquisition time for the potential, and some possible improvements to the technique that may be made in the future.

Before this, however, it is important that we take a step back to understand the anatomy and physiology of the auditory system, the underlying neural potentials involved with auditory monitoring, and the pathology associated with Ménière's disease. The following chapter sections will outline each of these in greater detail with a thorough review of the current literature.

1.1 The auditory system

The anatomy and physiology of the afferent and efferent auditory pathways is fundamental to understanding the function of the auditory system as a whole, and therefore auditory evoked potentials and the hearing threshold of the individual it represents. It is therefore the starting point for this literature review, building a basis of understanding for the topics investigated in this thesis.

1.1.1 Afferent auditory pathway

The outer, middle, and inner portions of the afferent auditory pathway transform sound waves from particle vibrations in the air; a mechanical signal to neural electrical signal. The sound waves travel down the external auditory canal to the tympanic membrane. This displaces the membrane, causing the ossicular chain of the malleus, incus and stapes bones

to concentrate this movement by a factor of 22 onto the round window of the cochlea (Patuzzi, 1996). This is known as impedance matching. This movement on the round window causes the fluid within the cochlea to create a longitudinal pressure wave. This pressure causes the basilar membrane to move vertically, creating a transverse travelling wave moving from the base of the cochlea to the apex (Von Békésy & Wever, 1960). Sound waves have alternating phases of rarefaction and condensation. The frequency of the stimulus interacts with the mass and stiffness of the basilar membrane to determine the maximal peak of the transverse wave, and therefore the hair cells stimulated within the cochlea, creating hair cells that respond to a characteristic frequency (Fettiplace & Hackney, 2006). The basal turn of the cochlea responds to the high frequency spectrum, while the apex responds to the lower frequencies humans can hear (Von Békésy & Wever, 1960). The stiffness, width, and damping of the basilar membrane creates the tonotopic organisation of the cochlea via a graded variation in its resonant frequency. The stiffness of the basilar membrane increases from the

apex to base, while the mass decreases from apex to the base (Oghalai, 2004). Figure 1 shows the structures from the outer, middle and inner ear.

The organ of Corti sits atop the basilar membrane, and consists of sensory hair cells, known as inner hair cells (IHCs) and outer hair cells (OHCs) and supporting cells. The OHCs stereocillia are embedded within the tectorial membrane, which forms the top of the organ of Corti. When the basilar membrane is displaced, it causes the tips of the stereocillia of the OHCs to bend against the tectorial membrane, which is known as radial shear. Radial shearing causes the OHCs to fire (Billone & Raynor, 1973). The IHCs stereocillia are not imbedded within the tectorial membrane, and are thought to be displaced by the velocity of the basilar membrane movement, as opposed to the physical displacement like the OHCs stereocillia (Fettiplace, 2006).

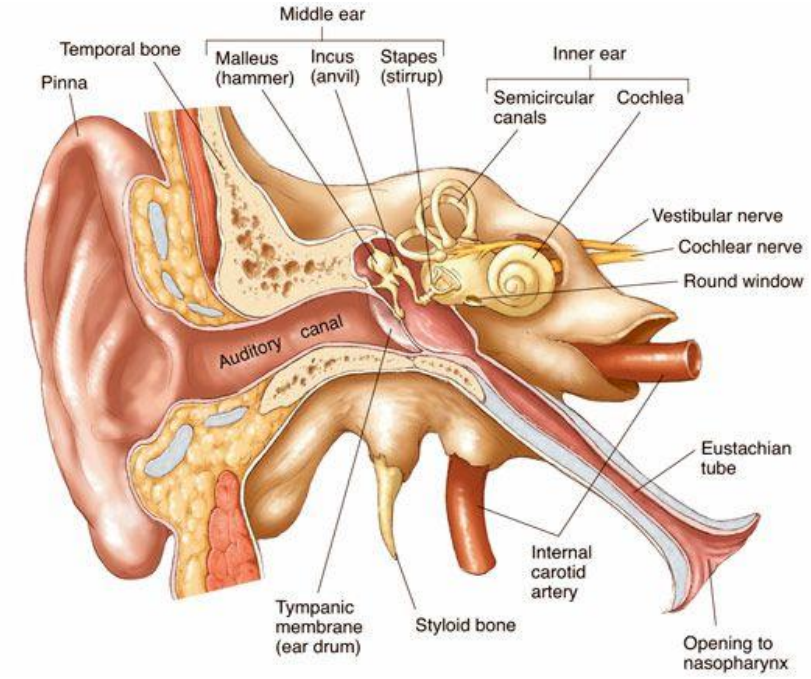

Figure 1: The anatomy of the outer, middle and inner ear. Retrieved from *http://www.biographixmedia.com/human/ear-anatomy.html*.

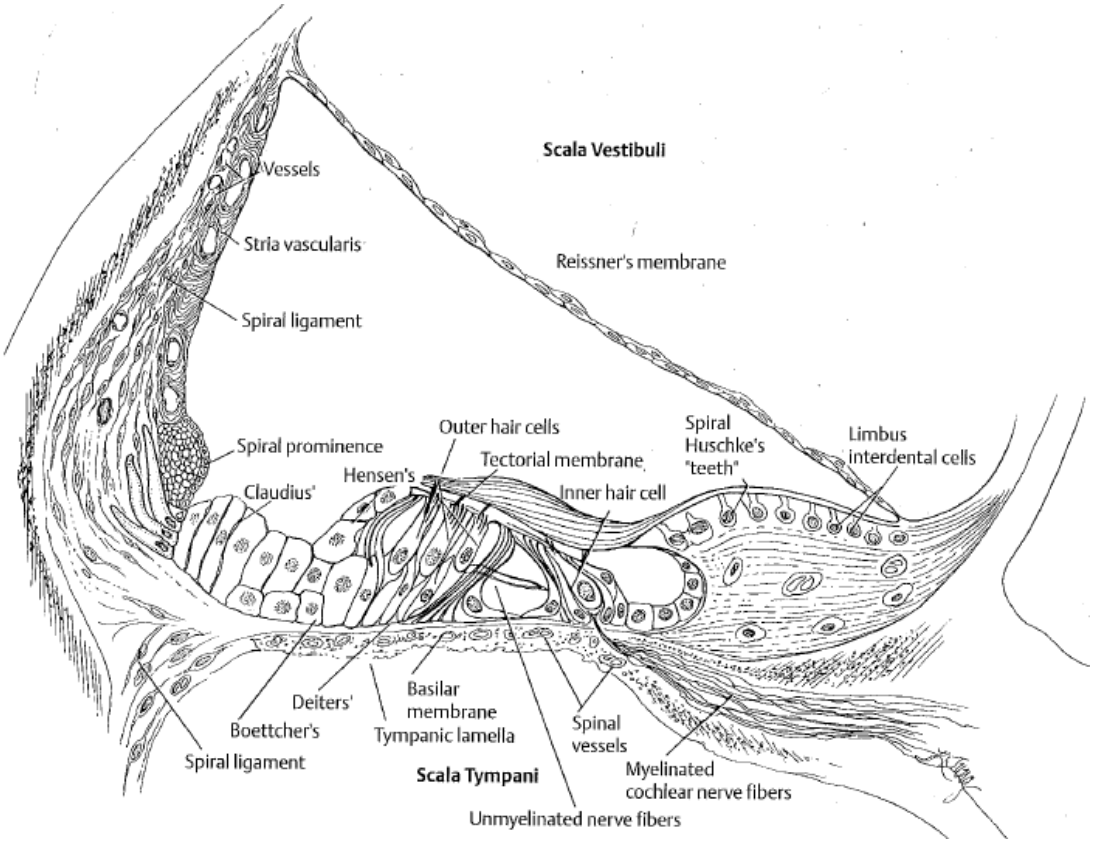

Figure 2: The components of the Organ of Corti and the cochlear fluids (Hughes & Pensak, 2011)

The cochlear is filled with three types of fluid; endolymph, perilymph, and intrastrial fluid (Wangemann, 2006). The fluids of the cochlea helps to regulate the process known as mechonelectrical conduction. It does this via the composition of endolymph and perilymph involving concentration gradients of potassium (K^+), sodium (Na^+), Calcium (Ca^{2+}) and chloride (Cl^-) (Wangemann, 2006). Endolymph is present within the scala media, and the perilymph within the scala tympani and vestibuli. The perilymph has a high concentration of Na^+ and low K^+ concentration. Potassium is pumped into the endolymph of the scala media from the stria vascularis, creating the endolymphatic potential; a high concentration of K^+ between the Reissner's and basilar membranes, and the surrounding cochlear fluids (a ratio of approximately 157mM to 6mM), as well as a low Ca^{2+} concentration (Wangemann, 2006). This potential difference allows for mechonelectrical transduction or *MET*; a mechanism that allows mechanical energy to be converted into electrical energy (Gillespie & Walker, 2001).

In this case, oscillations from the basilar membrane deflect inner hair cells, causing MET ion channels within the cell membranes to open, resulting in a surge of K^+ from the endolymph into the inner hair cell, causing a depolarisation with the possibility of an electrical potential (Gillespie & Walker, 2001). The ion channels responsible for MET use the gating spring model; the ion channel on the hair cell's stereocillium is attached via an extracellular filament (or *tip link*) to the adjacent stereocillium, so that when they are pulled in the activating direction, toward scala vestibuli, the ion channel is pulled open by the filament, allowing the flow of ions (Gillespie & Walker, 2001).

The efferent auditory pathway consists of the descending neural fibres, but unlike the afferent auditory pathway, the physiology behind it is not yet as well understood. The pathway starts in the temporal lobe, and generally follows the opposite of the afferent auditory pathway. The nerve fibres travel through the MGB, the olivocochlear system, through the brainstem and the IAC, to synapse with the outer hair cells and primary afferent neurones in the cochlea (Huffman, & Henson, 1990).

1.1.2 Efferent auditory pathway

The efferent auditory pathway consists of the descending neural fibres, but unlike the afferent auditory pathway, the physiology behind it is not yet as well understood. The pathway starts in the temporal lobe, and generally follows the opposite of the afferent auditory pathway. The nerve fibres travel through the MGB, the olivocochlear system, through the brainstem and the IAC, to synapse with the outer hair cells and primary afferent neurones in the cochlea (Huffman, & Henson, 1990).

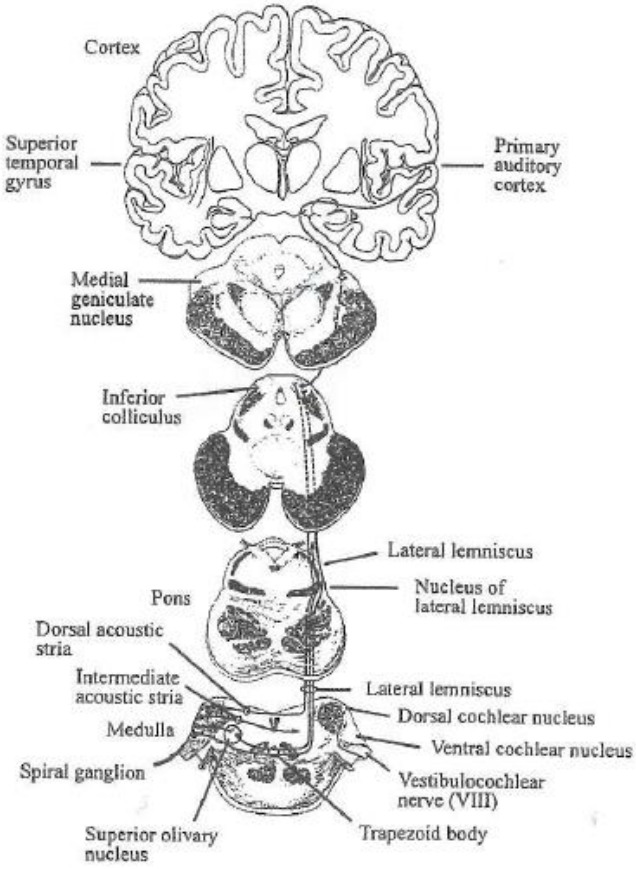

Figure 3: The afferent auditory pathway from the spiral ganglion to the primary auditory cortex (Katz, 2009).

The olivary complex is the thought to be an important part in the efferent auditory pathway. It can be divided into the lateral olivocochlear complex (LOC) and the medial olivocochlear complex (MOC) (Warr, & Guinan Jr, 1979). The LOC innervate the type I afferent nerve fibres, and in some cases the IHCs directly (Liberman, 1980a; Warr, & Guinan Jr, 1979; Wersinger, & Fuchs, 2011), whereas MOC neurons synapse directly onto the base of the OHCs (Warr, & Guinan Jr, 1979; Wilson, Henson, & Henson, 1991). While the lateral LOC efferents predominantly innervate the ipsilateral cochlea, 60-75% of the MOC efferents innervate the contralateral OHCs (Guinan, Warr, & Norris, 1983; Thompson, & Thompson, 1986; Warr, 1997; Wilson et al., 1991).

It is mostly agreed upon within the research that the efferent auditory pathway is involved with regulating the inputs from the afferent auditory pathway (Guinan Jr., 2006). Recent

research has shown that this regulation may be either inhibitory or excitatory in nature, rather than being purely inhibitory as first theorised (Galambos, 1956; Le Prell, Halsey, Hughes, Dolan, & Bledsoe Jr, 2005; Le Prell, Shore, Hughes, & Bledsoe Jr, 2003). Activation of the efferent olivocochlear complex creates an inhibitory signal onto the afferent auditory nerve (Galambos, 1956; Gifford & Guinan, 1987). However excitatory signals have been discovered from the MOC contralateral neurons, and create an effect known as the anti-masking effect. The anti-masking effect describes the excitatory stimulus produced on the auditory nerve when masking noise in the form of high intensity stimuli is applied (Dolan, & Nuttall, 1988; Nieder, & Nieder, 1970). The resulting effect is that the auditory nerve, when high level masking noise is applied with a signal, produces a greater response than with the high intensity masking noise alone. When low level masking stimuli was applied with a target signal, the resulting auditory nerve response was lower than the low intensity masking alone (Dolan & Nuttall, 1988). This may play a role in signal to noise detection, which would help with situations of discriminating auditory signals in background noise (Giraud, Garnier, Micheyl, Lina, Chays, & Chery-Croze, 1997; Harkrider & Smith, 2005; Musiek & Baran, 2007).

The MOC efferent nerve fibres can also have an effect on the peripheral auditory system. It has been found that the inhibitory responses from the MOC fibres can reduce the oscillations of the basilar membrane, and thus dampen the OHCs electromotile effect, and therefore is thought to have an influence on the cochlear amplifier (Cooper, & Guinan, 2006; Guinan, 2005; Guinan Jr., & Cooper, 2008; Murugasu, & Russell, 1996; Nam, & Guinan, 2011; Russell, & Murugasu, 1997). The LOC efferent nerve fibre influences are less well known than the MOC fibres, and can be difficult to assess using electrophysiology due to their relatively small fibres (Groff, & Liberman, 2003). Groff and Liberman (2003) found that LOC fibres may have an influence over the strength of auditory nerve firing, slowly increasing or decreasing

the neural response produced. However there is still conflicting evidence surrounding the LOC fibres and their excitatory and/or inhibitory role within the efferent auditory pathway, such as found with the opposing findings of Le Prell et al. (2003; 2005), and Darrow, Maison, and Liberman (2007). Le Prell et al.'s (2003; 2005) research indicates that LOC fibres are primarily excitatory, while Darrow et al. (2007) have found them to have an inhibitory role. Overall, the efferent auditory system requires further research to be done to fully understand the processes it is involved with within the auditory system.

1.2 Action potentials

The auditory system relies on a network of neurons to transfer information from the periphery to the central nervous system (the brain) and back, as discussed within the previous chapter section. It is important to understand the process of how this auditory signal information is conveyed once transformed into an electrical neural signal.

"Typical" neurons have a few basic features which aide in the physiology of information transferral. The body of the neuron, or the *soma*, receives synaptic inputs from other surrounding neural cells, usually via the processes off the cell known as dendrites. The axon, surrounded by myelinating neural cells, is the main mode of passing on the electrical signal. The axon ends in terminals known as synapses, which connect with neighbouring cells of which to pass on the signal. Within the synapses, are vesicles that contain neurotransmitter, chemicals that can activate or inhibit an electrical potential in the connected neuron (Siegel & Sapru, 2006).

The electrical potential that conveys the auditory signal through the nervous system is known as the action potential (AP) or compound action potential (CAP). The AP occurs across the neuron's membrane, caused mainly by the concentration gradients of Na^+ and K^+ (Siegel & Sapru, 2006). Neurons contain high extracellular concentrations of Na^+ (approximately 140

mM) and low K^+ (approximately 5 mM), and high intracellular concentrations of K^+ (approximately 140 mM) and low Na^+ (approximately 12 mM) (Siegel & Sapru, 2006). The concentration gradient is maintained via a protein pump (Na^+–K^+ ATPase), so that the overall intracellular potential is approximately -70 mV in a resting state (Siegel & Sapru, 2006).

When a neuron is stimulated, the result is a change in it its intracellular potential, which is either excitatory (depolarising the membrane) or inhibitory (hyperpolarising it) A depolarisation of the cell's membrane causes voltage gated Na^+ channels to open, allowing Na^+ to flood into the neuron, causing the intracellular potential to become even more positive. If the intracellular potential reaches over -55 mV, then an action potential occurs, causing even more Na^+ to enter the cell, and rapidly making the intracellular potential highly positive (approximately +40 mV) (Siegel & Sapru, 2006). The AP is known as an all-or-none response that doesn't alter in amplitude at the single neuron level. As the intracellular potential reaches a maximal positive potential, the voltage gated Na^+ channels begin to inactivate and close. As the Na^+ channels close, the voltage gated K^+ channels become activated due to the intracellular potential, transporting K^+ out of the cell. This phase of the AP is known as repolarising. As all the Na^+ channels are closed and the K^+ channels are open, the intracellular potential is hyperpolarised at -80 mV, which then causes the voltage gated K^+ channels to start closing. The cellular potential then returns to its resting state of -70 mV (Siegel & Sapru, 2006). See *figure 4* for a pictorial representation of the action potential.

The time of which another action potential can occur after one has just been, depends on the activation states of the cell's voltage gated ion channels. The absolute refractory period occurs when majority of voltage gated Na^+ channels are active, resulting in no chance of another AP being initiated. The relative refractory period occurs when the voltage gated K^+ channels are open, and the cell membrane is hyperpolarised (approximately 2ms after the

original AP). It is possible for another AP to be generated during this period, however it requires greater depolarisation to initiate (Siegel & Sapru, 2006).

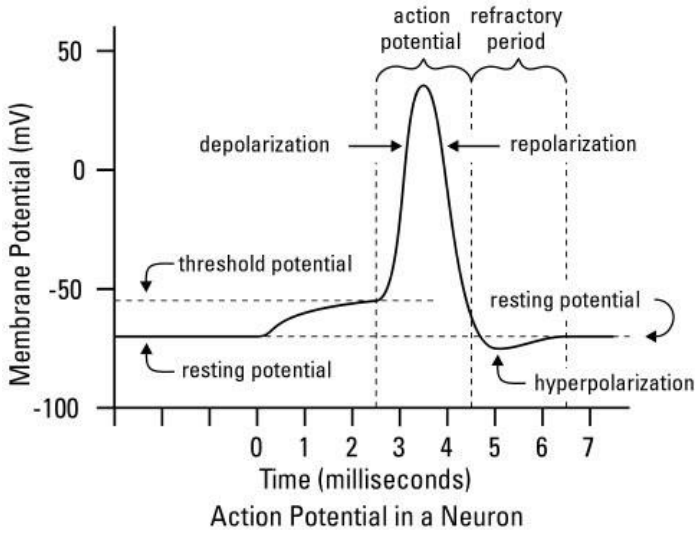

Figure 4: The elements of the action potential. Retrieved from http://www.dummies.com/how-to/content/understanding-the-transmission-of-nerve-impulses.html.

The AP does not simply travel down the axon in a wave of depolarisation, this would take too long to pass a signal from the periphery to the auditory centres of the brain (Siegel & Sapru, 2006). The Schwann cells' myelin surrounding the axon act as insulation. The depolarisations of the APs occur at the nodes of Ranvier, where myelin is absent, which causes the AP to travel down the axon by "jumping" between nodes. This is known as saltatory conduction, and increases electrical conduction velocity by up to 10-100 times. Other factors that increase conduction velocity along the axon are increase in the nerve diameter, change in extracellular environment, and changes in temperature (Siegel & Sapru, 2006).

Once the AP has reached the nerve terminals, the depolarisation causes Ca^{2+} to enter the terminals. Calcium acts to fuse the vesicles containing the neurotransmitter, glutamate, to the synapse membrane, and release its contents into the synaptic cleft (Berlin, 1997). The glutamate diffuses across the synaptic cleft to the post synaptic neuron dendrite, where it binds with ligand gated Na^{+} channels. This causes either an excitatory or inhibitory post

synaptic potential (EPSP or IPSP) (Berlin, 1997). This influx of Na^+ can then potentially cause a depolarisation within this neuron, and hence creating another AP if intracellular potential threshold is met (-55 mV), passing on the electrical signal (Siegel & Sapru, 2006).

Excitatory postsynaptic potentials do not necessarily result in APs being transferred onto that neuron. The dendrites of the neuron receive many synaptic inputs, some excitatory and some inhibitory, the sum of which determines if an AP will proceed. The summation of the inputs must reach conduction threshold (-55 mV) which will activate the voltage gated Na^+ channels and result in an AP. EPSP can be summated by either temporal or spatial means; either have two or more excitations occur close together time wise, or close together on the dendrite (Siegel & Sapru, 2006). However an action potential alone does not convey much auditory stimulus information. The rate at which APs occur, as well as the number of neurons responding help to convey the strength of an auditory signal (Pickles, 2012). The measurements of these CAPs, as well as the timing, location, and summation of CAPs can be useful clinically to assess auditory functioning.

1.3 Auditory Evoked Potentials

Neural responses to auditory stimuli can be represented by different neural patterns and intensities, caused by the culmination of actions potentials in certain anatomical points. The primary sensory cells of the auditory pathway are the IHCs, which are depolarised when stimulated, causing an AP in the primary afferent nerve fibres, along the auditory pathway, to the auditory cortex. Neural responses are also sent from the central nervous system back out to the periphery. Measuring these neural events can be useful clinically, to objectively measure auditory thresholds and give indications on the functioning of the auditory pathway (Katz, 2009; Pickles, 2012).

1.3.1 Electrocochleography (ECochG)

The earliest electrical potential that can be measured from the auditory pathway is known as electrocochleography (ECochG), and was first described by Wever and Bray in 1930. The waveform of ECochG is comprised of the cochlear microphonic (CM), the summating potential (SP) and the compound action potential (CAP). The response gives an indication of the electrical activity of the hair cells and the beginnings of the auditory nerve (Hall, 2006). ECochG responses are evoked using stimuli of rarefaction and condensation polarity, which can be summed or subtracted to amplify the components of the ECochG. When the response to opposite stimulus polarities are summed, the SP and AP components are enlarged, while the CM becomes evident when the stimulus polarities are subtracted (American Speech-Language-Hearing Association, 1988).

The cochlear microphonic (CM) is produced from the OHCs deflection, and results in an electrical potential that is an alternating current (AC) (Dallos and Cheatham, 1976). The overall AC electrical potential has been found to only come from the OHC receptors, and that any contribution from the IHCs do not significantly contribute to the CM (Choi, Chertoff, Bian, & Lerner, 2004; Dallos & Wang, 1974; Patuzzi, Yates, & Johnstone, 1989). The acoustic stimulus determines the frequency of the CM produced, as the CM copies the frequency of the acoustic stimulus (Patuzzi et al., 1989). The amplitude of the CM also increases with the intensity of the acoustic stimulus, until the maximum intensity of the potential is reached (Patuzzi et al., 1989). This is due to the potential reaching a saturation point, and showing little change with increasing acoustic stimulus intensity from this point (Johnstone, Patuzzi, & Yates, 1986). As the CM is at the frequency of its evoking stimulus, changing the polarity of the stimulus changes the polarity of the CM. When the opposing stimuli are used in combination (an alternating stimulus), the CM is minimised or cancelled (Katz, 2009). This can

be useful clinically, to assess the functioning of the OHCs, which can help to assess auditory neuropathy.

While the main contributor to the CM is the OHCs, the summating potential portion of the ECochG is produced mainly from the IHCs, with some contribution from the OHCs (Durrant, Wang, Ding, & Salvi, 1998; Zheng, Ding, McFadden, & Henderson, 1997). The summating potential is seen as a direct current (DC), mirroring the displacement of the basilar membrane (Zheng et al., 1997). Originally, it was thought that the OHCs were the main contributors of this potential, however SPs recorded found a basal weighting in the potentials, and the basal OHCs do not produce large DC potentials at higher frequencies (Russell & Kossl, 1992). The SP copies the stimulus temporal envelope, resulting in a DC potential of the polarity of the stimulus, which can be positive or negative depending on the stimulus and the electrode placement (Eggermont & Odenthal, 1974; Davis, Deatherage, Eldredge, & Smith, 1958, Van Deelen & Smoorenburg, 1986). The DC potential of the SP is seen prior to the CAP, as a deviation away from the ECochG baseline recording, and can be seen with the CM and CAP in figure 5.

The compound action potential (CAP) is the sum of the action potentials produced from the acoustic nerve fibres (Johnstone, Alder, Johnstone, & Robertson, 1979). It is seen as a negative peak known as N1, followed by a positive response or P1, and then another negative peak known as N2 (Katz, 2009). N2 is only present occasionally, and depends on the intensity of the stimulus used (Gibson & Beagley, 1976). The first peak (N1) of the CAP is identical to the first wave (Wave I) of the auditory brainstem response (ABR), with only minor differences in the evoked potential source with low intensity clicks in cases of hearing loss (Ferarro & Ferguson, 1989; Coats & Martin, 1977). These peaks represent the beginnings of the auditory nerve, the portion closest to the cochlear (Moller & Janetta, 1985). As the CAP

is the sum of APs from the distal cochlear nerve, the greater intensity of the acoustic stimulus, the more nerve fibres recruited, and therefore the greater the evoked potential (Naunton & Zerlin, 1976). As well as this, with increased stimulus intensity CAP latency decreases, seen as the most effective at lower frequencies (Eggermont, 1974). Even with minimal IHCs present, a CAP will still occur if the remaining IHCs are sufficiently stimulated (Spoendlin & Baumgartner, 1977).

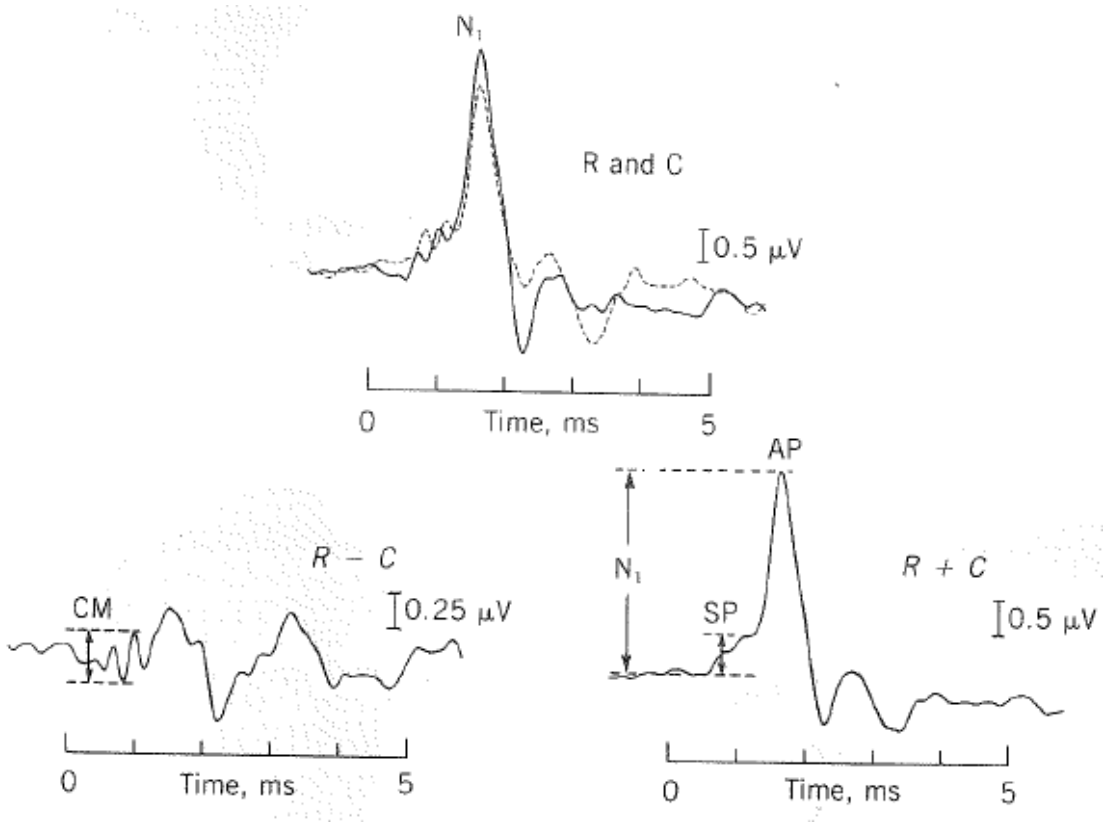

Figure 5: Showing (*top*) rarefaction and condensation responses overlaid; (*left*) the rarefaction and condensation responses subtracted to amplify the CM; (*right*) the rarefaction and condensation waveforms added to amplify the SP and CAP, (Coats, 1981)

Each portion of the ECochG can be used to infer the integrity of the anatomical parts that produce this evoked potential. This can be used as part of a medical and audiological test battery to come to a diagnosis about the site of lesion causing an individual's hearing loss. The ECochG can also be used clinically to assess audiometric threshold using tone burst stimuli using the AP amplitude (Spoor & Eggermont, 1976). All of the components of the ECochG can

be measured for their amplitude and latency, but the amplitude is more commonly used clinically and within the research, as latency changes with the frequency being stimulated as well as the intensity of the stimulus used (Katz, 2009). Figure 6 shows the locations along the ECochG waveform that are measured for amplitude (Katz, 2009). Low frequencies have longer onset latencies than higher frequencies (Eggermont, 1974). The CAP waveforms of the different frequency responses changes too. At below 2 kHz, the nerve fibres are locked and synchronised with the onset stimulus sine wave, and related to the actual hair cell movement (Deatherage & Eldredge, 1959). This can be seen as a near sinusoidal wave in response the low frequency stimulus (Dallos & Cheatham, 1976). At 2 kHz and above, adaption occurs resulting in smaller AP responses over time; this is known as the on-effect, and is demonstrated in figure 7 (Eggermont, 1974). The reliability of ECochG recordings accurately measuring responses from the cochlea hair cells, and therefore threshold diminishes below

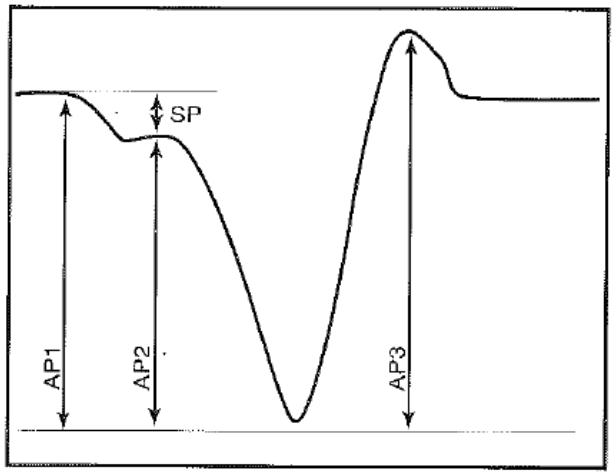

Figure 6 (above): Indicates three possible places of amplitude measurement (Katz, 2009).

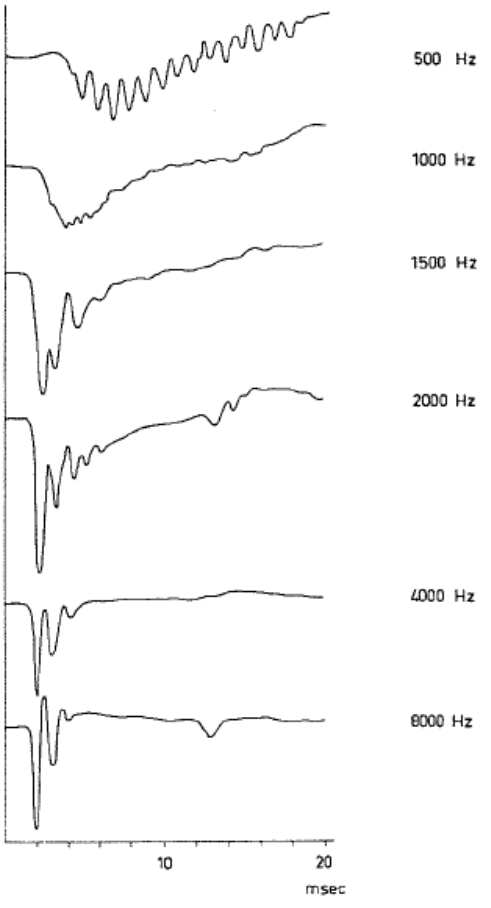

Figure 7 (right): Shows the changes in both latency onset and wave morphology with stimulus frequency (Eggermont, 1974).

500Hz (Eggermont, 1974; Laureano, McGrady, & Campbell, 1995). This represents a challenge to using electrocochleography for determining threshold at these low frequencies.

The different use of onset stimuli can also be utilised clinically. Click stimuli, with a rapid onset, stimulates a wide frequency range, and therefore stimulating more nerve fibres. Although click stimuli is a wide frequency stimulus, there is evidence to suggest that responses evoked by click stimuli primarily represent the higher frequency range, and therefore may not represent the nerve as a whole (Hyde, Riko, & Malizia, 1990). As previously stated, frequency specific tone burst stimuli can be utilised to threshold seek, although the resulting potential may not be as robust as rapid onset click stimulus (Pickles, 2012). This objective measure of hearing threshold can be used clinically to measure intraoperatively or to enhance wave I of the ABR (Ruth, Lambert, & Ferraro, 1988), and as one method for estimating hearing thresholds of young children unable to respond subjectively (Spoor & Eggermont, 1976). The SP can also be evoked using tone bursts, however it has been found that SP amplitude evoked with clicks is more reliable as a clinical measure (Coats, 1981; Eggermont 1979; Gibson, Moffat, & Ramsden 1977). Using SP/AP ratio can be a useful measure in diagnosing endolymphatic hydrops associated with Ménière's disease, which will be discussed further in *Chapter 1.5*. The AP with an amplitude greater than 1μV is more reliable when using the AP/SP ratio diagnostically (Hough & Baker, 2004).

There are a few different recording electrode sites that are able to be used for ECochG. They differ in how close to the evoked potentials they are i.e. how close to the cochlea, as well as whether they are invasive or non-invasive. The closer to the site of the evoked potential response the active electrode is, the more robust the signal will be, and will require less signal averaging to obtain a true response (Katz, 2009). The two types of placements that

are used for ECochG are transtympanic (invasive) and extratympanic (noninvasive). Transtympanic involves placing a needle electrode down the ear canal, through the tympanic membrane, and as close to the cochlea (promontory or round window) as possible. However Krueger & Wagner (1997) have shown that the precise placement of the needle does not impinge on the SP/AP recorded, and that any abnormalities can be attributed to pathologies, rather than needle placement. While other studies have shown that needle placement does have effect on the SP and AP, and changing position of the electrode can change the amplitude of the potentials (Van Deelen & Smoorenburg, 1986). While the transtympanic electrode yields good results it is still an invasive procedure, with possible complications. Ng, Srireddy, Horlbeck, & Niparko (2001) found that some of the complications faced by those that underwent transtympanic electrocochleography were persistent tympanic membrane perforation, hearing loss, otitis media and externa, hemotympanium, and pain. They however concluded that the complications were infrequent enough to be acceptable diagnostically, and that those involved tolerated the invasive procedure well (Ng et al., 2001).

Extra tympanic does not involve piercing the tympanic membrane, but varies in placement site; from resting on the tympanic membrane to sitting within the external auditory meatus in a conducting fluid (Carpi & Migliorini, 2009). The evoked potential recordings from the tympanic membrane does reduce the strength of the signal detected by the electrode. This reduces the signal to noise ratio, reducing the measured response, and allowing for electrical noise to overshadow the ECochG (Kumaragamage, Lithgow, & Moussavi, 2015). However it is possible to record SP information, even with tone bursts, from a tympanic membrane placed electrode (Ferraro, Thedinger, Mediavilla, & Blackwell, 1994a). Ferraro, Thedinger, Mediavilla, & Blackwell (1994b) found that the SP amplitudes were approximately four times greater with transtympanic than with extratympanic from the same

ear, however the evoked potentials of both had the same morphology, allowing for diagnosis, regardless of decreased amplitude. Schoonhoven, Fabius, & Grote (1995) found similar results, and concluded that for low level stimuli, more signal averaging was required to get an accurate response with extratympanic placement compare to transtympanic. Bonucci and Hyppolito (2009) concluded that extratympanic placement was better, as although the amplitude was decreased and the reproducibility was lesser than transtympanic, it also decreased discomfort during the procedure and the electrode was easier to place. Noninvasive ECochG has also been found to have good inter-test reliability (Mori, Matsunaga, & Asai, 1981). Posterior inferior placement on the tympanic membrane has been found to increase amplitude of AP/SP responses, with the thought that it decreases the conduction pathway between the electrode and the cochlea (Cullen, Ellis, Berlin, & Lousteau, 1972; Mason, Singh, & Brown, 1980).

1.3.2 Auditory Brainstem Response (ABR)

Auditory brainstem responses (ABRs) can be used to assess the eighth cranial nerve and the auditory neural pathway. ABRs can be seen as a set of seven waveforms that extend from stimulus onset to around 15ms (Katz, 2009). The peaks and troughs of these waveforms were

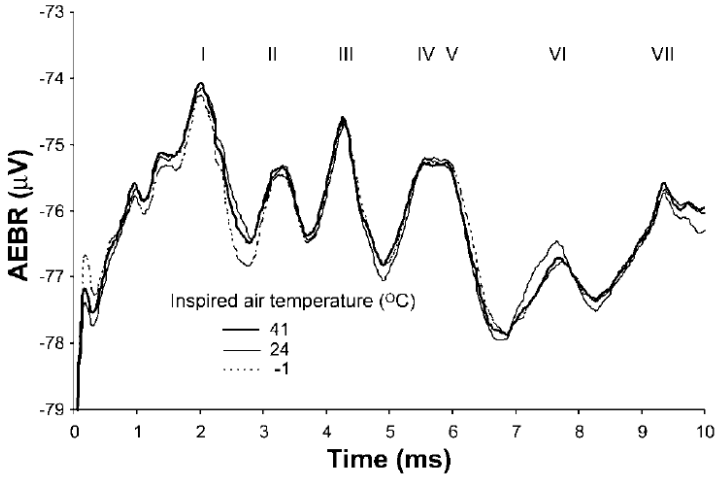

Figure 8: ABR waveform, labelled using the Jewett and Williston nomenclature (Mekjavic, 2002)

first named by Jewett and Williston (1971) and coincide with sums of neural activations along the auditory neural pathway (Katz, 2009), see figure 8 for the morphology of the ABR waves. Wave I is considered peripheral auditory nerve, while wave II and above is considered central auditory nerve, with wave V resulting from upper brainstem activation (O'Beirne, 2014). These waveforms are recorded by electrodes placed on the scalp, with the active electrode being placed on the vertex or forehead, the reference electrodes placed on the mastoid or the ear lobe, and the ground electrodes placed on the clavicle or the neck.

The ABR peaks and troughs can then be used diagnostically by looking at the latency and amplitude of different aspects of the seven waves. Peak latencies are established by several mechanisms within the auditory pathway, such as delay from the cochlea to site of activation, filter impulse response time of the activation site, the synaptic delay between the inner hair cells and the auditory nerve fibres, and nerve conduction time, as well as any other synaptic delays within the brainstem (Katz, 2009). Amplitude can be measured from the peak of a wave to the trough, and can depend on the synchronisation of neural activity (such as seen with click compared to chirp stimuli), and also the intensity of stimulation. Hearing loss, pathologies, and age can also affect the peak amplitudes (Katz, 2009). Latency measures can include wave V latencies, comparing peak latencies between ears, measuring the latencies between different peaks (such as I-III, III-V, and I-V), and comparing these interpeak differences between ears (Katz, 2009). Amplitude measurements can include wave V amplitude and comparing to the opposite ear, using wave V and wave I amplitudes to form a ratio, and then again comparing between ears (Katz, 2009).

Jewett and Williston (1971) found that the seven wave peaks they had measured occurred within 9 ms of the stimulus onset, and that waves I to V increased in magnitude. They also

found that the amplitudes of these waves were similar between normal hearing adults, around 0.6 - 1.4 μV, and similar latencies, with wave V occurring around 4.6 - 5.1 ms, however the morphology of the waves differed between participants (Jewett & Williston, 1971). Salamy, McKean, and Buda (1975) looked at the differences in latencies between adults and infants. They found that from birth with increase in age, the latency of wave V decreased, and by around age 2.5 years old responses were adult like in latency (around 5.5ms). They found that waves I to IV were also prolonged in younger participants. They concluded that peripheral maturity is achieved earlier than central (Salamy et al., 1975). Hecox and Galambos (1974) found very similar results to these in their ABR latency experiment with adults and infants, but also that latency increases with decrease in stimulus (click) intensity. Starr, Amlie, Martin, and Sanders (1977) looked specifically at newborn latency of wave V, and found again that latency decreased with maturation, for example at 65 dB SL presentation of click stimulus, wave V peak was present at 9.9ms at 26weeks gestation, and 6.9ms at 40weeks. During their study they found five children whose ABRs were abnormal, with delayed latency or altered amplitude at normal presentation levels. These children were found to have varying disorders of the brainstem and central nervous system. They go onto suggest that auditory brainstem potentials allow for an objective measurement of infant sensory function (Starr et al., 1977).

ABR can be used clinically to objectively detect hearing loss that may be present in young children, or adults who are unable to respond to subjective threshold testing. Cone-Wesson, Dowell, Tomlin, Rance, and Ming (2002) used click ABRs to predict hearing loss in children, compared to auditory steady state responses. They found that click ABRs were slightly better at predicting thresholds, and that tone burst ABR was also a good predictor of adult thresholds. This can then be used as a screening tool to pick up any children with a hearing

loss; such is as done with the new born hearing screen. Mason and Herrmann (1998) used ABR to screen 10,372 infants for hearing loss. They found that it had a 96% success rate, and that those infants that were identified and amplified before 6 months had normal speech and language development (Mason & Herrmann, 1998). McGee and Clemis (1981) found that conductive losses can cause a shift in wave V latency intensity function, which correlates with the air bone gap found in the audiogram. However when there is a mixed loss, the wave V latency due to the sensorineural/retrocochlear aspect of the loss may be masked by the conductive component. Starr and Achor (1975) used ABRs to evaluate the usefulness in identifying neurological conditions. They found that ABRs were useful in localising tumours in the brainstem, demyelination of the brainstem, as well as decreased blood flow to the brainstem (Starr & Achor, 1975).

Different stimuli can be used to elicit ABRs. Typically click stimuli activate the high frequency region of the basal part of the cochlea, found to be linked with auditory thresholds at 2 kHz and 4 kHz (Folsom, 1984; Gorga et al., 2006; Hyde, Riko, & Malizia, 1990). It is this that drives the wave V peak latencies. However when there is a high frequency hearing loss, the apical low frequency part of the cochlea produce more of wave V, causing a longer latency (Katz, 2009). Chirp stimuli are frequency swept to compensate for this basilar membrane travelling wave delay that clicks produce (Chertoff, Lichtenhan, & Willis, 2010). Chertoff et al. (2010) found that chirp stimuli had shallower latency intensity functions in compound action potentials, compared to clicks. They concluded that this was due to auditory nerve fibres responding more in unison with chirp stimuli than clicks, due to the frequency compensation (Chertoff et al., 2010). Riedel and Kollmeier (2002) found that chirps resulted in larger wave V amplitudes for all levels, and resulted in better ABR results compared to clicks. They also

concluded that this was due to greater activation of the high and low frequency neurons simultaneously, as opposed to high frequency activation followed through to low frequency activation as with clicks (Riedel & Kollmeier, 2002). Maloff and Hood (2014) found that chirps increased the peak to peak amplitude of wave V, especially at lower intensities, and that chirp stimuli were closer to estimating hearing thresholds than clicks. However the most robust ABRs are best produced with transient stimuli with a rapid onset, which causes synchronous firing of a great number of neurons, creating a stronger response recorded (Hall, 2006).

1.3.3 Direct Eighth Nerve Monitoring (DENM)

Direct eighth nerve monitoring (DENM) is the measurement of the collective evoked potential from the vestibulocochlear nerve (CN VIII). The measurement of this potential was first developed by Moller and Jannetta (1983). This monitoring technique is only able to be used during surgery which allows access to the cerebellopontine angle (CPA), as the active electrode needs to be placed on the proximal end of the vestibulocochlear nerve, within the CPA. One modern active electrode used in these recordings is a C shaped electrode, made to sit around the eighth nerve, while allowing for the nerve to safely move out of the electrode in the case of movement (Cueva, Morris, & Prioleau, 1998).

The cochlear nerve action potentials (CNAPs) are similar in morphology to CAPs, only differing in location along the cochlear nerve. The response has a large positive peak (P1), followed by a negative peak (N1), a second positive peak (P2), and a second negative peak (N2), which can be seen in figure 9. Smaller neural activity can also be seen in the trace, before and after the CNAP, showing the neural electrical activity moving towards and away from the DENM electrode (Roberson, Senne, Brackmann, Hitselberger, & Saunders, 1996). CNAPs can be evoked using click stimuli, causing a greater response than tone burst stimuli, as it causes greater recruitment of neural fibres. Tone burst stimuli, however, are useful at creating frequency specific responses, making it possible to record audiometric thresholds (Jannetta, Møller, & Møller, 1984; Møller & Jannetta, 1983).

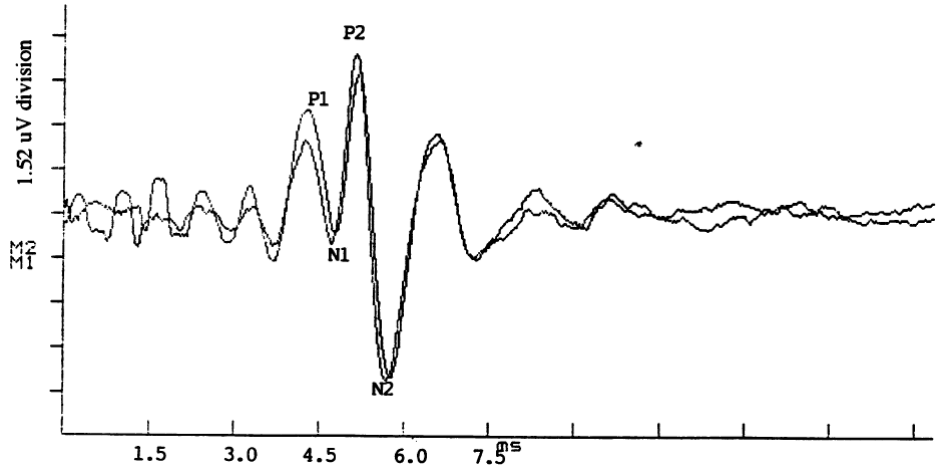

Figure 9: The CNAP waveform amplitude and morphology (Ruckenstein, 1997)

Both amplitude and latency can be used for evaluating the CNAP. The amplitude measured from the DENM can vary around 5 µV to 70 µV, and changes with degree of hearing loss (Cueva, Morris, & Prioleau, 1998). The amplitude of the response is taken as the voltage difference between the trough of N1 and the peak of P1, and is a large response given to the proximity to the electrical source, minimising the need for large amounts averaging (Aihara et al., 2009). The difference in amplitude is almost a hundred fold comparing ABR and DENM responses (Jackson & Roberson, 2000). The onset latency of the DENM CNAP occurs within

two to five seconds. Comparing this to ABR traces, the averaging of the DENM takes less time, and requires less averaging overall due to the intensity of the waveform. In terms of obtaining results, DENM is almost instantaneous, meaning that the responses can be used as a measure of immediate auditory functioning of the cochlear nerve (Battista et al., 2000; Danner et al., 2004). Batista et al. (2000) commented on the latency of the DENM response, which can vary between individuals due to placement on the nerve. Placement closer to the cochlea, results in a shorter CNAP latency. Therefore, latency measures must have a reference point from an individual taken before comparing latency changes (Battista et al., 2000).

1.3.4 Otoacoustic Emissions

Otoacoustic emissions (OAEs) are not auditory evoked electrical potentials, rather they are auditory evoked sounds produced from the outer hair cells within cochlea. Kemp (1978) discovered delayed acoustic energy produced in in the ear after being present with click stimuli. The sounds produced were not reflections from the cochlea, and indicated a nonlinear mechanism within the cochlea (Kemp, 1978). The OHCs, as discussed in an earlier chapter, contribute to this nonlinear process, through the feedback system known as the cochlear amplifier, which contributes to producing the OAEs. As such, OAEs are an objective measure of OHC functioning, and can be used clinically to measure low level intensity responses. The OAEs are conducted out of the cochlea, through the middle ear, into the external ear canal. OAEs cannot be measured in those with mild to moderate hearing losses (Kemp, 1978; Prieve et al., 1993). As the responses are acoustic in response, rather than electrical, OAE testing must be conducted in an acoustically quiet environment to stop background noise interference.

There are three types of OAEs that are used within research and clinically. Spontaneous OAEs (SOAEs) are the sounds produced by random oscillation of OHCs without

being acoustically stimulated, which can be heard in the external auditory meatus. This occurs naturally in at least 30-50% of the normal hearing population in at least one frequency (Probst et al., 1986). SOAEs, however, are not much use diagnostically, as they only apply for very specific and varying frequencies in different individuals, if at all. Transient OAEs (TEOAEs) are sounds produced by the cochlea in response to a click or tone burst stimulation. Imperfections within the basilar membrane cause sounds to be echoed back, creating an OAE that is representative of approximately 500 Hz to 4000 Hz, with 2000 Hz to 4000 Hz being the most repeatable, reliable, and indicator of hearing loss (Prieve et al., 1993). TEOAEs measure an acoustic signal in background noise, and as such, much be performed in relatively quiet conditions to detect the low level OAE produced. Distortion product OAEs (DPOAEs) are produced by stimulating the cochlea with two primary tones, which causes intermodulation of the two tones overlapping in the cochlea, resulting in a third tone known as a distortion product, which is produced as an OAEs. These OAEs result from a broad spectrum of the cochlea, but are still relatively frequency specific in nature (Shera & Guinan, 2008).

When compared, DPOAEs and TEOAEs both did equally well at diagnosing a hearing loss at 2000Hz, while DPOAEs predicted hearing loss better at 4000 Hz, and TEOAEs better at 1000Hz (Gorga et al., 1993). Both DPOAEs and TEOAEs were unable to accurately predict hearing loss at 500Hz, and this frequency was especially effected by background noise (Gorga et al., 1993). Both DPOAEs and TEOAEs were found to have consistent retest reliability (Franklin, McCoy, Martin, Lonsbury-Martin, 1992; Gorga et al., 1993). Another study found that 2000 to 6000 Hz were most reliable predictors of audiometric threshold, while frequencies above and below were less accurate (Rogers, Burke, Kopun, Tan, Neely, & Gorga, 2010). Overall OAEs are a good indication of absence or presence of hearing loss at frequencies above 1000 Hz, but unlike other evoked potential discussed, they are not able to

be used to threshold seek, only indicate presence or absence of OHC function. Knowing this, persons with middle ear abnormalities will not produce OAEs.

1.4 An Historical Review of Evoked Potentials

The CM was first discovered by Wever and Bray in 1930, in their experiments with cats. They named what they had discovered the Wever-Bray effect, and concluded that the waveform was from the auditory nerve. Davis and Derbyshire (1934) replicated Wever and Bray's experiment and came to the conclusion that the Wever-Bray effect was not from the nerve, but from the cochlea. The first experiments to obtain the CM, as well as the subsequent waveforms in humans was conducted by Fromm, Nylen, and Zotterman in 1935, using transtympanic recording electrodes. Fiscii and Ruben in 1962 measured the CAP from the round window of the cochlea and the CNAP from the eighth cranial nerve in cats. Moore was the first to record the CM and CAP using noninvasive electrode in 1971. This then paved the way for the use of recording the CM and CAP clinically.

Around the same time, in 1967, Sohmer and Feinmesser recorded ABR waveforms using noninvasive surface electrodes, while Yoshie, Ohashi, and Suzuki (1967) were conducting electrocochleography still using invasive techniques. The discovery by Hecox and Galambos (1974) that ABR could be used as an objective measure of auditory threshold in both adults and children, as well as noninvasively, added to the appeal of researching into ABR compared to ECochG for threshold estimation. The concern with noninvasive ECochG recording compared with noninvasive ABR recording was the signal to noise ratio, and the strength of the signal obtained. Extratympanic recording produces a weaker ECochG signal than transtympanic, making it more susceptible to interference from noise. This overall make the extratympanic recording less reproducible and strong than transtympanic (Bonucci & Hyppolito, 2009; Ruth & Lambert, 1989). Ghosh, Gupta, & Mann (2002) found that

extratympanic ECochG recordings had reduced sensitivity (from 100% to 90%) and reduced specificity (from 90% to 80%) compared to transtympanic ECochG. Kumaragamage, Lithgow, and Moussavi (2015) found that the main noise contributing to the degradation of the extratympanic signals was background biological noise and thermal noise from electrode impedances. Due to the noise influence that noninvasive ECochG can encounter, ECochG has mainly used in the research of and to diagnose Ménière's disease, rather than in the use of objective threshold seeking, where invasive recording techniques can be applied (Kumaragamage, Lithgow, & Moussavi, 2015).

The use of Google Ngram Viewer and PubMed results by year timeline can show the effect the influences mentioned above had on the uses of electrocochleography and auditory brainstem response within the literature. Google Ngram Viewer is a search engine that finds specific words or phrases found in printed books from the 1500s until 2008. The comparison of electrocochleography and auditory brainstem response is covered in figures 10 and 11. Figure 10 shows the raw data (the exact number of time the word was used in a given year) of the word electrocochleography per year compared to auditory brainstem response. Figure 11 gives the same data, except that it has been smoothed for the purposes of identifying a trend more easily within the data. The overall trend that can be seen is the earlier use of

electrocochleography, until the early 1980s, where ABR became more popular within the written literature.

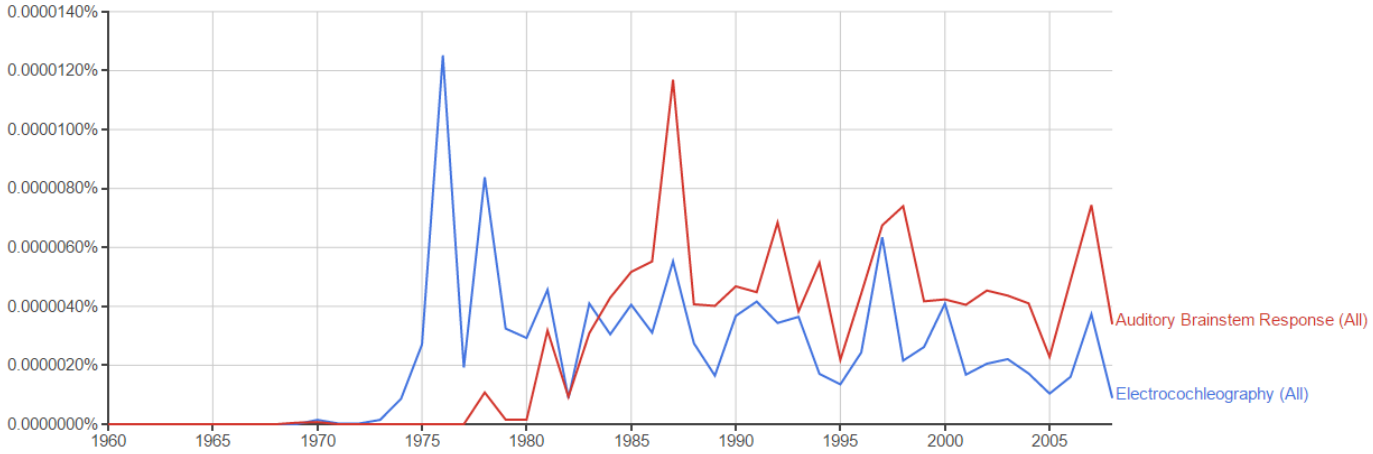

Figure 10 (*above*): shows raw data of the word electrocochleography (blue) compared to auditory brainstem response (red) usage in books from 1960 until 2008. *Figure 11* (*below*): The same data as in figure eleven that has been smoothed for the purpose of observing trends within the data

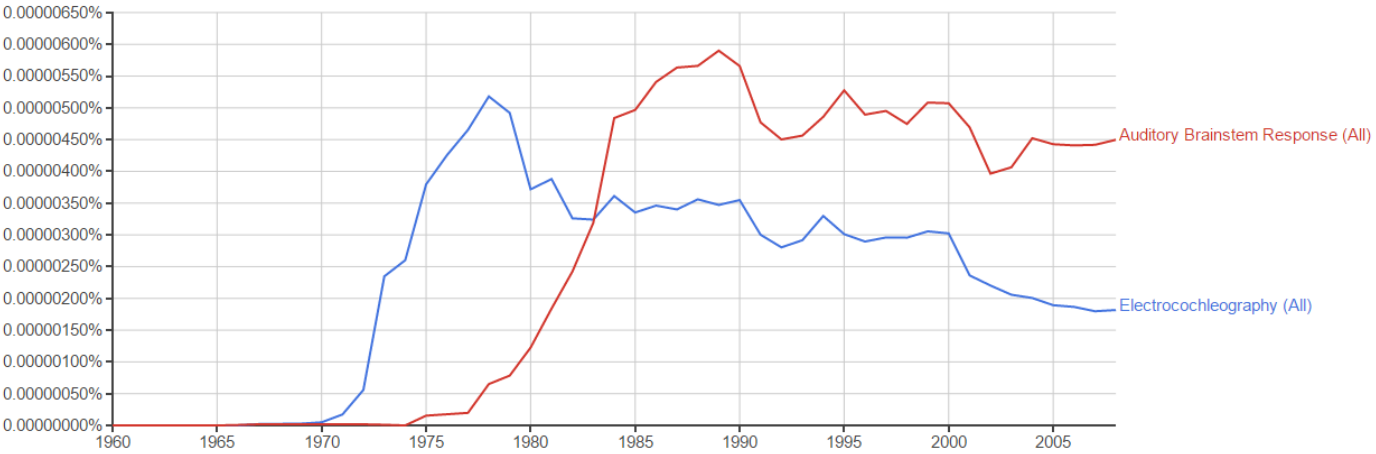

The other data to examine is the use of ECochG and ABR within research papers published. This was done through PubMed by searching for both electrocochleography and auditory brainstem response, and using the timeline data to create figure 12. The graph shows the use of the word electrocochleography compared to auditory brainstem response in published research papers over the years of 1960 until 2016. Again the overall trend shows the popularity of ABR use in research compared to ECochG, beginning in the early

1980s.

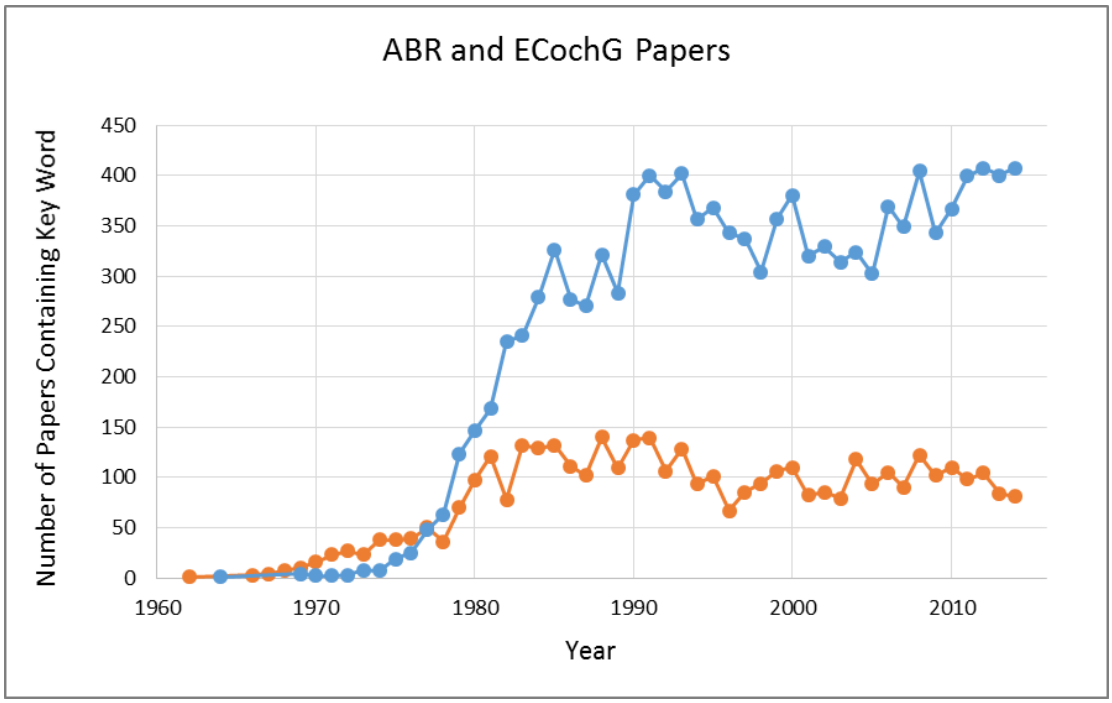

Figure 12: The raw data of the word electrocochleography (orange) compared to auditory brainstem response (blue) usage in published papers from 1960 until 2014.

Both Google Ngram Viewer and PubMed timeline indicate the current popularity of ABR compared to ECochG within the research. The suspected reasoning behind these trends has also been outlined; the invasive nature of transtympanic ECochG, and the better sensitivity and specificity of noninvasive ABR compared to noninvasive ECochG.

1.5 Ménière's Disease

Ménière's disease has a range of symptoms consisting of vertigo attacks, tinnitus, aural fullness, and hearing loss, and can affect one or both ears (Hughes & Pensak, 2011; Ruckenstein, 2010). It is described by the American Academy of Otolaryngology-Head and Neck Surgery (1995) in table 1 as comparing the range of symptoms felt with the possibility of having Ménière's disease. Ménière's disease can also be defined into three different stages defined by hearing loss associated with the disease (Kumagami, Nishida, & Baba, 1982). First stage: hearing recovers between attacks of Ménière's. Second stage: a fluctuating hearing

threshold which does not recover between attacks. Third stage: a fixed hearing loss, greater than 60 dB HL. The attacks of vertigo give the sensation of spinning, which can last for several hours, also often inducing nausea and emesis. The attacks can occur in groups, over a few days. Hearing, aural fullness, and tinnitus can all get worse prior to an onset of an attack, but can recover afterward (Ruckenstein, 2010).

Table 1: Shows the diagnosis of Ménière's disease from the patient's symptoms

Possible Ménière's Disease	1. Episodic vertigo of the Ménière's type without documented hearing loss or sensorineural hearing loss (fluctuating or fixed) with disequilibrium but without episodes 2. Other causes excluded
Probable Ménière's Disease	1. One definitive episode of vertigo 2. Audiometrically documented hearing loss on at least one occasion 3. Tinnitus or aural fullness in the treated ear 4. Other causes excluded
Definite Ménière's Disease	1. Two or more episode of vertigo lasting 20 minutes or longer 2. Audiometrically documented hearing loss on at least one occasion 3. Tinnitus or aural fullness in the treated ear 4. Other causes excluded
Certain Ménière's Disease	1. Definite Ménière's Disease, plus histopathologic confirmation

An alternative measure of Ménière's is the Gibson Score. It uses the combination of the four main symptoms of Ménière's and assigns points depending on the severity. A score of 7 or over indicates Ménière's disease, with a maximum of 10 points possible. One point is given to each of the following if present: rotational vertigo; attacks of rotational vertigo lasting over 10 minutes; rotational vertigo associated with hearing loss, tinnitus, or aural pressure; sensorineural hearing loss; fluctuating sensorineural hearing loss; hearing loss or fluctuation associated with vertigo, tinnitus, or aural pressure; tinnitus lasting over 5 minutes; tinnitus fluctuating with vertigo, hearing loss, or aural pressure; aural pressure lasting over 5

minutes; fluctuating aural pressure with vertigo, hearing loss, or tinnitus (William, 1991). The above methods of identifying patients with Ménière's disease rely on their subjective symptoms and personal information (Hornibrook, Kalin, Lin, O'Beirne, & Gourley, 2012).

The main identified cause of Ménière's disease is endolymphatic hydrops, discovered by both Yamakawa (1938), and Hallpike and Cairns (1938) in their separate histopathology research. Hydrops can be described as a fluctuating excess of endolymph fluid in the cochlea and vestibular system, causing distortion to the fine inner structures of both the cochlea and the vestibular saccule (Hughes & Pensak, 2011). In some cases the Reissner's membrane becomes enlarged, causing the accumulation of endolymph within the scala media to fill the space of the scala vestibuli. This can also lead to rupturing of the membranes within the inner ear, which can histologically confirm the presence of hydrops (Hughes & Pensak, 2011). Figure 13 shows a diagram of what endolymphatic hydrops looks like within the cochlea. The exact cause of endolymphatic hydrops is still not fully known.

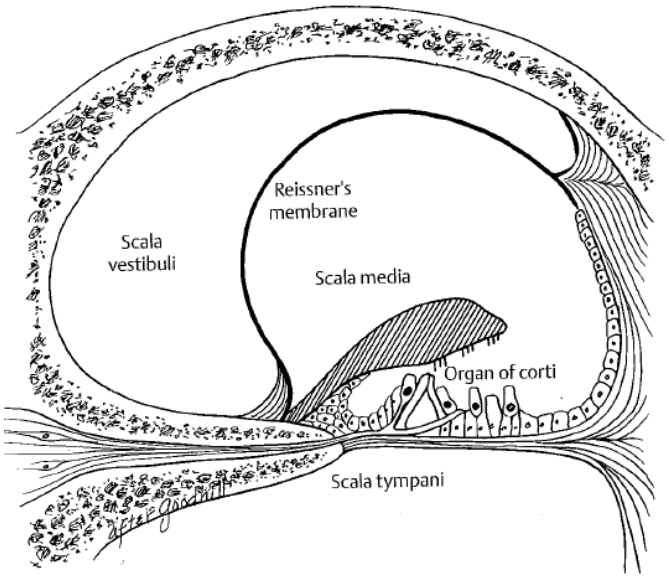

Figure 13: shows the effect endolymphatic hydrops has on the cochlear structures (Hughes & Pensak, 2011)

The objective measure of detecting endolymphatic hydrops using ECochG was explored by Gibson, Moffat, & Ramsden (1977), Gibson, Prasher, & Kilkenny (1983), and Coats

(1981), using invasive and noninvasive techniques, as well as clicks and tone burst stimuli. They used the SP and AP to define the difference between normal ears and with hydrops present, with an enlarged SP giving an indication of hydrops. Margolis, Rieks, Fournier, & Levine (1995) found that SP/AP ratio, and tone burst SP were useful in diagnosing hydrops. Clinical norms were developed from the research, currently used at Christchurch Public Hospital, which can be seen in table 2. The effect of hydrops, and the resulting Ménière's disease, has on ECochG tone burst and click recordings can be seen respectively in figures 14 and 15. Gibson (1993) found that the lower frequencies of 500 and 1000 Hz were more effective at diagnosing Ménière's disease using the SP compared to higher frequency of 4000 Hz. Gibson (2009) compared the sensitivity between tone burst and click ECochG for confirming hydrops. He found that tone burst stimuli, especially at 500, 1000, and 2000 Hz, was a more sensitive measure of hydrops than click stimuli (Gibson, 2009). Hornibrook et al. (2015) found similar results, concluding that tone burst ECochG was a more sensitive measure than both MRI detection and click stimulus ECochG.

Table 2: showing researched norms for diagnosing endolymphatic hydrops for clinical use

Click Stimulus	Abnormal if SP/AP ratio > 0.50 (50%)	
Tone Burst Stimulus:	**Hearing Level (dB HL)**	**Abnormal if SP >**
500 Hz (75 dB HL)	Under 25	-2 µV
	20 - 35	-2 µV
	40 - 55	-2 µV
	60 - 75	-1 µV
1000 Hz (90 dB HL)	Under 25	-6 µV
	20 - 35	-6 µV
	40 - 55	-6 µV
	60 - 75	-3 µV
2000 Hz (100 dB HL)	Under 25	-9 µV
	20 - 35	-7 µV
	40 - 55	-5 µV
	60 - 75	-5 µV
4000 Hz (75 dB HL)	Under 25	-9 µV
	20 - 35	-5 µV
	40 - 55	-5 µV
	60 - 75	-5 µV

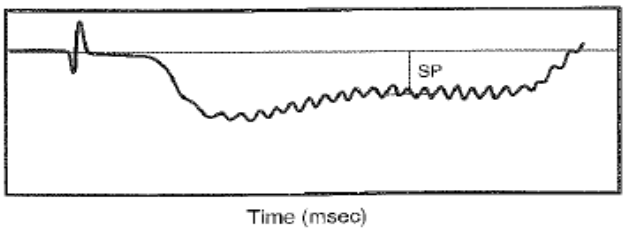

Figure 14: A tone burst ECochG response example of a patient with endolymphatic hydrops, causing an enlarged SP amplitude (Katz, 2009).

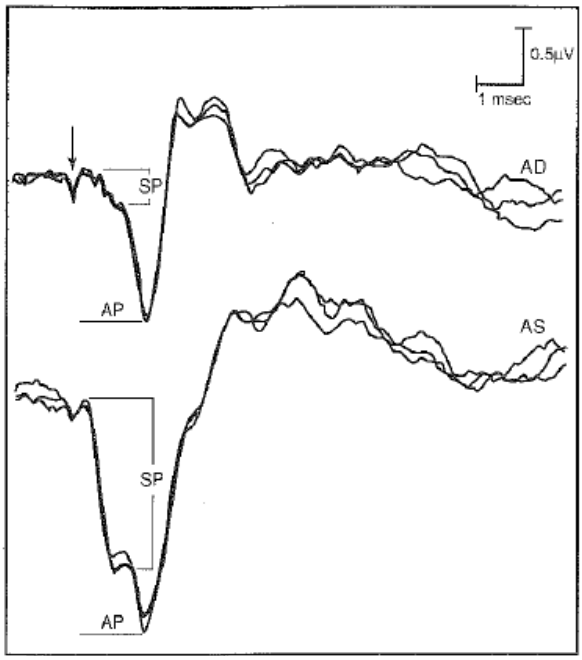

Figure 15: A click ECochG response example of a normal patient (top waveform) and a patient with endolymphatic hydrops (bottom waveform), causing an enlarged SP amplitude (Katz, 2009).

There is no definitive treatment for Meniere's disease, but there are management strategies. The strategies involve trying to decrease the amount of endolymph, increasing the circulation within the inner ear, or attempting to remove the blockage of the endolymphatic duct that may be causing symptoms (Hughes & Pensak, 2011). Ruckenstein, Rutka, & Hawke (1991) evaluated different Ménière's disease treatments and came to the conclusion that none of the supposed treatments had been shown to be effect in controlled double blind

studies. Management strategies involve either conservative measures, or surgical or destructive measures. Conservative methods involve a low sodium diet and diuretics to try and decrease the amount of endolymph. Betahistine can be prescribed in an attempt to reduce vertigo or dizziness (Lacour, van de Heyning, Novotny, & Tighilet, 2007). Invasive and destructive procedures such as endolymphatic sac surgery, gentamicin injections, vestibular nerve resection, or inner ear destruction can be implemented if the symptoms of Ménière's have become severe, and other management strategies have been tried and failed. From these destructive management strategies, rehabilitation is necessary, as both sensitivity of hearing and balance for the effected side will be severely diminished or absent.

1.6 Limitations to current clinical methods of monitoring thresholds

Although there are many benefits to the current methods of monitoring thresholds using auditory evoked potentials, there are also some limitations, which could be improved upon by another method. The main methods of objective threshold measurements using auditory evoked potentials are discussed below.

1.6.1 ECochG

As discussed in chapter 1.3 ECochG is useful in its ability to compare different aspects of the cochlea; the functioning of the OHCs, the IHCs, and the beginnings of the auditory nerve. It is also one of the leading ways in helping to diagnose Ménière's disease. However there are limitations to this method when it comes to objectively measuring hearing threshold. Laureano, McGrady, and Campbell (1995) found that lower frequencies did not correlate with behavioural audiometric thresholds when using an extratympanic electrode. Higher frequencies of 2000 and 4000 Hz did correlate, but from 1000 Hz and below, the ECochG became an unreliable method of measuring threshold (Laureano, McGrady, & Campbell, 1995). Schoonhoven, Prijis, and Grote (1996) conducted a similar study, except compared

both extratympanic and transtympanic electrodes with pure tone thresholds. They found that both methods of measurement correlated with frequency specific audiometric thresholds except for 500 Hz by extratympanic measurement, and that extratympanic thresholds yielded more uncertainty. They concluded that ECochG measurements take into account cochlear sensitivity, but subjectively thresholds also take into account reduced temporal integration (Schoonhoven, Prijis, & Grote, 1996). Spoor and Eggermont (1976) found that for lower frequencies of 500 Hz gave greater range of differences in threshold, as well as, on average, predicting the subjective threshold as 10dB better than it actually was. These studies have found good correlation of high frequency ECochG responses with audiometric threshold, but poor correlation with low frequency stimuli.

Another problem with ECochG being used for threshold stimulation is the reduced response with extratympanic ECochG. The response, due to the decreased amplitude, can be subject to other neural potentials interfering with the recording (Patuzzi, Yates, & Johnstone, 1989). And as such, requires greater averaging to obtain a true response, requiring more time, and thus not being an instantaneous measure of hearing. Humphries, Ashcroft, and Douek (1977) found that extratympanic ECochG predicted subjective threshold with 30dB, which they considered to be a good indicator of threshold. Transtympanic can remove some of these problems, however the invasiveness of this procedure remains a problem for those not requiring special ear treatments i.e. those with normal auditory system functioning.

The final consideration of ECochG is the subjective nature of the interpretation of the waveforms. In terms of Ménière's disease, the SP/AP ratio can be critical in diagnosis and therefore management. Roland and Roth (1997) evaluated the variability of clinician's interpretations of ECochG, specifically the SP and AP amplitudes. They found that the more

difficult or no response traces had the greatest inter-clinician variability, resulting in significant differences in diagnosis (Roland & Roth, 1997).

1.6.2 ABR

As with ECochG, ABR has problems of lower frequency not correlating to behavioural threshold as well as the higher frequencies. Sininger, Abdala, and Cone-Wesson (1997) found a high correlation between frequency tone burst stimuli and the corresponding auditory thresholds in infants. These results showed elevated thresholds compared with adult thresholds, especially with 8000 Hz, suggesting the auditory system not fully developed in terms of high frequency thresholds (Sininger, Abdala, & Cone-Wesson, 1997). While Sininger (2007) found that the responses to the low frequency tone bursts did not correlate as well to behavioural thresholds. Tone burst stimuli are preferred in estimating threshold, as click stimuli produce a response from the auditory nerve as a whole, with a possible bias for the higher frequencies due to phase cancellation of responses from lower frequencies (Hyde, Riko, and Malizia, 1990; Katz, 2009). It has been found that ABR can be an accurate measurement of auditory thresholds from 500 to 4000 Hz in neonates, young children, and adults (Stapells, 2000; Stapells & Oates, 1997). Threshold measurement at 500 Hz in neonates is attempted using a correction factor, to allow for inaccuracy at this frequency, as providing estimated hearing amplification at this frequency is better than none at all. Stapells (2000) found that the correction factor used often varies among patients, which adds a level of uncertainty to the actual threshold, as well as any hearing aid amplification that may be prescribed. As a result ABR is commonly used as an objective threshold measure in neonates and young children who are yet unable to subjectively respond. This has advantaged over ECochG, as ABR yields good responses using noninvasive electrode placement.

Like ECochG responses, auditory brainstem responses need to be averaged to highlight and enhance the ABR waveform within the background electrical and myogenic noise (Hall, 2006). The responses can be biased by myogenic potentials, which are larger in amplitude (as seen with the PAMR or post auricular muscle response), which can then influence the resulting waveform (Don & Elberling, 1994). This is why the testing must occur while the patient is at rest, and with eyes closed. Bayesian weighting to the responses can help to minimise the noise recorded, helping to improve the strength of the response, overall reducing averaging time (Don & Elberling, 1994).

1.7 Auditory Nerve Overlapped Waveform (ANOW)

The Auditory Nerve Overlapped Waveform (ANOW) was first defined by Lichtenhan, Cooper and Guinan (2013). It is described as a neural response obtainable from what is usually considered the cochlear microphonic waveform. If the cochlear microphonic is produced with a low frequency tone burst, and then averaged with the opposite polarity CM elicited using the same frequency, the overall CM gets abolished, and produces a neural response that is twice the tone cycle. This is the auditory nerve overlapped waveform (ANOW).

Lichtenhan, Cooper, and Guinan Jr. (2013) designed the study to develop a method of objectively measuring thresholds accurately below 1000 Hz, as both ECochG and ABR do not accurately do this. They used the reasoning described in previous papers from Henry (1995), Eggermont (1974), Ferraro, Blackwell, Mediavilla, and Thedinger (1994) to try and quantify the technique to a clinically viable test. At low frequencies the OHCs respond to stimuli as a sinusoidal wave almost copying the stimulus frequency (Dallos & Cheatham, 1976). While the underlying neural response to low frequency stimuli is to activate with one polarity of a stimulus wave, causing IHCs depolarise, and with the other polarity of the wave, to stop firing. This is known as phase locked responses (Palmer & Russell, 1986).

Lichtenhan et al. (2013) measured the CM within cats at 300, and subtracted the waveforms of opposite polarity, to leave the underlying (phase locked) neural component.

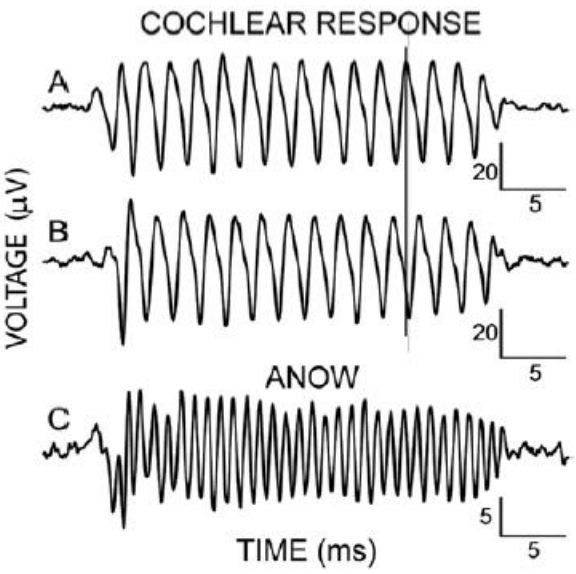

Figure 16: Shows the two CMs of opposite polarity (*A & B*), and the ANOW (*C*) of the averaged top traces (Lichtenhan et al., 2013).

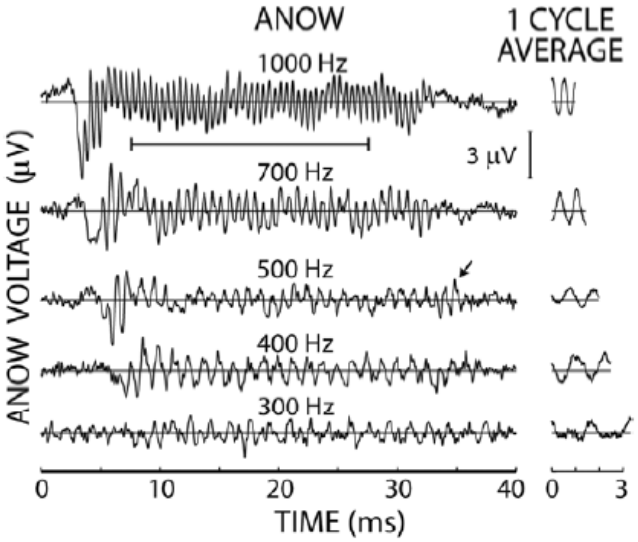

Figure 17: Shows the ANOW obtained from different low frequency stimuli. The wave cycles to the right of the ANOWs shows the double tone cycle produced from the original stimulus (Lichtenhan et al., 2013).

This resultant waveform is what they termed the ANOW, and can be seen as twice the cycle of the overlying cochlear responses, similar to the auditory nerve neurophonic residual, as described by Henry (1995). The ANOW can be seen in figures 16 and 17, from the Lichtenhan, Cooper, and Guinan Jr. (2013) paper. They compared the measured ANOWs from 300 to 1000 Hz with single auditory nerve fibre responses at the same frequencies. This showed that the ANOW is a useful measure from 700 Hz and below. From their work, in combination with Henry's (1995) paper, they conclude that the ANOW is a useful technique to be developed further as a measure of low frequency neural auditory threshold.

Lichtenhan, Hartsock, Gill, Guinan Jr, and Salt (2014) examined the neural origins of the ANOW. They used tetrodotoxin injected into the cochlear apex to slowly stop neural functioning from the apex to the base in guinea pigs. The frequencies of 353, 500, and 707 Hz were tested. They found that the cochlear responses that they were recording from the

guinea pigs were not purely from the OHCs, and that the summed responses produced the CM, not the ANOW, as was previously thought in the Lichtenhan et al. (2013) paper. They used a very similar, but different technique from Lichtenhan et al. paper (2013) to produce the ANOW. The ANOW was achieved by summing the two cochlear responses of diffing polarities, smoothing the sum trace, then subtracting it from the original sum, leaving only ANOW (double the stimulus frequency) around a baseline of zero. This can be seen in figure 18. From this study they concluded that the ANOW was neural in origin, and originated from

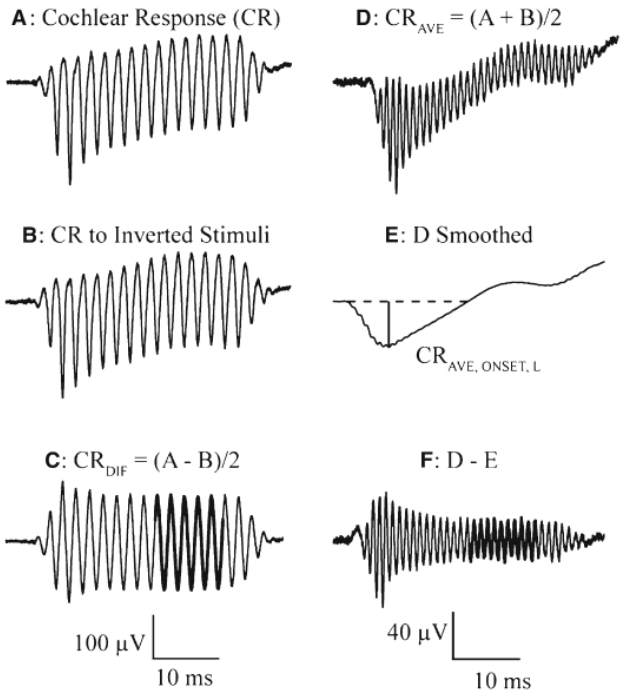

Figure 18: (**A**) shows the cochlear response. (**B**) Cochlear response of opposite polarity. (**C**) The difference between A & B, resulting in the CM. (**D**) The average of A & B. (**E**) the smoothed response of D, can be seen as the CAP. (**F**) The response from D minus E, showing the purely neural component or ANOW. (Lichtenhan et al., 2014).

the apex (low frequency) of the cochlea (Lichtenhan et al., 2014).

Kaf, Abdelhakiem, Zahirsha, and Lichtenhan (2015) discuss the possible implications of using ANOW in the diagnosis of Ménière's disease. They concluded that low frequency responses were more efficient at diagnosing Ménière's disease, however current methods of threshold monitoring were not accurate at measuring low frequency hearing loss (Kaf et al., 2015). They also stated that within the current research of ANOW results had only been

obtain from animal models, and that further development would be required to take this technology for use in human subjects, and in diagnosis for Ménière's disease (Kaf et el., 2015).

Choudhury, Fitzpatrick, Buchman, Wei, Dillon, He and Adunka (2012) researched into the use of the auditory nerve neurophonic or ANN, which is similar to the ANOW, and developed from the same past research. They recorded electrical potentials from the round windows during cochlear implantation in humans to investigate the preservation of residual hearing. They measured the CM, SP, CAP, and ANN intraoperatively. From this they concluded that they were able to measure the hair cell and neural states of the participants, especially at frequencies lower than 1000 Hz. However it should be noted that while the Choudhury et al. (2012) paper claims that the ANN they measured was from auditory neural activity from the round window in humans, only Lichtenhan et al. (2014) demonstrated that what they recorded (the ANOW) was purely neural in origin. The Choudhury et al. (2012) paper also involved a highly invasive surgical measure of reported neural activity prior to cochlear implantation, not practical to those patients not having their round window surgically exposed.

1.8 Aims and Hypothesis

The aim of this study is to advance the techniques formed in the animal models of the Lichtenhan et al. papers (2013; 2014), and develop the use of the ANOW in humans, specifically in those with Ménière's disease, as suggested in Kaf et al. (2015). We aim to gain some normative data from the participants with suspected Ménière's disease, as well as objectively track their threshold and compare to their subjective thresholds, and their ECochG responses. This will allow us to develop both the technique of aiding current subjective

methods of diagnosing Ménière's disease, as well as further developing the serious clinical need for objective low frequency threshold monitoring.

We will compare both neural and hair cell functioning from our results (CM compared to ANOW), and hope to find a difference between those affected with Ménière's disease, and those with normal cochlear pathology. We also hope to develop the ANOW monitoring technique so it can be applied to not only those with suspected Ménière's disease, but those with normal hearing, other auditory system pathologies, and also to be used intraoperatively.

Based upon the current minimal literature available on the topic of ANOW, we hypothesise that the ANOW monitoring technique will accurately predict thresholds at lower frequencies, which current methods are not capable of. We also hypothesise that the ANOW norms developed in this study will be the beginning to a clinically viable low frequency monitoring technique, useful clinically across a range of auditory pathologies to be further developed.

Chapter Two: Verification of Equipment

2.1 Equipment Setup

A laptop containing the software for this experiment, was connected via USB port to an electrically isolated, battery powered preamplifier (NIcDAQ9174 Chassis). This preamplifier contained an analog input (NI9222) and an analog output (NI9269). Both input and output sites contained four channels. The output from this preamplifier connected to a battery powered Rolls Stereo mini mx 28 amplifier, which amplified the signal from the analog output unit and drove the magnetically shielded headphones. The electrodes connected to the participants feed into an electrically isolated, mains powered amplifier, which connected into the NIcDAQ9174 Chassis preamplifier analog input. A connection also ran between the input and output of the preamplifier, acting to synchronise and trigger. The Rolls Stereo amplifier was used to drive the headphone output as the NI9269 output was not capable. This amplifier contained adjustable output amplification dials, the calibration of which will be discussed in following chapters. The amplifier that fed into the NIcDAQ9174 Chassis preamplifier analog input was the Amplaid MK 15, which was also included in the recording of ECochG signals, via the electrodiagnostic system (Amplaid MK 15, Milan, Italy).

2.2 Software

The electrophysiological data was recorded using custom-written intraoperative monitoring software called Te Pihareinga (O'Beirne, 2015). The software presents chained stimuli at multiple frequencies and intensities, which allows waveforms obtained using different stimuli to be reliably compared (as they are recorded concurrently, thereby limiting the influence of differences in recording conditions and noise levels). In the initial recordings (Participants 1 to 3), the averaged ECochG waveforms (n = 300 averages) were saved to tab-delimited text files for later processing. However, in later recording sessions (Participants 4

and 5) this processing was incorporated directly into the software and the ANOW waveforms were saved directly along with the averaged ECochG recordings.

As illustrated in Figure 19 below, the following steps of processing were applied:

1. DC offsets (calculated over the 5 ms prior to the stimulus onset) were first removed from both the condensation (CON) and rarefaction (RAR) waveforms.
2. The RAR waveform was subtracted from the CON waveform and divided by two to produce the difference (DIFF) waveform. The DIFF waveform accentuates the cochlear microphonic, and attenuates neural activity.
3. The CON and RAR were added together and divided by two to form the SUM waveform. The SUM waveform accentuates neural potentials and cancels the cochlear microphonic.
4. The SUM waveform was then smoothed to remove any residual compound action potential or summating potential. This SUMsmoothed waveform was produced by applying a bandpass filter (0.01 Hz to 525 Hz, 3rd order Butterworth), reversing the filtered waveform in the time domain, repeating the filtering, and then returning the waveform to its normal orientation in time. This double reversal process helped eliminate any phase shifts imposed by the filters.
5. The SUMsmoothed waveform was then subtracted from the SUM waveform to produce the ANOW waveform, which contains cycle-by-cycle neural activity.

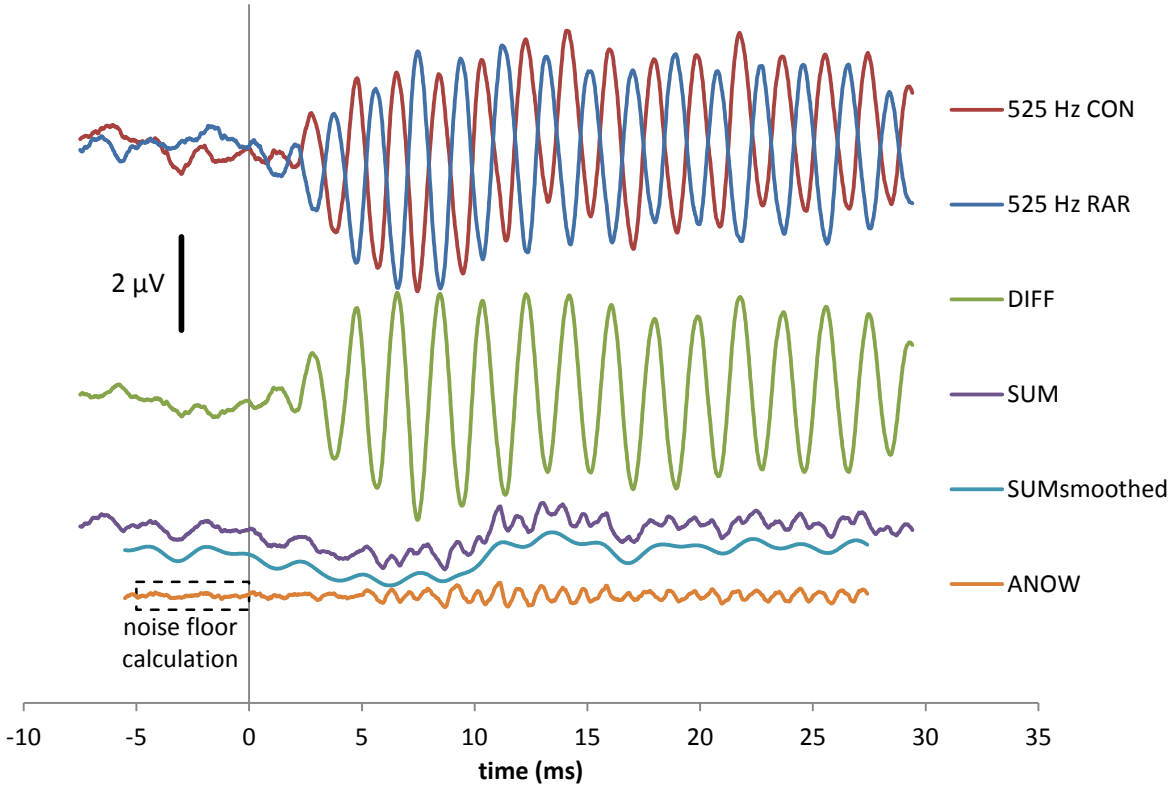

Figure 19: Data from Participant 3 (525 Hz, 94 dB peSPL) illustrating the processing applied to derive the ANOW waveform. The noise floors reported and plotted in this thesis refer to those of the ANOW trace, recorded in the 5 ms prior to stimulus onset.

As illustrated in Figure 20 below, a further averaging step was performed to improve the noise-floor of the recording. The region of the waveforms between 8 and 26 ms was divided into as many whole single cycles as would fit (i.e. 6 for 360 Hz, 9 for 525 Hz, and 13 for 725 Hz). Averaging these individual single cycles together further improved the noise floor by factors of 2.4 ($\sqrt{6}$), 3 ($\sqrt{9}$), and 3.6 ($\sqrt{13}$) respectively. The waveform RMS amplitude measures reported and plotted in this thesis therefore consist of a mean and standard deviation, the n of which is either 6, 9, or 13 depending on the frequency (360, 525, or 725 Hz).

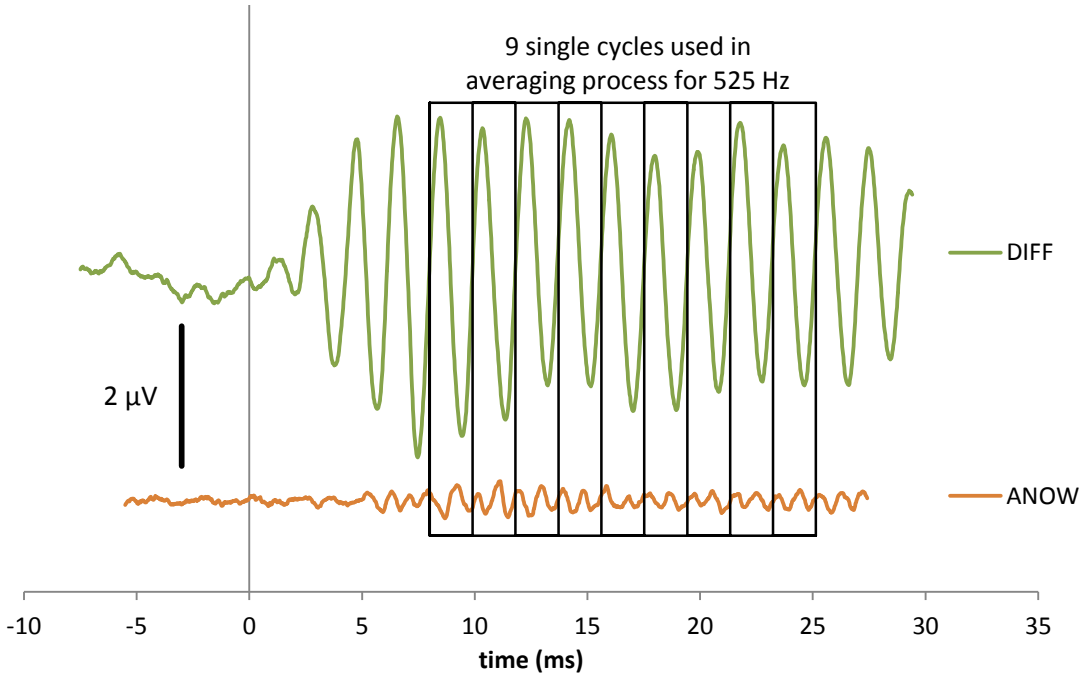

Figure 20: Illustration of the segmentation procedure for single-cycle analysis of the DIFF and ANOW waveforms. In this 525 Hz recording (94 dB peSPL) from Participant 3, averaged DIFF and ANOW waveforms (n = 302) were divided into 9 single cycles which were then averaged together (total n = 2718).

2.3 Calibration of Headphones

The output level and frequency response of the combination of the audio amplifier and headphone were measured using a Brüel & Kjær Type 4128 Head and Torso Simulator (HATS) connected to a Brüel & Kjær 7539 5/1-ch. Input/Output Controller Module. Sinusoidal voltage signals of 500 mV pp at varying frequencies were produced by the NI 9269 analog output module for this analysis, and enabled calibration of the output tone bursts in dB peSPL.

Comparison of tone-burst evoked potential thresholds to human audiometric thresholds would require measurement of peak-to-peak equivalent Reference Equivalent Threshold Sound Pressure Levels (peRETSPLs) from a large number of normal-hearing individuals using the 30 ms tone bursts played through the supra-aural headphones. Due to

the late stage at which this equipment was selected, such calibration was unable to be performed.

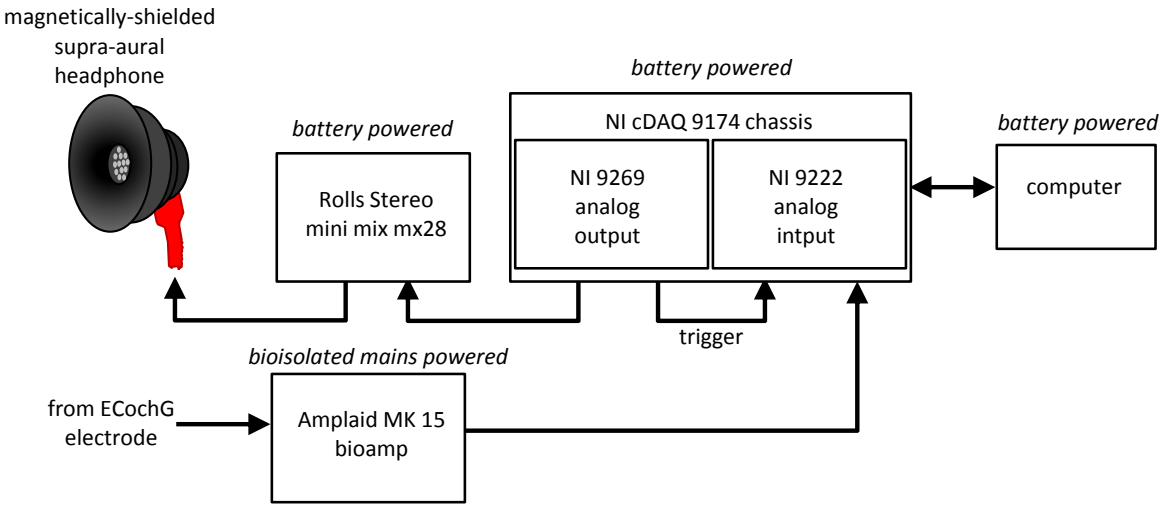

Figure 21: Block diagram of the experimental set-up used to elicit and record the ANOW waveform from human participants.

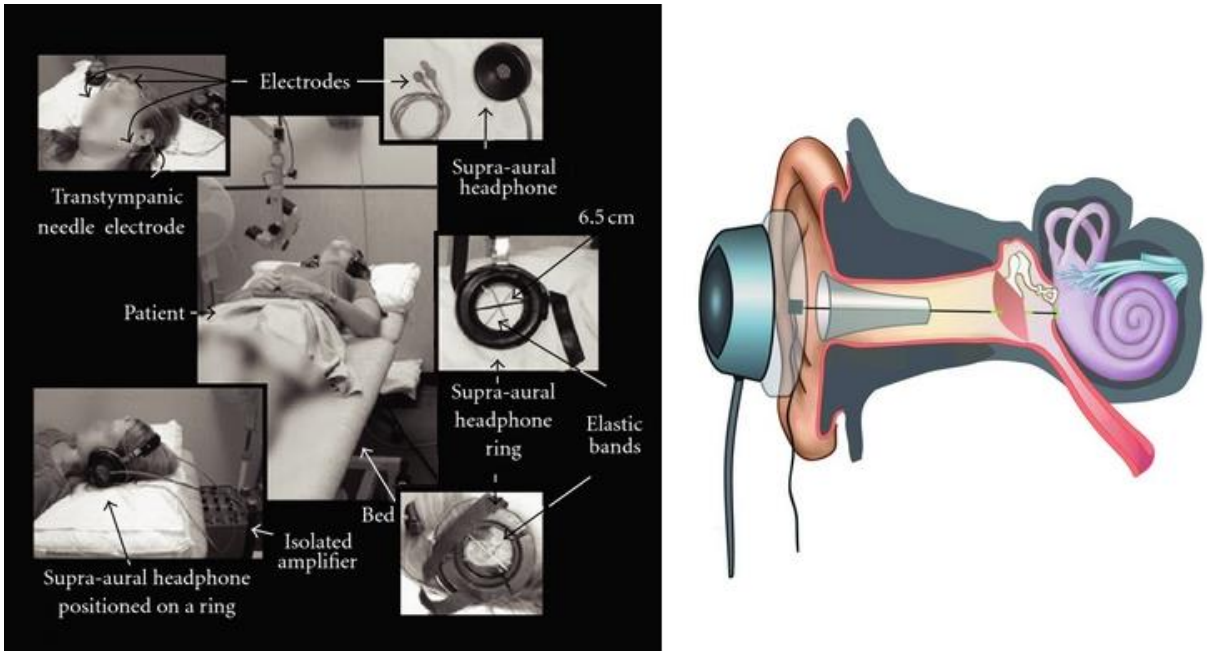

Figure 22: This figure adapted from Hornibrook et al. (2012) shows part of the experimental set-up and the placement of the transtympanic electrode. An analog output from the Amplaid MK15 biological amplifier was fed to the NI 9222 analog input unit shown in Figure 22.

The headphones were placed on the head and torso simulator (HATs), which allowed measurement of the continuous sine wave output for the input signal. The input was a 500mV peak to peak amplitude driven into the headphones via the amplifier. HATs provides a way of realistically reproducing the acoustic properties of the average adult human head and torso.

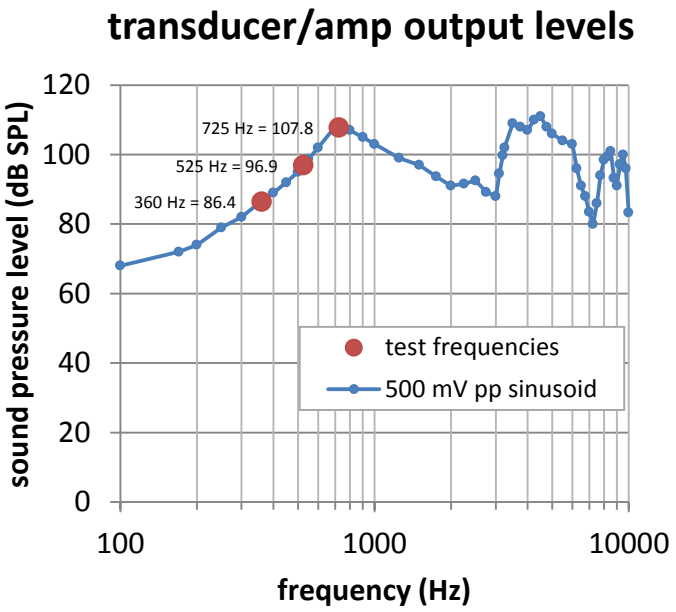

Figure 23: Frequency response of the combined Rolls audio amplifier and supra-aural headphone combination for a 500 mV pp sinusoid. Frequencies used in ANOW testing are shown by red circles.

The integration of the headphone calibration data into the testing protocols took place subsequent to the final data collection session. Therefore, one limitation of the study presented here is that the sound levels at which testing took place generally exceeded the 65 dB SPL level which *in the guinea pig* ensures that the ANOW waveforms recorded are purely neural in origin (Lichtenhan et al., 2014). The corresponding level in human participants is still unknown.

In addition, the calibration process revealed that amplifier settings used for Participants One and Two were such that acoustic stimuli were significantly distorted at the

intensities tested, rendering the meaningful interpretation of their data impossible. For this reason, the DIFF and ANOW data from these two participants has been omitted from this thesis.

Chapter Three: Investigations into the Auditory Nerve Overlapped Waveform

3.1 Transtympanic Electrocochleography in Suspected Ménière's Patients

3.1.1 Participants

Participants were recruited through Mr. Jeremy Hornibrook (Otolaryngologist). All the participants were taking part in a routine transtympanic ECochG as part of the diagnosis for suspected Ménière's disease. There were no exclusion criteria for this study.

3.1.2 Ethical Considerations

Ethical approval from the Southern Health and Disability Ethics Committee was granted on 18th July 2014 (Ethics Ref: 14/STH/92). Written informed consent was obtained from each participant prior to testing (Appendix), and participant confidentiality was strictly maintained in accordance with the conditions outlined in the ethics application.

3.1.3 General Outline of Procedure

3.1.3.1 Pre-Electrocochleography Hearing Test

Testing occurred in sound treated rooms, at Christchurch Public Hospital. All testing was conducted by either Ms Ashleigh Allsop, a Master of Audiology Student; or an MNZAS audiologist employed by the Canterbury District Health Board prior to non-invasive electrocochleography. Testing consisted of:

1. Otoscopy and full pure tone air- and bone- conduction audiometry bilaterally, including the standard audiometric frequencies. Air conduction frequencies tested included 0.25 to 8 kHz in half octave steps. Bone conduction was measured at 0.5 to 4 kHz in one octave steps. Thresholds were measured using the Modified Hughson-Westlake procedure, in 5dB steps. A Grayson-Stadler GSI 61 clinical audiometer was used to present the stimuli to the participants. ER-3A insert earphones were used to present the standard audiometric frequencies (unless contraindicated), and Radioear

B-71 bone conduction vibrator was used to present bone conducted pure tone audiometry. When interaural attenuation between the air conduction of the test ear and non-test ear was exceeded, or bone conduction exceeded air conduction by 15dB HL, then narrow band masking noise was applied to the non test ear to mask.

2. Tympanometry was also conducted using Grayson-Stadler GSI Tympstar tympanometer, using 226Hz probe tone at 200daPa/s sweep rate. Tympanometry was classified using the Jerger classification system.

3.1.3.2 Transtympanic Electrocochleography

All testing occurred in the Electrocochleography room of the Audiology department at Christchurch Public Hospital. Participants were firstly instructed on the procedure for transtympanic electrocochleography by Mr Jeremy Hornibrook. They were instructed to "relax, close eyes, and maintain head position" whilst in the supine position. The participants' external auditory meatus and tympanic membrane were observed through otoscopy, and any debris carefully removed prior to electrode placement. The skin of the participant was prepared using abrasive techniques to the cheek, high forehead, and both mastoids. Electrodes were then placed on the cheek or forehead (ground and indifferent electrodes) and on the contralateral mastoid (non-inverting electrode). The skin electrodes used were Ambu® Blue Sensor N Ag/AgCl ECG electrodes. The transtympanic electrode acted as the active, inverting electrode for the ECochG recordings.

Phenol, an analgesic was placed within the participant's ear canal onto the tympanic membrane, to reduce the discomfort of the procedure. The electrodes used were TECA™ Disposable Monopolar Needles (CareFusion, WI, USA) which were 37 mm long and 28 gauge diameter. The electrodes were placed by Mr. Jeremy Hornibrook, an Otolaryngological surgeon. The electrode was placed to rest on or near the promontory of the cochlea. The

electrode was then held in place by the custom made headphone holder, and the magnetically shielded supra-aural headphones placed over this (see figure 22).

The software and equipment set up used in this study is described in detail in *Chapter 2.* The software used in this study is custom designed to record evoked potentials, and was used to generate the stimuli and record the responses of ECochG. The software is run through a laptop, which is connected to an electrically isolated preamplifier, which was connected to the electrodes on the patient. The recordings were obtained by Ms Ashleigh Allsop and Assoc Prof Gregory O'Beirne. The stimuli used was primarily frequency specific tone bursts presented through the supra-aural earphones. The traces recorded for this study were collected after the otolaryngologist and charge audiologist had finished conducting their own electrocochleography. The equipment amplifier used by the otolaryngologist was able to be unplugged from the electrodes connected to the patient, which was then connected to the equipment used for this study.

The software recorded the raw ECochG traces, and saved them to the laptop for later analysis. A number of recordings were made, including the response threshold, the latency and amplitude of the ECochG compound action potential and low frequency neural responses in the form of the auditory nerve overlapped waveform (ANOW).

3.2 Individual Cases

All participant data was analysed using Equipment described in *Chapter 2.*

3.2.1 Case One

Participant One was a 70 year old male who presented with a fluctuating hearing loss in his left ear, with a persistent tinnitus. He did not have any vertigo or aural fullness. He presented with Type A tympanograms in bilaterally indicating normal middle ear functioning. Audiometry revealed essentially normal hearing in the right ear, and a fluctuating loss in the

left ear ranging from slight to moderate sensorineural loss on separate testing occasions. His audiogram from the day of testing is presented in figure 24. ECochG testing using click stimuli showed no significant increase in the SP/AP ratio in either ear. ECochG testing using tone bursts stimuli showed no significant increase in the SP amplitude at any frequency as per Gibson's norms. The overall pattern of results is consistent with no hydrops in either ear. The ECochG results are presented in table 3, indicating that Ménière's disease is not likely the cause of Participant One's symptoms.

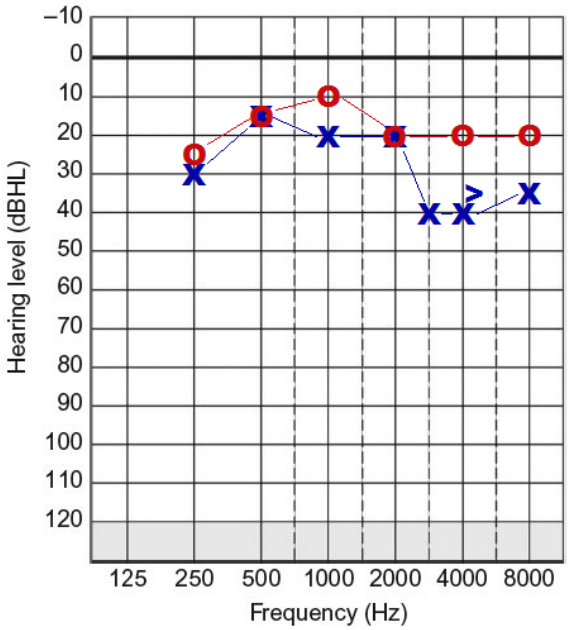

Figure 24: Participant One's audiological results; right ear showing essentially normal hearing, the left ear indicating a normal to mild sensorineural hearing loss

Table 3: Participant One's ECochG Results

			500 Hz	1000 Hz	2000 Hz	4000 Hz
Tone Bursts	Right	SP Amp (µV)	0.22	4.92	1.52	2.56
		Gibson Sig. Level (µV)	2.0	6.0	9.0	9.0
		AP Amp (µV)	3.56	5.76	5.36	8.76
		SP/AP ratio (%)	6.2%	85.4%	28.4%	29.2%
	Left	SP Amp (µV)	2.0	5.16	5.80	2.60
		Gibson Sig. Level (µV)	2.0	6.0	9.0	5.0
		AP Amp (µV)	4.32	7.84	9.08	6.84
		SP/AP ratio (%)	46.3%	65.8%	63.9%	38%
Clicks	Right	SP Amp (µV)	5.00			

		AP Amp (µV)	29.50
		SP/AP ratio (%)	16.9%
	Left	SP Amp (µV)	3.0
		AP Amp (µV)	17.80
		SP/AP ratio (%)	16.9%

Participant One's data was analysed and graphed using the same methods as the other participants. Unfortunately, the responses recorded from Participant One were derived from distorted acoustic signals containing frequency components in addition to those specified, which did not permit analysis of DIFF and ANOW responses.

3.2.2 Case Two

Participant Two was a 37 year old female. She was referred to the otolaryngology department in mid- 2015 with a sudden low frequency hearing loss in her left ear. She also experienced a loud tinnitus associated with the loss, and a sore throat and headache prior to the loss. She did not have any vertigo or aural fullness. She also did not have any prior noise exposure, ototoxic medications, or any other ear related medical history. Balance and vestibular ocular tests were normal, and her MRI was unremarkable. She presented with a Type A tympanogram in her right ear indicating normal middle ear functioning, and were unable to obtain a seal on her left ear. She has not presented with any middle ear pathologies in the past. Audiometry revealed normal hearing in her right ear, with a moderately severe rising to normal sensorineural hearing loss in her left ear. This data is presented in figure 25. ECochG testing using click stimuli showed no significant increase in the SP/AP ratio in either ear. ECochG testing using tone bursts stimuli showed no significant increase in the SP

amplitude at any frequency as per Gibson's norms. The overall pattern of results is consistent with no hydrops in either ear. The ECochG results are presented in table 4.

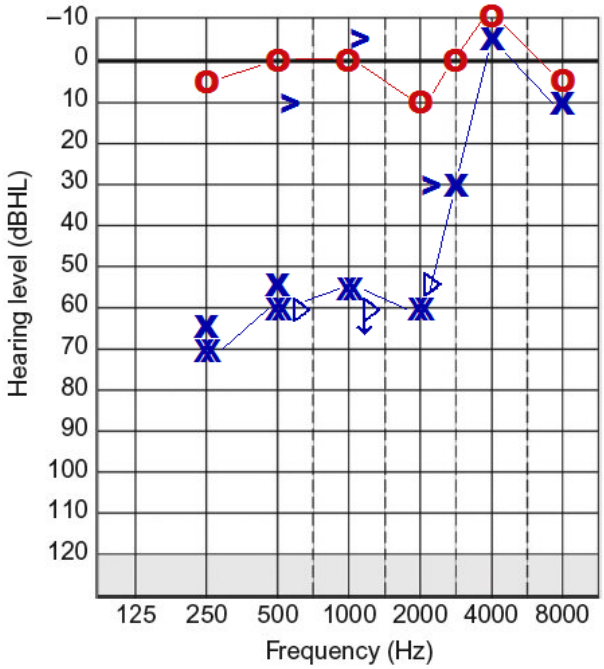

Figure 25: Participant Two's audiological results; right ear normal hearing, the left ear indicating a moderately severe sensorineural hearing loss in the low to mid frequencies rising to normal in the high frequencies

Table 4: Participant Two's ECochG Results

			500 Hz	1000 Hz	2000 Hz	4000 Hz
Tone Bursts	Right	SP Amp (µV)	-	1.28	3.72	5.04
		Gibson Sig. Level (µV)	2.0	6.0	9.0	9.0
		AP Amp (µV)	-	5.36	11.32	12.40
		SP/AP ratio (%)	-	23.9%	32.9%	40.6%
	Left	SP Amp (µV)	-	-	1.68	4.0
		Gibson Sig. Level (µV)	1.0	6.0	5.0	9.0
		AP Amp (µV)	-	-	4.56	10.0
		SP/AP ratio (%)	-	-	36.8%	40%
Clicks	Right	SP Amp (µV)	9.72			
		AP Amp (µV)	34.76			
		SP/AP ratio (%)	28%			
	Left	SP Amp (µV)	8.10			
		AP Amp (µV)	37.30			
		SP/AP ratio (%)	21.7%			

Participant Two's data was analysed and graphed using the same methods as the other participants. Unfortunately, as with Participant One, the responses recorded from Participant Two were derived from distorted acoustic signals containing frequency

components in addition to those specified, which did not permit analysis of DIFF and ANOW responses.

3.2.3 Case Three

Participant Three was a 46 year old female. In mid- 2015 she experienced a vertigo attack, with a feeling of nausea and aural fullness in her right ear, which persisted for three days. She then developed tinnitus in her right ear following this episode. There was a significant decrease in her low frequency hearing of her right ear following the attack also. Balance and vestibular ocular tests were normal. She had no other prior relevant medical history. She presented with Type A tympanograms bilaterally, indicating normal middle ear functioning. Audiometry revealed normal hearing sloping to a mild high frequency sensorineural hearing loss in her left ear, and essentially normal sloping to severe high frequency sensorineural hearing loss in her right ear. Her pure tone audiometry from the day of testing is presented in figure 26. ECochG testing using click stimuli showed no significant

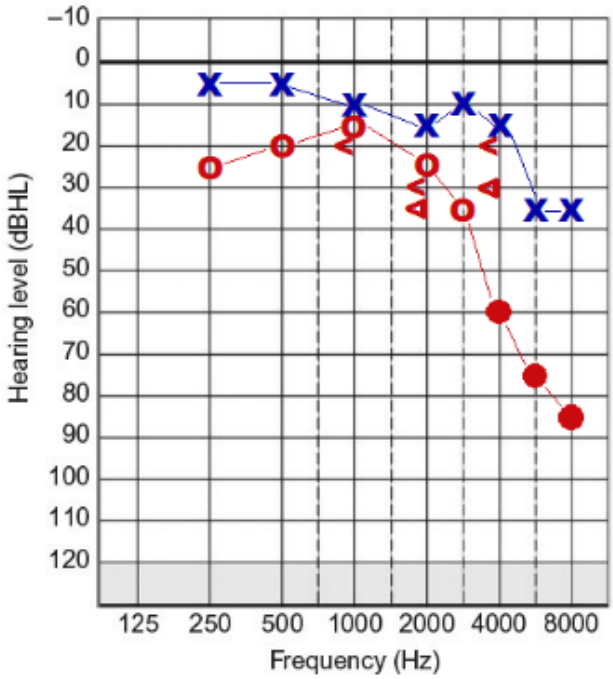

Figure 26: Participant Three's audiological results. The right ear showing essentially normal hearing sloping to a severe high frequency sensorineural hearing loss; the left ear indicating normal hearing through the low to mid frequencies, sloping to a mild sensorineural hearing loss in the high frequencies.

increase in the SP/AP ratio in either ear. ECochG testing using tone bursts stimuli showed a significant increase in the SP amplitude at 1000 Hz and 2000 Hz in the right ear only, as per Gibson's norms. The overall pattern of results is consistent with hydrops in the right ear only. The ECochG results are presented in table 5.

Table 5: Participant Three's ECochG Results

			500 Hz	1000 Hz	2000 Hz	4000 Hz
Tone Bursts	Right	SP Amp (µV)	2.48	17.74	12.84	2.4
		Gibson Sig. Level (µV)	2.0	6.0	7.0	5.0
		AP Amp (µV)	5.60	16.62	15.94	4.0
		SP/AP ratio (%)	44.2%	6%	80.5%	60%
	Left	SP Amp (µV)	0.68	2.20	2.36	1.72
		Gibson Sig. Level (µV)	2.0	6.0	9.0	9.0
		AP Amp (µV)	5.12	6.32	8.52	9.12
		SP/AP ratio (%)	13.2%	34.8%	27.7%	18.9%
Clicks	Right	SP Amp (µV)	9.22			
		AP Amp (µV)	26.66			
		SP/AP ratio (%)	34.6%			
	Left	SP Amp (µV)	13.50			
		AP Amp (µV)	57.60			
		SP/AP ratio (%)	23.4%			

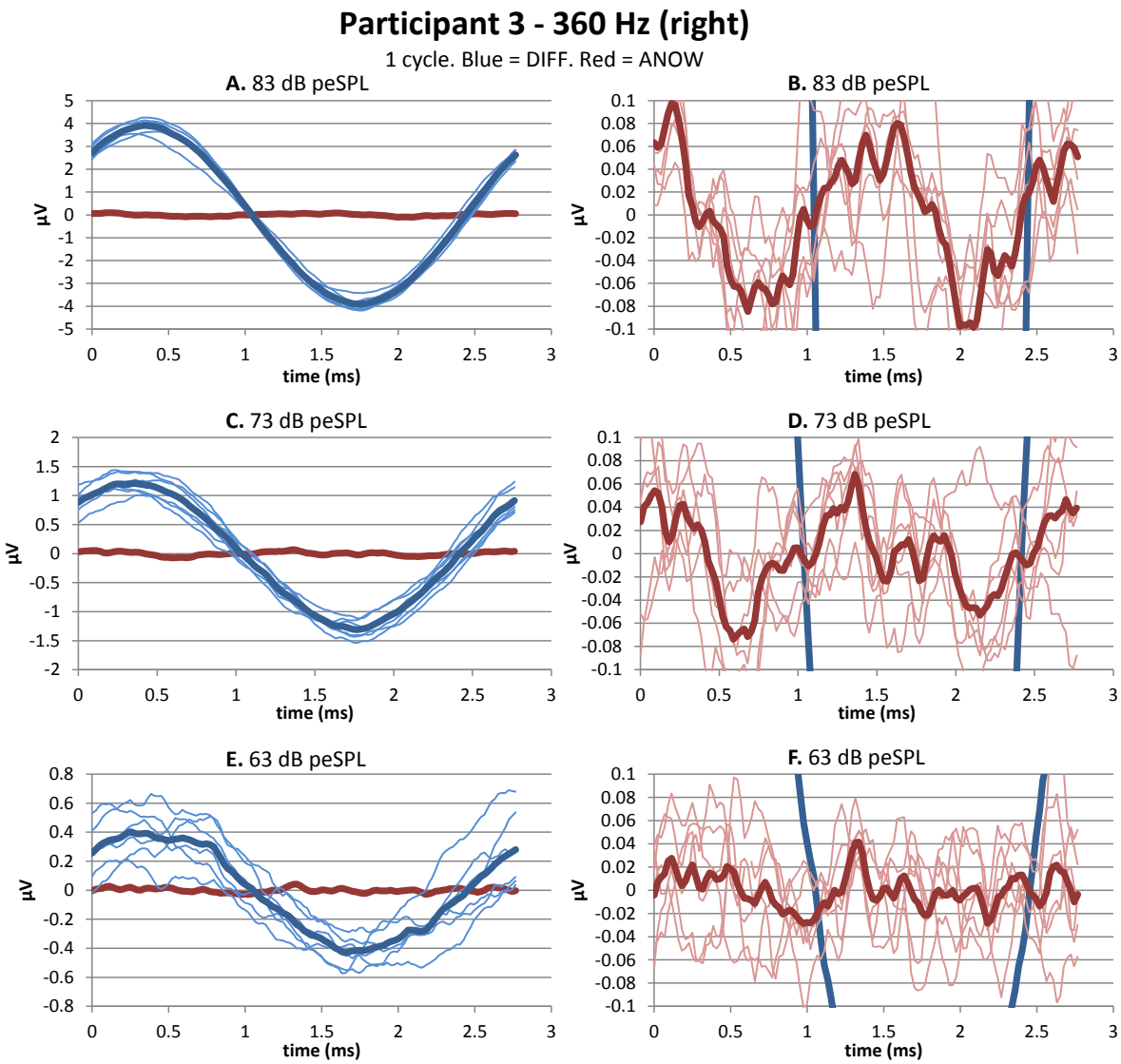

Figure 27: Participant 3's 360 Hz overlaid single-cycle DIFF (blue) and ANOW (red) waveforms elicited in the right ear at 83, 73, 63 dB peSPL. Plots B, D, and F, represent zoomed-in versions of the waveforms in A, C, and E respectively. The bold traces represent the mean overlaid waveform (n=1818) derived from 302 stimulus presentations. The light traces are the mean of 302 presentations.

Table 6: Mean (± standard deviation) RMS amplitudes for Participant 3's 360 Hz right-ear ANOW and DIFF waveforms at three intensity levels.

level (dB peSPL)	83	73	63
Mean ANOW amplitude (nV RMS)	69	53	40
StdDev ANOW amplitude (nV RMS)	± 9	± 11	± 4
Mean DIFF amplitude (nV RMS)	2743	887	323
StdDev DIFF amplitude (nV RMS)	± 194	± 118	± 71
n (sub-averages)	6	6	6

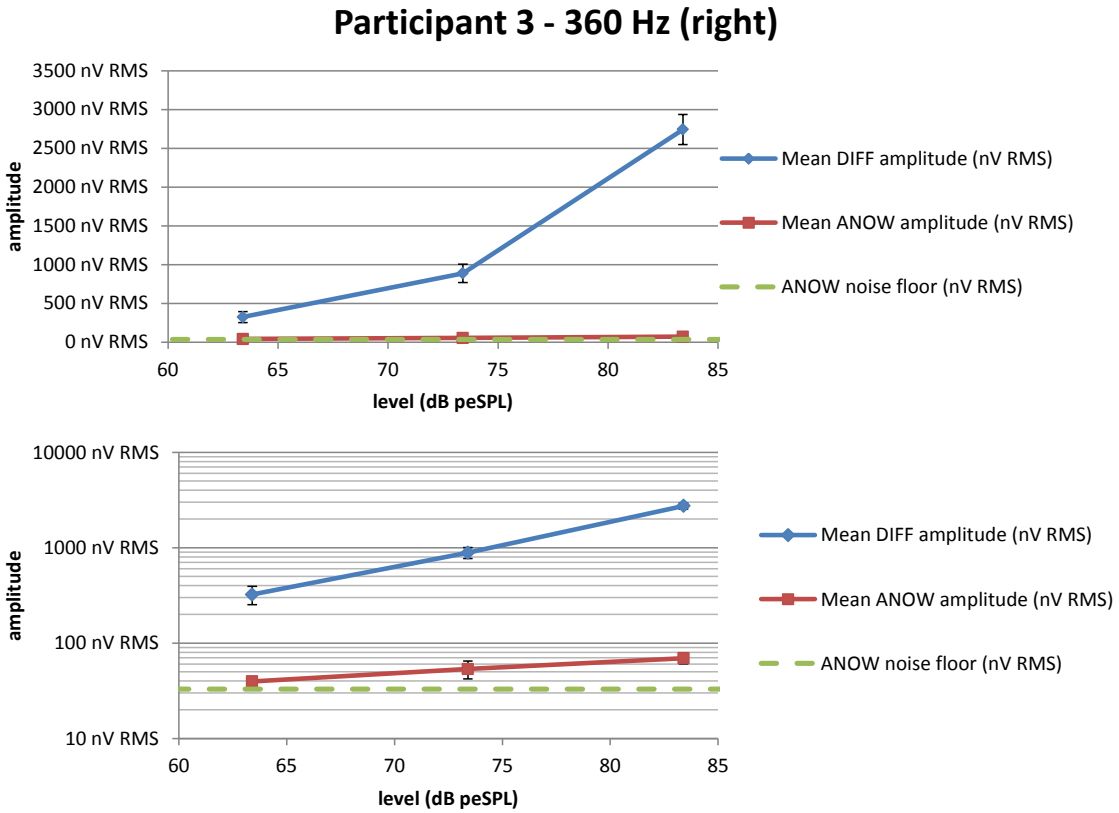

Figure 28: Input/output functions for Participant 3's 360 Hz right-ear DIFF (blue) and ANOW (red) waveforms respectively, shown on a linear amplitude scale (top) and a logarithmic one (bottom). The figure shows the ANOW waveform emerging above the 33 nV noise floor between 63 and 73 dB peSPL

The overall data from participant Three indicated the ANOW was present for 360 Hz in her right ear. Presence of the CM can be seen in all recorded cases in the DIFF waveform, seen in figure 27. At 360 Hz, the presence of the CM occurs from around 300 nV RMS, with increasing amplitude from 63 dB peSPL. At 360 Hz, the ANOW can be distinguished from the noise floor between at 73 dB peSPL (but not 63 dB peSPL) with an amplitude of 53 nV RMS, as seen in figure 28.

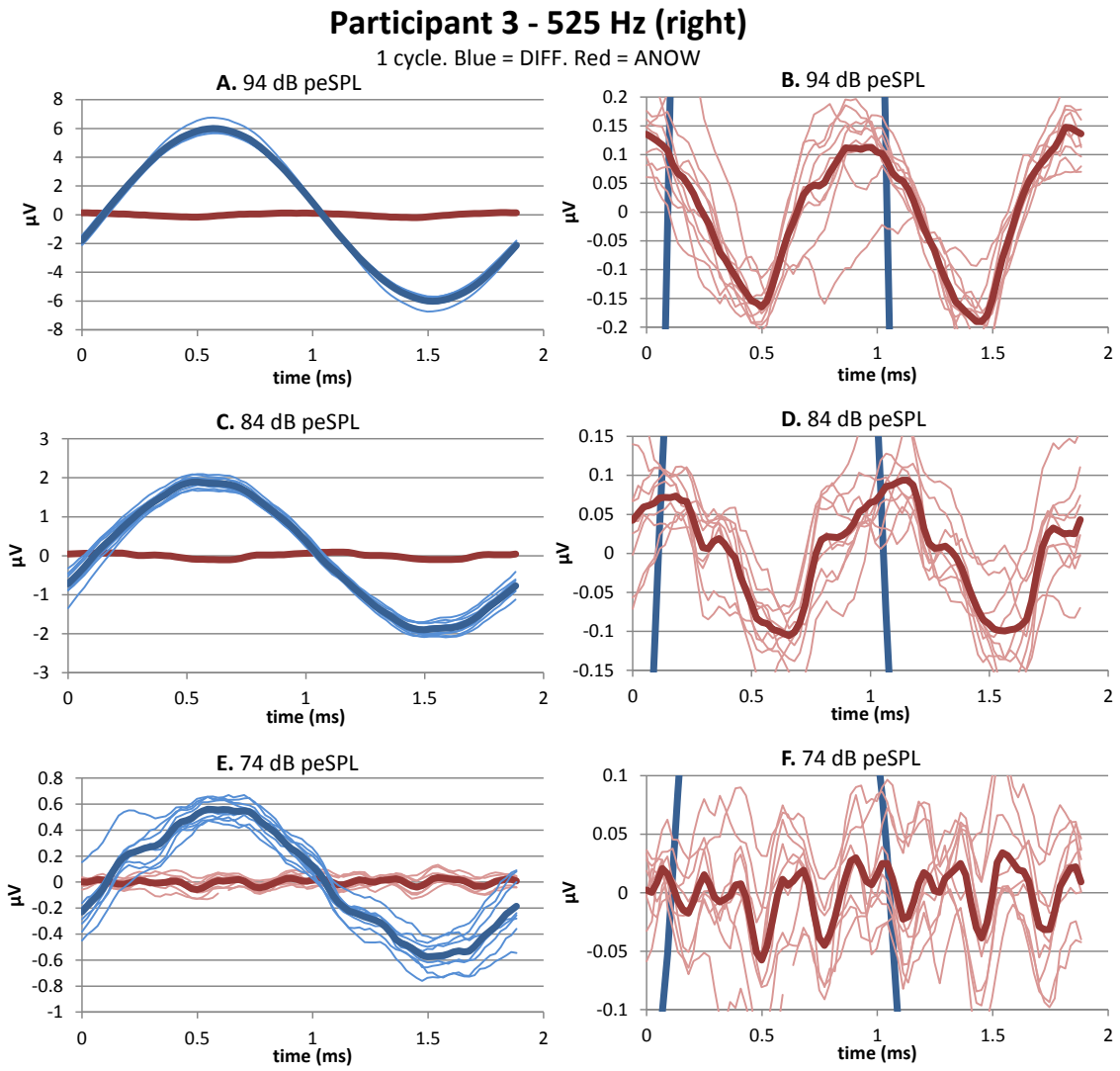

Figure 29: Participant 3's 525 Hz overlaid single-cycle DIFF (blue) and ANOW (red) waveforms elicited in the right ear at 94, 84, and 74 dB peSPL. Plots B, D, and F, represent zoomed-in versions of the waveforms in A, C, and E respectively. The bold traces represent the mean overlaid waveform (n=2718) derived from 302 stimulus presentations. The light traces are the mean of 302 presentations.

Table 7: Mean (± standard deviation) RMS amplitudes for Participant 3's 525 Hz right-ear ANOW and DIFF waveforms at three intensity levels.

level (dB peSPL)	94	84	74
Mean ANOW amplitude (nV RMS)	117	77	45
StdDev ANOW amplitude (nV RMS)	± 15	± 13	± 11
Mean DIFF amplitude (nV RMS)	4204	1338	397
StdDev DIFF amplitude (nV RMS)	± 218	± 107	± 80
n (sub-averages)	9	9	9

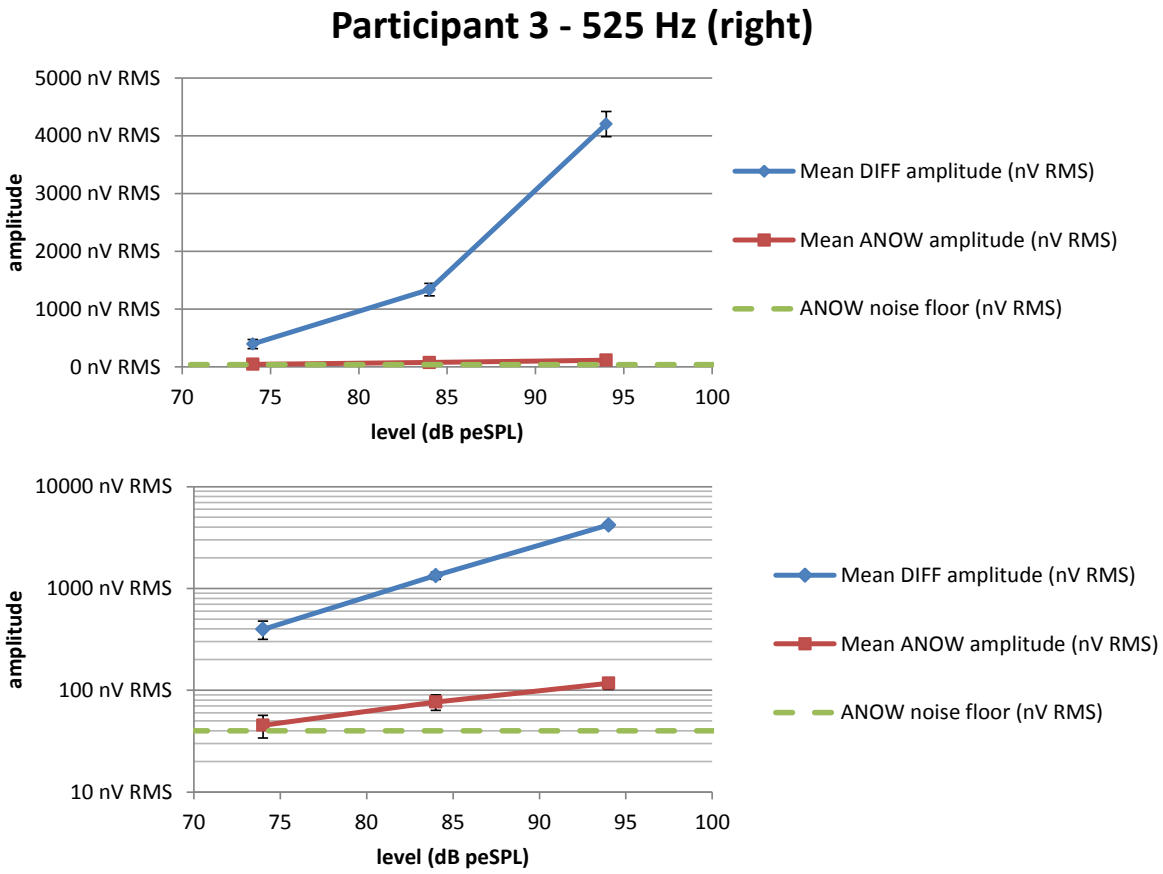

Figure 30: Input/output functions for Participant 3's 525 Hz right-ear DIFF (blue) and ANOW (red) waveforms respectively, shown on a linear amplitude scale (top) and a logarithmic one (bottom). The figure shows the ANOW waveform emerging above the 40 nV noise floor between 74 and 84 dB peSPL.

The data from participant Three indicated the ANOW was present for 525 Hz in her right ear. Presence of the CM can be seen in all recorded cases in the DIFF waveform, seen in figure 29. At 525 Hz, the presence of the CM occurs from around 397 nV RMS, with increasing amplitude from 74 dB peSPL. At 525 Hz, the presence of the ANOW can be distinguished from the noise floor at 84 dB peSPL (but not 74 dB peSPL), first appearing with an amplitude of around77 nV RMS, as seen in figure 30.

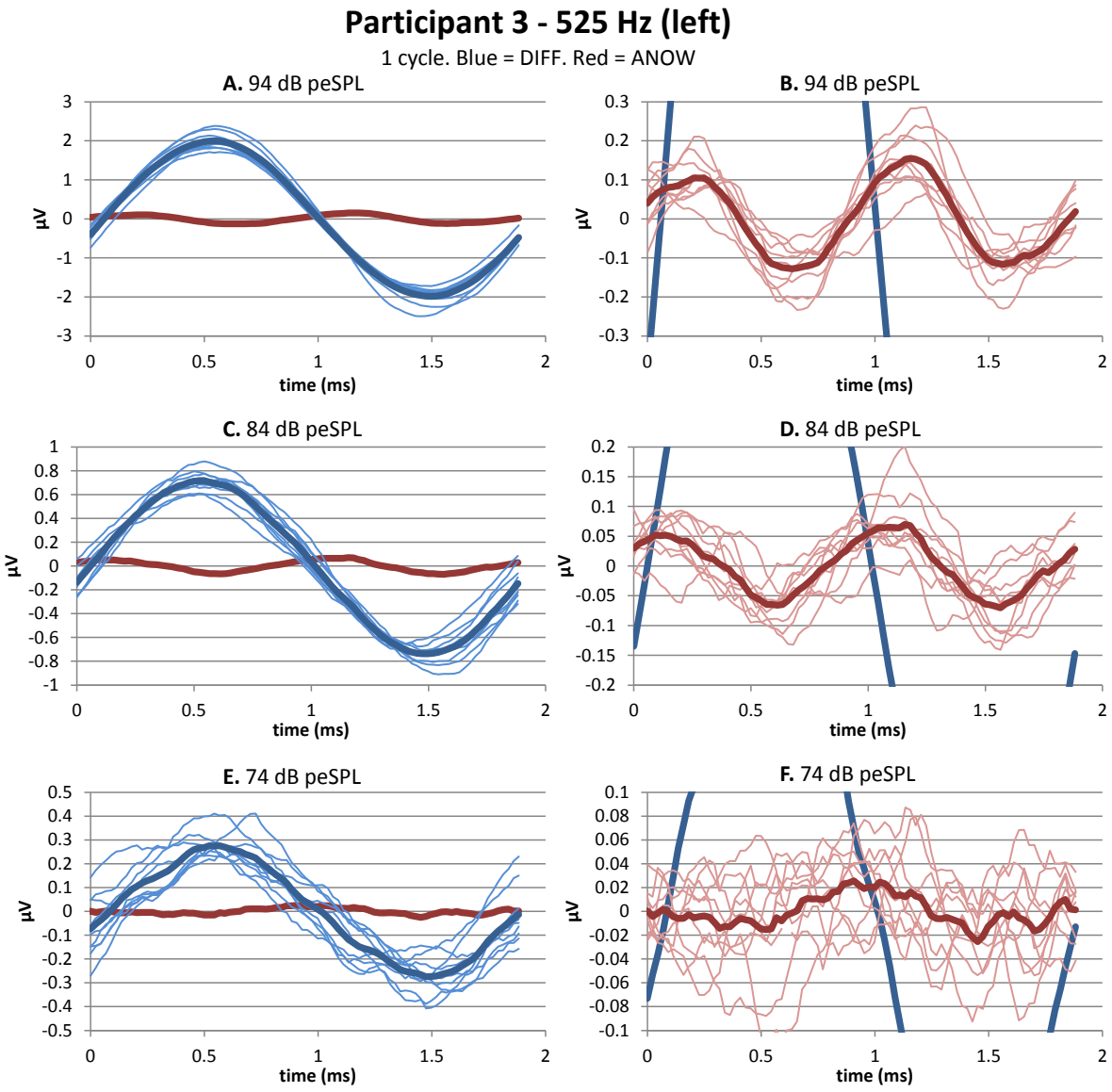

Figure 31: Participant 3's 525 Hz overlaid single-cycle DIFF (blue) and ANOW (red) waveforms elicited in the left ear at 74, 84, and 94 dB peSPL. Plots B, D, and F, represent zoomed-in versions of the waveforms in A, C, and E respectively. The bold traces represent the mean overlaid waveform (n=2733) derived from 302 stimulus presentations. The light traces are the mean of 302 presentations.

Table 8: Mean (± standard deviation) RMS amplitudes for Participant 3's 525 Hz left-ear ANOW and DIFF waveforms at three intensity levels.

level (dB peSPL)	94	84	74
Mean ANOW amplitude (nV RMS)	102	58	35
StdDev ANOW amplitude (nV RMS)	± 28	± 14	± 9
Mean DIFF amplitude (nV RMS)	1398	507	197
StdDev DIFF amplitude (nV RMS)	± 159	± 62	± 41
n (sub-averages)	9	9	9

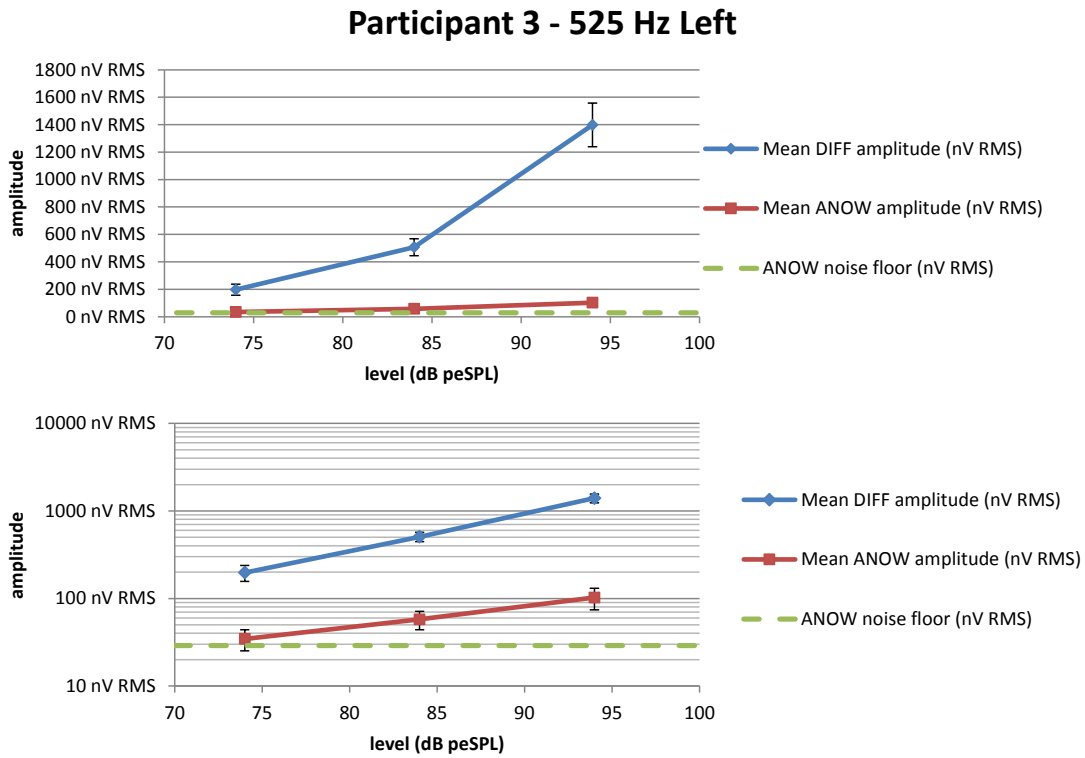

Figure 32: Input/output functions for Participant 3's 525 Hz left-ear DIFF (blue) and ANOW (red) waveforms respectively, shown on a linear amplitude scale (top) and a logarithmic one (bottom). The figure shows the ANOW waveform emerging above the 29 nV noise floor between 74 and 84 dB peSPL.

The data from participant Three indicated the ANOW was present for 525 Hz in her left ear. Presence of the CM can be seen in the DIFF waveform, seen in figure 31. At 525 Hz, the presence of the CM occurs significantly above the noise floor from around 200 nV RMS, with increasing amplitude from 74 dB peSPL. In this case, the SPL was not reduced enough to record the CM reduced to the level of the noise floor. At 525 Hz in the left ear, the presence of the ANOW can be faintly distinguished from the noise floor at the lowest level tested – 74 dB peSPL – with an amplitude of around 35 nV RMS, as seen in figure 32.

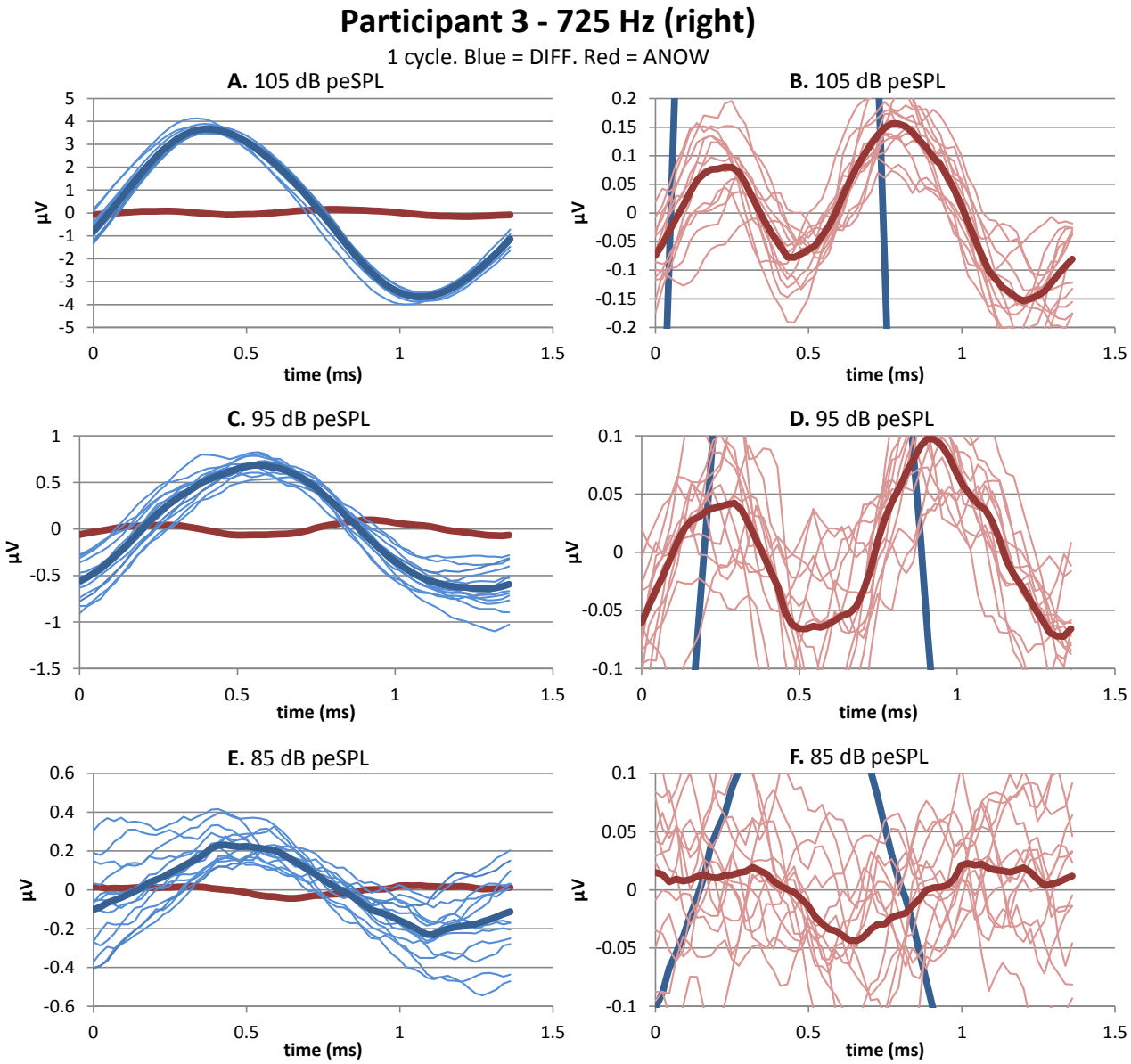

Figure 33: Participant 3's 725 Hz overlaid single-cycle DIFF (blue) and ANOW (red) waveforms elicited in the right ear at 105, 95, and 85 dB peSPL. Plots B, D, and F, represent zoomed-in versions of the waveforms in A, C, and E respectively. The bold traces represent the mean overlaid waveform (n=3948 approx.) derived from around 300 stimulus presentations. The light traces are the mean of around 300 presentations.

Table 9: Mean (± standard deviation) RMS amplitudes for Participant 3's 725 Hz right-ear ANOW and DIFF waveforms at three intensity levels.

level (dB peSPL)	105	95	85
Mean ANOW amplitude (nV RMS)	106	66	52
StdDev ANOW amplitude (nV RMS)	± 12	± 15	± 18
Mean DIFF amplitude (nV RMS)	2563	499	224

StdDev DIFF amplitude (nV RMS)	± 118	± 63	± 62
n (sub-averages)	13	13	13

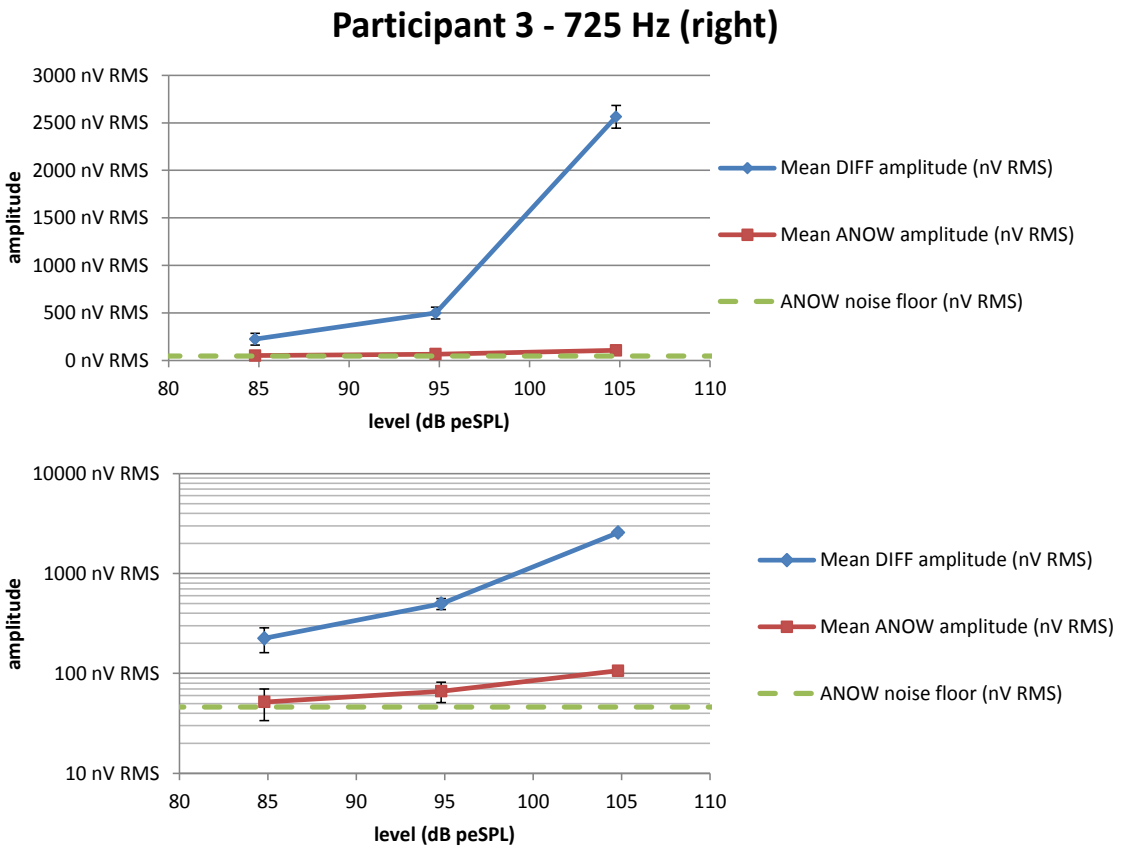

Figure 34: Input/output functions for Participant 3's 725 Hz right-ear DIFF (blue) and ANOW (red) waveforms respectively, shown on a linear amplitude scale (top) and a logarithmic one (bottom). The figure shows the ANOW waveform emerging above the 46 nV noise floor at 85 peSPL.

The data from participant Three indicated the ANOW was present for 725 Hz in her right ear. Presence of the CM can be seen in all recorded cases in the DIFF waveform, seen in figure 33. At 725 Hz, the presence of the CM occurs from around 224 nV RMS, with increasing amplitude from 85 dB peSPL. At 725 Hz, the presence of the ANOW can be distinguished from the noise floor at the lowest level tested – 85 dB peSPL – with the amplitude of around 52 nV RMS, as seen in figure 34.

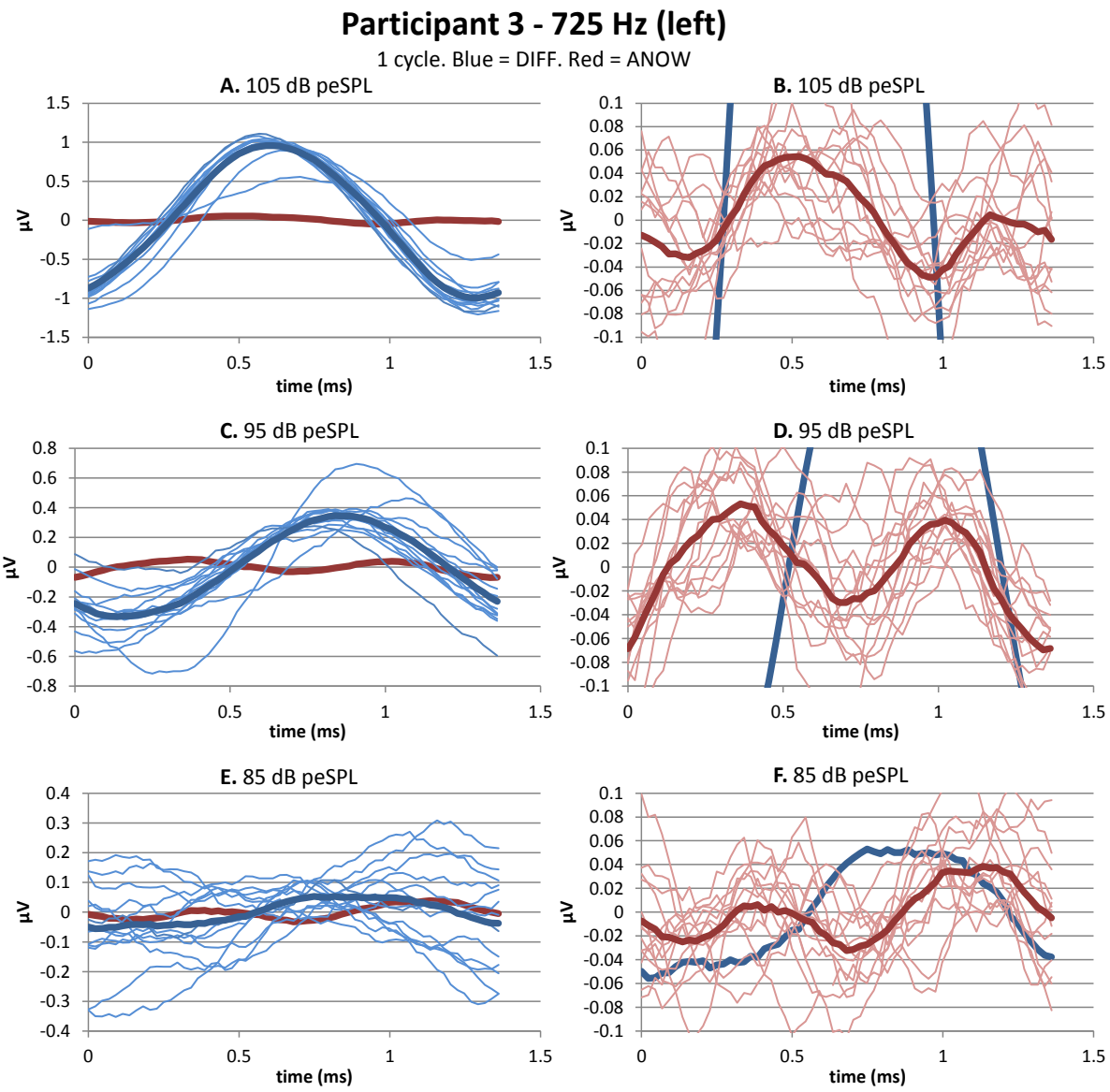

Figure 35: Participant 3's 725 Hz overlaid single-cycle DIFF (blue) and ANOW (red) waveforms elicited in the left ear at 105, 95, and 85 dB peSPL. Plots B, D, and F, represent zoomed-in versions of the waveforms in A, C, and E respectively. The bold traces represent the mean overlaid waveform (n=3948 approx.) derived from around 300 stimulus presentations. The light traces are the mean of around 301 presentations.

Table 10: Mean (± standard deviation) RMS amplitudes for Participant 3's 725 Hz left-ear ANOW and DIFF waveforms at three intensity levels.

level (dB peSPL)	105	95	85
Mean ANOW amplitude (nV RMS)	50	50	39
StdDev ANOW amplitude (nV RMS)	± 18	± 9	± 13
Mean DIFF amplitude (nV RMS)	694	270	117
StdDev DIFF amplitude (nV RMS)	± 76	± 80	± 54
n (sub-averages)	13	13	13

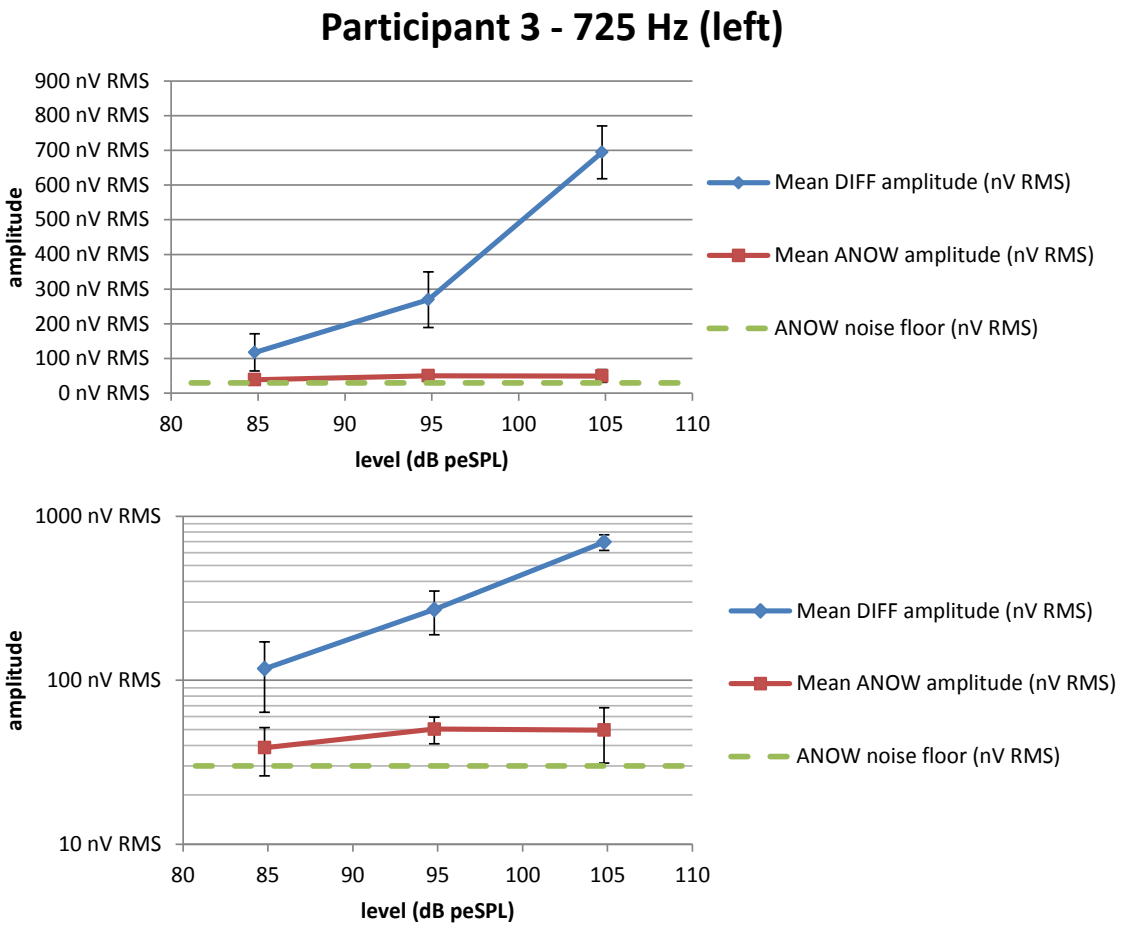

Figure 36: Input/output functions for Participant 3's 725 Hz left-ear DIFF (blue) and ANOW (red) waveforms respectively, shown on a linear amplitude scale (top) and a logarithmic one (bottom). The figure shows the ANOW waveform emerging above the 30 nV noise floor from 85 dB peSPL.

The data from participant Three indicated the ANOW was present her left ear at 725 Hz. Presence of the CM can be seen in all recorded cases in the DIFF waveform, seen in figure 37. At 725 Hz, the presence of the CM occurs from around 117 nV RMS, with increasing amplitude from 85 dB peSPL. At 725 Hz, the presence of the ANOW can be distinguished from the noise floor at the lowest level tested – 85 dB peSPL – with an amplitude of 39 nV RMS, as seen in figure 36.

3.2.4 Case Four

Participant Four was a 54 year old female. She presented to the otolaryngologist in late 2015 with a vertigo attack with right beating nystagmus. She has had a history of vertigo attacks, as well as headaches, and a history of migraine attacks. In 2003 she had a left blind sac closure, which closed off her left ear canal. An MRI scan revealed nothing specific for causing her vertigo attacks in either ear. It was suspected that one or both of her ears may have been causing Meniere's symptoms, resulting in the ECochG testing of her right ear. The left ear was unable to be tested in this manner. Tympanometry from her right ear revealed a Type Ad tympanogram, suggesting hypermobile middle ear functioning. The Left ear was unable to be tested due to the blind sac closure. Audiometry reveal a slight to mild sloping to a moderately severe sensorineural hearing loss in the high frequencies in her right ear. The left ear had no recordable hearing via pure tone air conduction testing at the limits of the audiometer. Bone conduction in the left ear was presented to the maximum before vibrotactile response was reported. Audiometry results are presented in figure 37. ECochG testing using click stimuli showed no significant increase in the SP/AP ratio in either ear. ECochG testing using tone bursts stimuli showed no significant increase in the SP amplitude at any frequency as per Gibson's norms. The overall pattern of results is consistent with no hydrops in her right ear. She was referred for MRI inner ear imaging with intravenous gadolinium testing to determine the state of the left ear. The ECochG results for her right ear are presented in table 11.

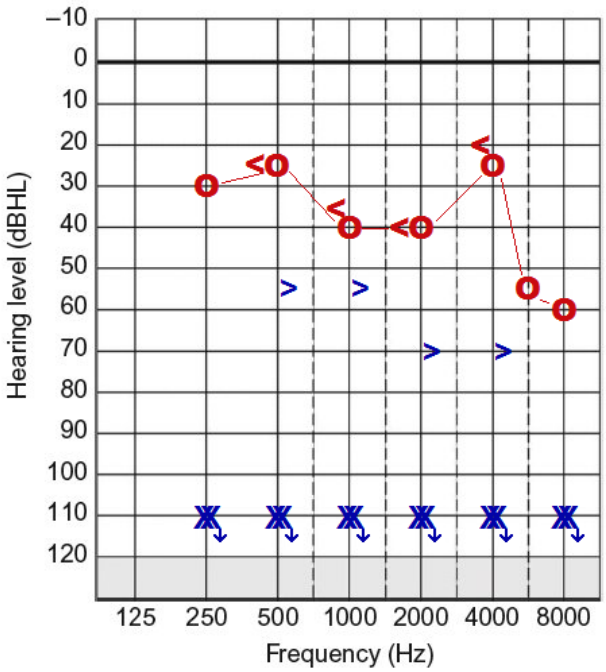

Figure 37: Participant Four's audiological results. The right ear showing a slight to mild sensorineural hearing loss sloping to moderately severe in the high frequencies. The left ear tested with no recordable hearing at the limitations of the audiometer.

Table 11: Participant Four's ECochG Results

			500 Hz	1000 Hz	2000 Hz	4000 Hz
Tone Bursts	Right	SP Amp (µV)	-	4.98	2.12	0.82
		Gibson Sig. Level (µV)	2.0	6.0	5.0	5.0
		AP Amp (µV)	4.44	7.36	10.64	11.52
		SP/AP ratio (%)	-	67.7%	19.9%	7.1%
	Left	SP Amp (µV)	-	-	-	-
		Gibson Sig. Level (µV)	-	-	-	-
		AP Amp (µV)	-	-	-	-
		SP/AP ratio (%)	-	-	-	-
Clicks	Right	SP Amp (µV)	10.0			
		AP Amp (µV)	71.7			
		SP/AP ratio (%)	13.95			
	Left	SP Amp (µV)	-			
		AP Amp (µV)	-			
		SP/AP ratio (%)	-			

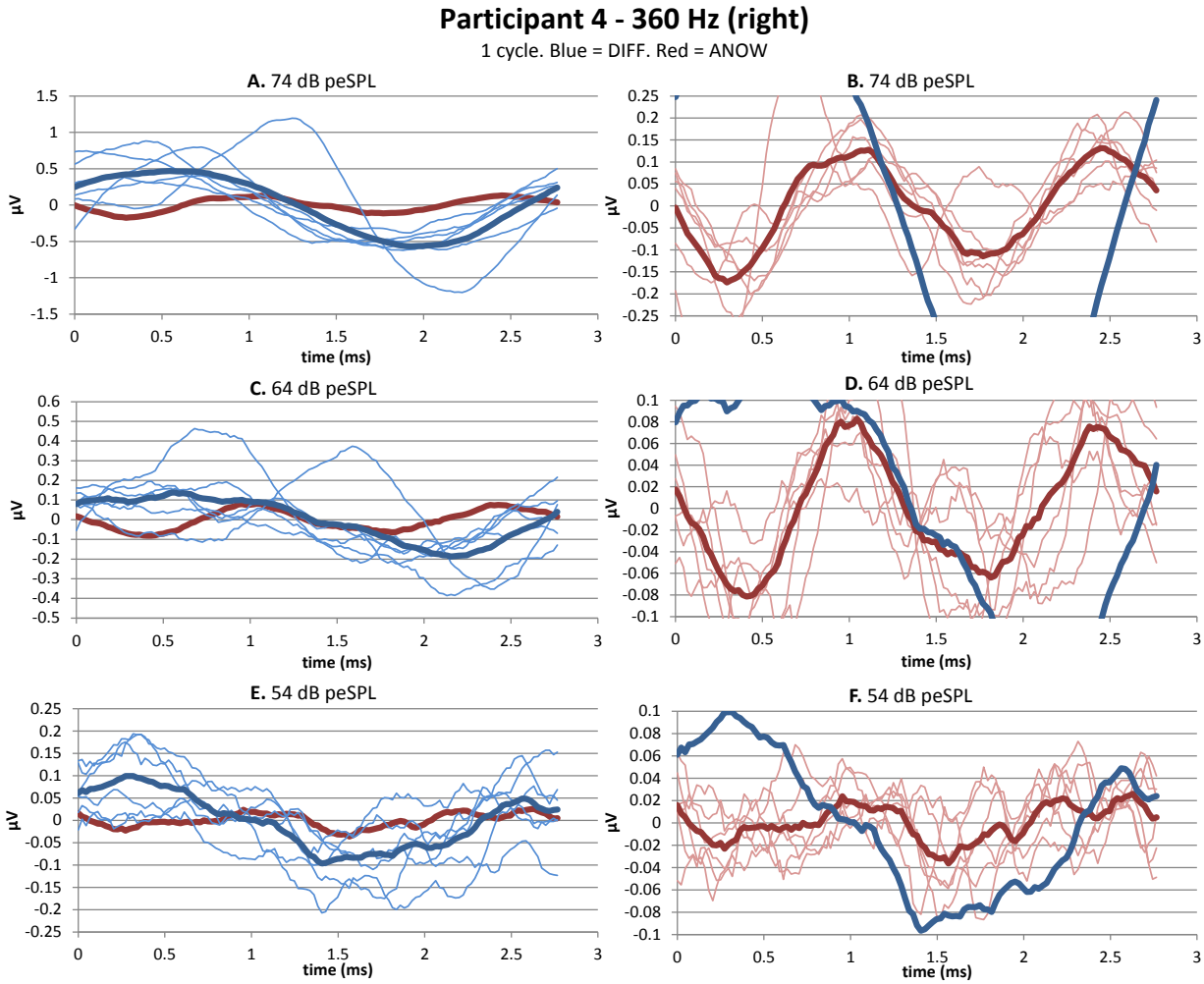

Figure 38: Participant 4's 360 Hz overlaid single-cycle DIFF (blue) and ANOW (red) waveforms elicited in the right ear at 74, 64, and 54 dB peSPL. Plots B, D, and F, represent zoomed-in versions of the waveforms in A, C, and E respectively. The bold traces represent the mean overlaid waveform (n=1852 approx.) derived from around 300 stimulus presentations. The light traces are the mean of around 300 presentations.

Table 12: Mean (± standard deviation) RMS amplitudes for Participant 4's 360 Hz right-ear ANOW and DIFF waveforms at three intensity levels.

level (dB peSPL)	73.8	63.8	53.8
Mean ANOW amplitude (nV RMS)	118	66	30
StdDev ANOW amplitude (nV RMS)	± 33	± 18	± 7
Mean DIFF amplitude (nV RMS)	455	152	96
StdDev DIFF amplitude (nV RMS)	± 167	± 70	± 29
n (sub-averages)	6	6	6

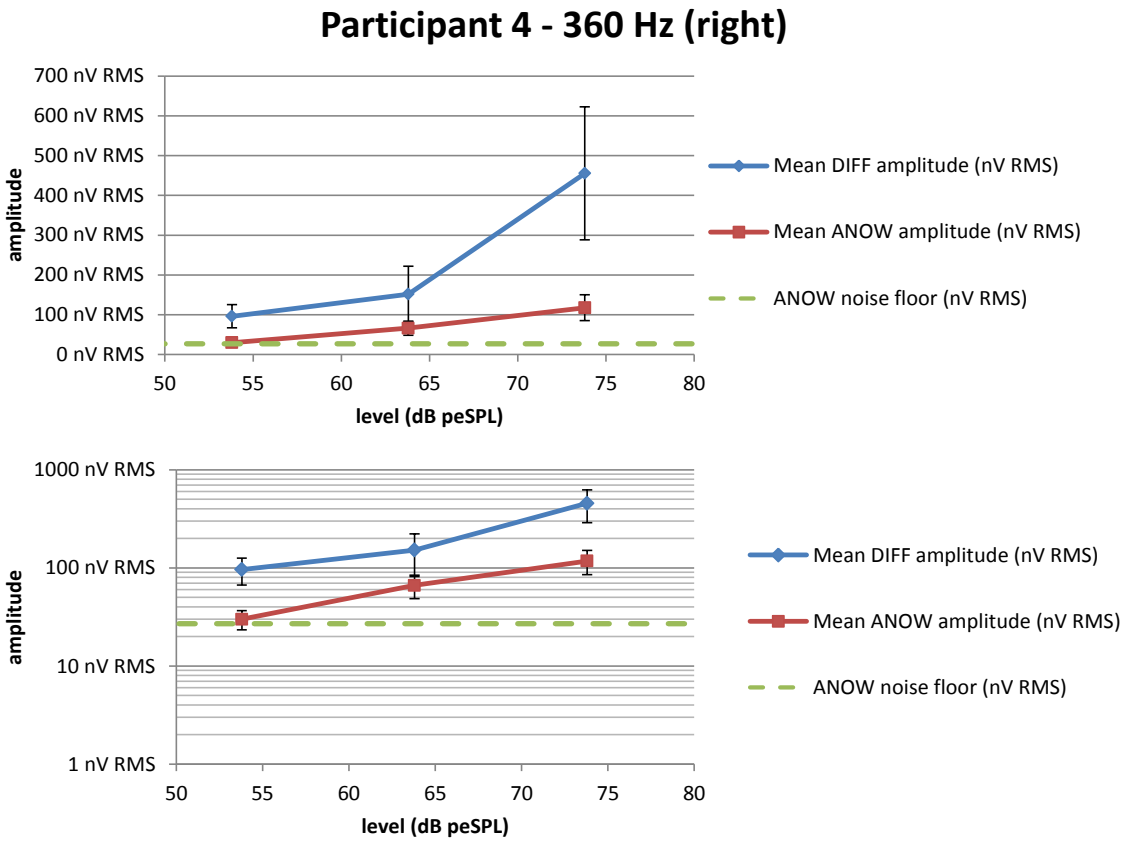

Figure 39: Input/output functions for Participant 4's 360 Hz right-ear DIFF (blue) and ANOW (red) waveforms respectively, shown on a linear amplitude scale (top) and a logarithmic one (bottom). The figure shows the ANOW waveform emerging above the 27 nV noise floor between 54 and 64 dB peSPL.

The data from participant Four indicated the ANOW was present for 360 Hz in her right ear. Presence of the CM can be seen in all recorded cases in the DIFF waveform, seen in figure 38. At 360 Hz, the presence of the CM occurs from around 100 nV RMS, with increasing amplitude from 54 dB peSPL. At 360 Hz, the presence of the ANOW can faintly be distinguished from the noise floor at 54 dB peSPL, with an amplitude of 30 nV RMS, as seen in figure 39.

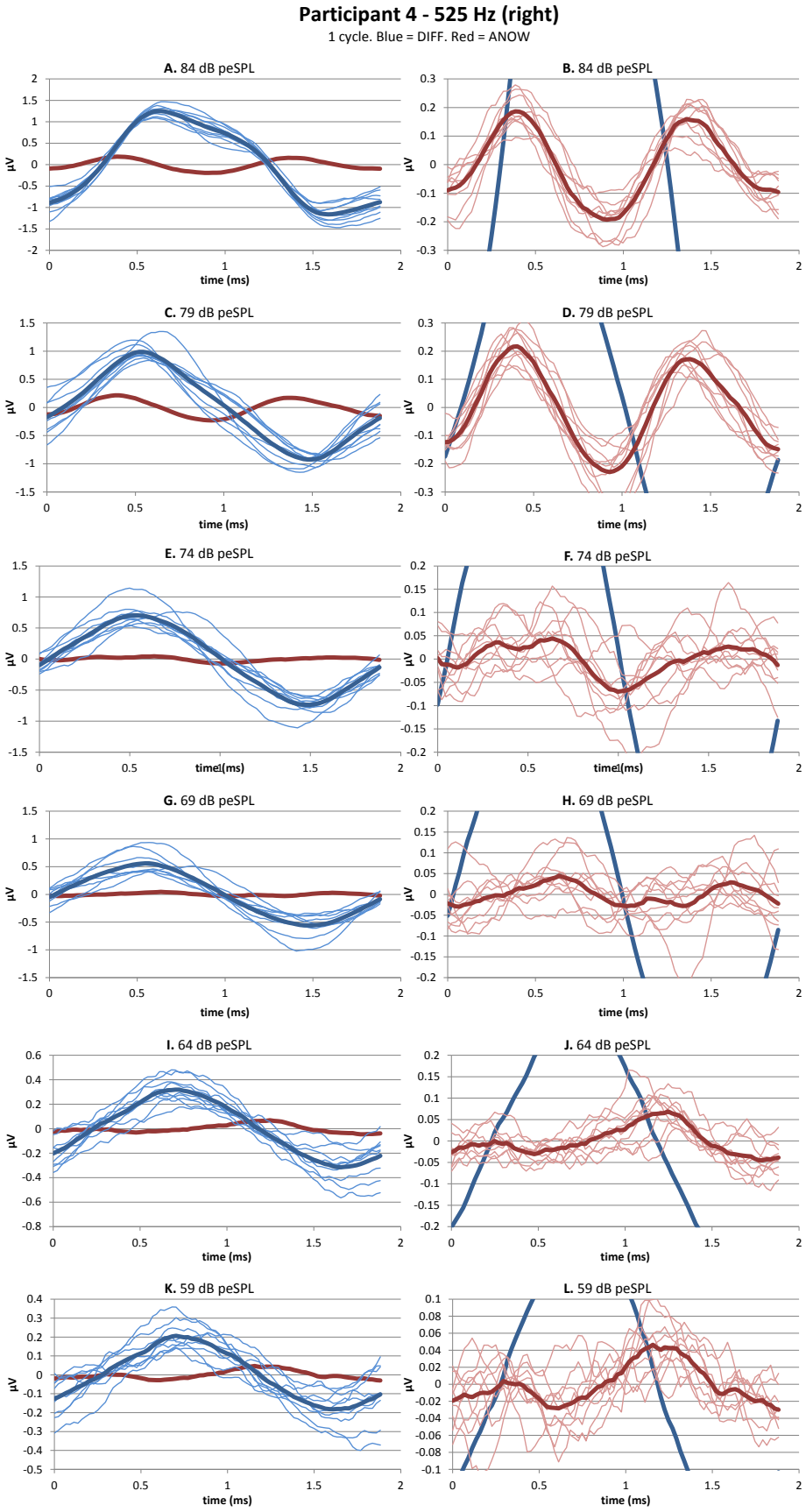

Figure 40: Participant 4's 525 Hz overlaid single-cycle DIFF (blue) and ANOW (red) waveforms elicited in the right ear at 84, 79, 74, 69, 64 and 59 dB peSPL. Plots B, D, F, H, J and L, represent zoomed-in versions of the waveforms in A, C, E, G, I and K respectively. The bold traces represent the mean overlaid waveform (n=2733 approx.) derived from around 300 stimulus presentations. The light traces are the mean of around 300 presentations.

Table 13: Mean (± standard deviation) RMS amplitudes for Participant 4's 525 Hz right-ear ANOW and DIFF waveforms at six intensity levels.

level (dB peSPL)	84.4	79.4	74.4	69.4	64.4	59.4
Mean ANOW amplitude (nV RMS)	125	148	56	49	45	34
StdDev ANOW amplitude (nV RMS)	± 39	± 35	± 25	± 23	± 15	± 11
Mean DIFF amplitude (nV RMS)	855	638	496	391	222	148
StdDev DIFF amplitude (nV RMS)	± 108	± 96	± 116	± 137	± 79	± 52
n (sub-averages)	9	9	9	9	9	9

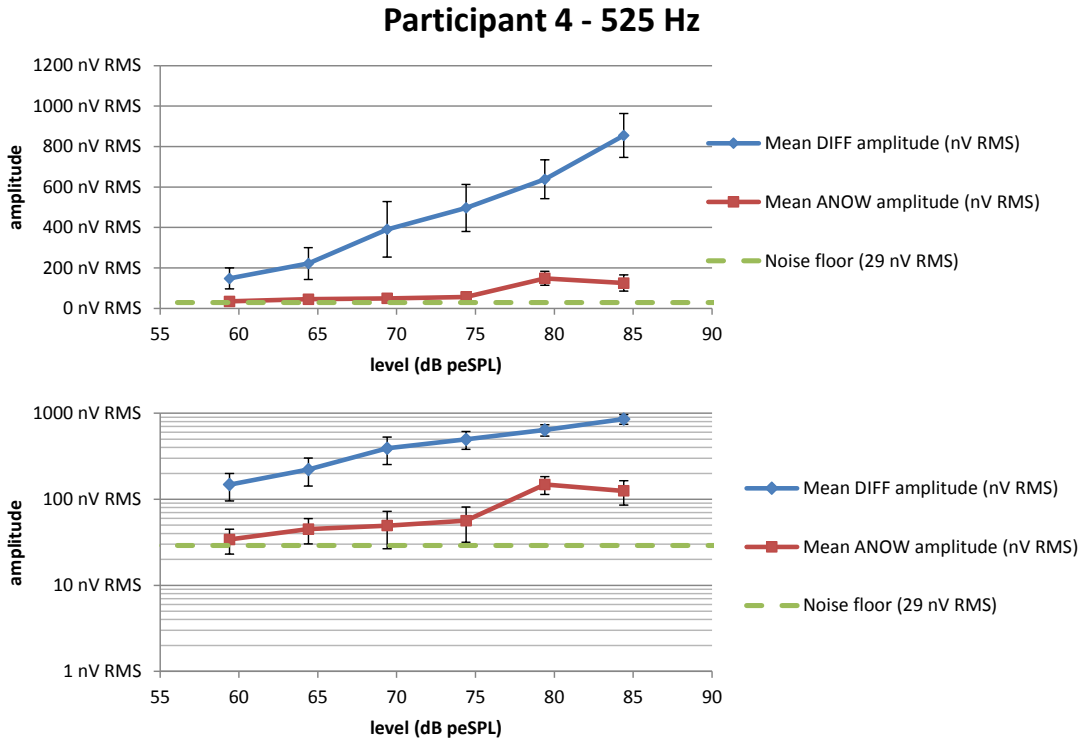

Figure 41: Input/output functions for Participant 4's 525 Hz right-ear DIFF (blue) and ANOW (red) waveforms respectively, shown on a linear amplitude scale (top) and a logarithmic one (bottom). The figure shows the ANOW waveform clearly above the 29 nV noise floor from 79 dB peSPL.

The data from participant Four indicated the ANOW was present for 525 Hz in her right ear. Presence of the CM can be seen in all recorded cases in the DIFF waveform, seen in figure 40. At 525 Hz, the presence of the CM occurs from around 150 nV RMS, with increasing amplitude from 59 dB peSPL. In this case, the recording did not show the CM reducing to the level of the noise floor at 29 nV. At 525 Hz in the right ear, the amplitude of the ANOW

increases sharply from 56 nV to 148 nV between 74 dB peSPL and 79 dB peSPL, as seen in figure 41.

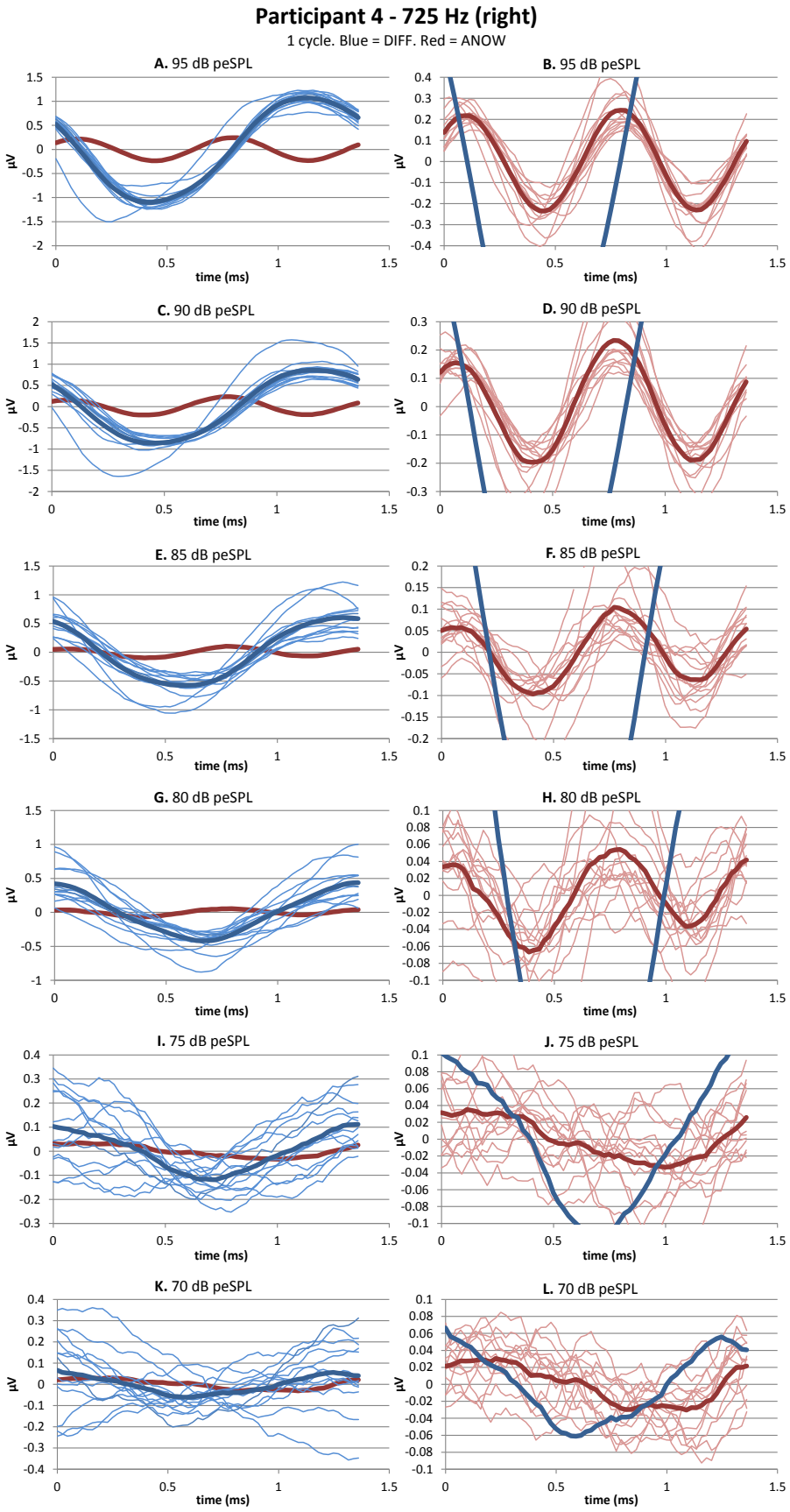

Figure 42: Participant 4's 725 Hz overlaid single-cycle DIFF (blue) and ANOW (red) waveforms elicited in the right ear at 95, 90, 85, 80, 75, and 70 dB peSPL. Plots B, D, F, H, J, and L, represent zoomed-in versions of the waveforms in A, C, E, G, I, and K respectively. The bold traces represent the mean overlaid waveform (n=2733 approx.) derived from around 300 stimulus presentations. The light traces are the mean of around 300 presentations.

Table 14: Mean (± standard deviation) RMS amplitudes for Participant 4's 725 Hz right-ear ANOW and DIFF waveforms at six intensity levels.

level (dB peSPL)	95.2	90.2	85.2	80.2	75.2	70.2
Mean ANOW amplitude (nV RMS)	174	150	76	54	42	37
StdDev ANOW amplitude (nV RMS)	± 51	± 56	± 37	± 27	± 24	± 8
Mean DIFF amplitude (nV RMS)	798	649	449	322	131	117
StdDev DIFF amplitude (nV RMS)	± 103	± 181	± 161	± 137	± 35	± 57
n (sub-averages)	13	13	13	13	13	13

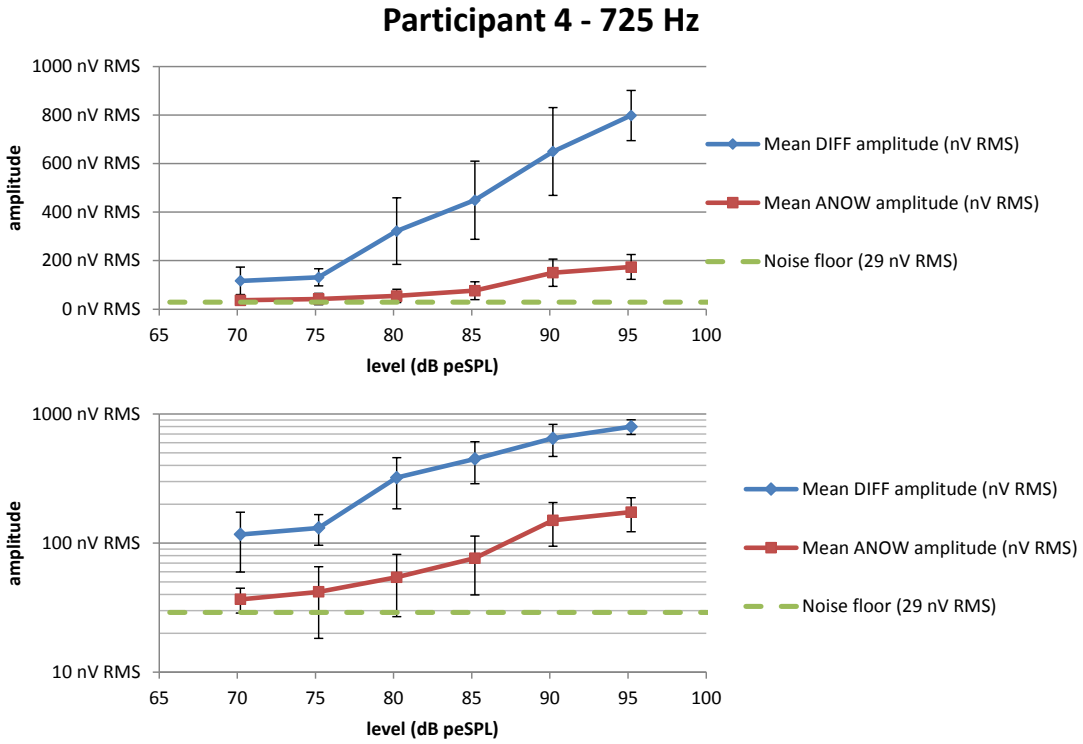

Figure 43: Input/output functions for Participant 4's 725 Hz right-ear DIFF (blue) and ANOW (red) waveforms respectively, shown on a linear amplitude scale (top) and a logarithmic one (bottom). The figure shows the ANOW waveform emerging above the 29 nV noise floor between 75 and 80 dB peSPL. The CM in the DIFF waveform was present at the lowest level tested.

The data from participant Four indicated the ANOW was present for 725 Hz in her right ear. Presence of the CM can be seen in all recorded cases in the DIFF waveform, seen in figure 42. At 725 Hz, the presence of the CM occurs from around 120 nV RMS, with increasing amplitude from 70 dB peSPL. In this case, the recording did not show the CM reducing to the level of the noise floor at 29 nV. At 725 Hz, the presence of the ANOW can be seen distinguishing from the noise floor between 80 and 85 dB peSPL, around 54 and 76 nV RMS,

as seen in figure 43. The waveforms in figure 44 show the presence of a slight latency shift to the left visible in the DIFF waveform in the top figure, and a small latency shift to the right visible in the ANOW in the bottom figure. This is analysed in greater detail below.

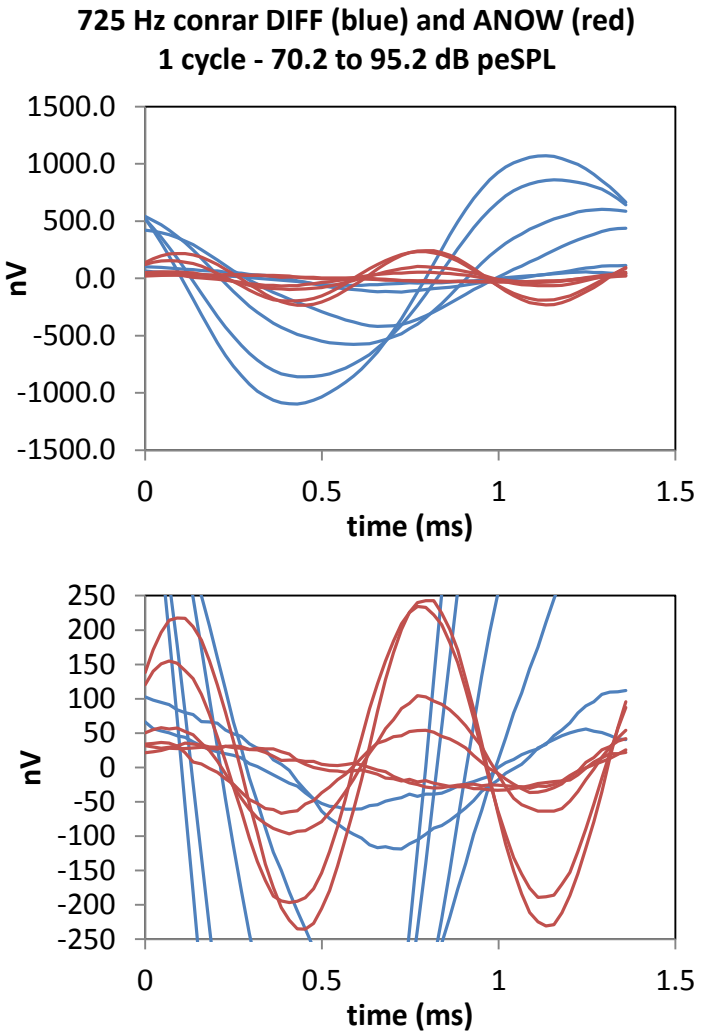

Figure 44: Participant Four's 725 Hz, right ear responses of the DIFF (blue) and ANOW (red) from all the levels tested from 95 – 70 dB peSPL. The bottom figure represents the zoomed-in version of the top figure waveforms.

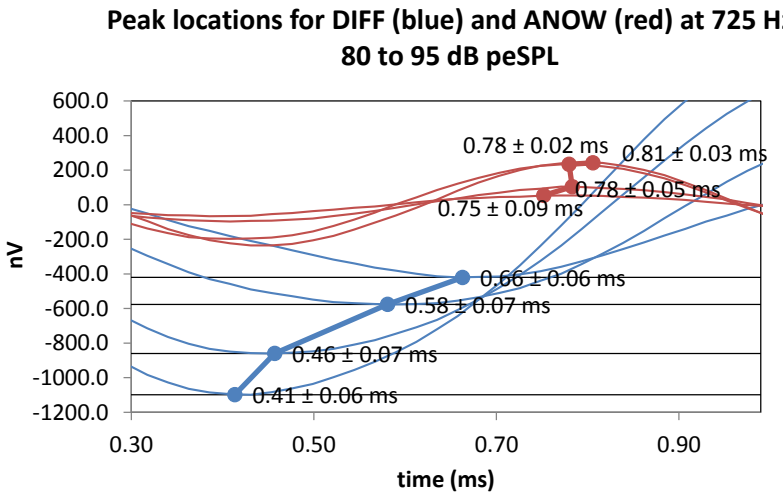

Figure 45: The mean (± st.dev) peak latencies for Participant 4's 725 Hz DIFF (negative peaks, blue) and ANOW (positive peaks, red) waveforms recorded between 80 and 95 dB peSPL.

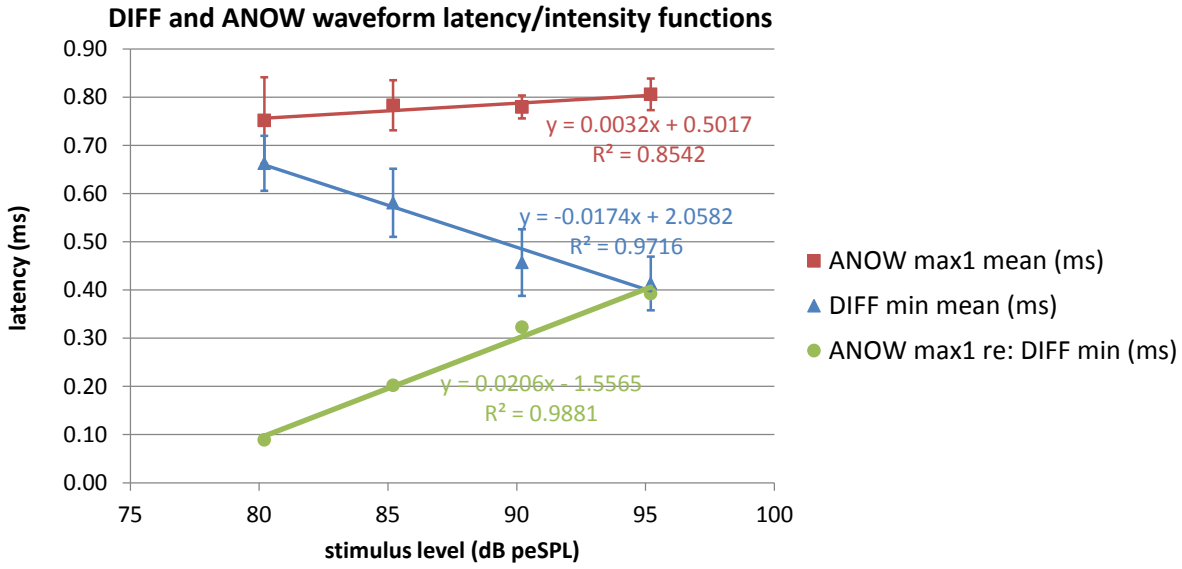

Figure 46: The DIFF wave negative peak latencies (blue trace), the ANOW positive peak latencies (red trace), and the latency difference between the two peaks (green trace). Measurements taken from the sub-averages (n = 300) that formed the waveforms shown in the previous figure.

As shown in Figure 45 above, the peak latencies for the DIFF waves (blue trace) decreased with increasing sound level at a rate of 17.4 µs/dB. By contrast, the ANOW peak latencies (red trace) actually increased with increasing sound level at a rate of 3.2 µs/dB – a trend which is unusual for a neural waveform – however, this value must be interpreted with

caution given the large error bars at the lower sound levels. If we assume that the phasic neural activity that gives rise to the ANOW is actually triggered by the hair cell potentials that give rise to the DIFF waveform, it makes sense to account for the latency function of the DIFF waveform when examining the ANOW waveform. This can be achieved by simple subtraction, as shown in Figure 46, where the latency difference between the two peaks (green trace) increased with increasing sound level at a rate of 20.6 μs/dB. However, once again, the large error bars on the DIFF and ANOW estimates indicate that further investigation of this issue (ideally with waveforms with higher signal-to-noise ratios) is warranted.

3.2.5 Case Five

Participant Five was a 51 year old male. He presented with a sudden hearing loss to his left ear, coupled with a vertigo attack in late 2014. He has previously has a vertigo attack 25 year prior to the current episode, but had none in between. He also commented on the humming tinnitus that was present in his left ear. He was given prednisone for the sudden hearing loss, which helped to improve the loss. The MRI scan showed no abnormality in either ear. He then presented with another two vertigo attacks, with the possibility of left aural fullness in early and mid- 2015. He had ongoing nausea and fluctuating hearing loss since his last attacks. Clinical vestibular ocular reflex testing was normal suggesting good peripheral vestibular functioning. Tympanograms showed Type A bilaterally, indicating normal middle ear functioning. Audiometry revealed essentially normal hearing in his right ear, and a moderate sloping to severe sensorineural hearing loss in his left ear. Audiometry results are presented in figure 47. Given his symptoms he presented with suspected Ménière's disease in his left ear. ECochG testing using click stimuli showed no significant increase in the SP/AP ratio in either ear. ECochG testing using tone bursts stimuli showed a significant increase in

the SP amplitude at 500 Hz, 1000 Hz, 2000 Hz, and 4000 Hz in the left ear only, as per Gibson's norms. The overall pattern of results is consistent with hydrops in the left ear only. The ECochG results are presented in table 15.

Table 15: Participant Five's ECochG Results

			500 Hz	1000 Hz	2000 Hz	4000 Hz
Tone Bursts	Right	SP Amp (µV)	0.0	3.5	3.0	3.80
		Gibson Sig. Level (µV)	2.0	6.0	9.0	9.0
		AP Amp (µV)	1.0	4.3	3.8	4.06
		SP/AP ratio (%)	-	81.4%	78.9%	93.6%
	Left	SP Amp (µV)	2.72	37.00	11.84	4.0
		Gibson Sig. Level (µV)	1.0	3.0	5.0	5.0
		AP Amp (µV)	3.88	26.0	12.06	7.0
		SP/AP ratio (%)	70.1%	142%	98.2%	57.1%
Clicks	Right	SP Amp (µV)	4.14			
		AP Amp (µV)	13.92			
		SP/AP ratio (%)	29.74			
	Left	SP Amp (µV)	14.00			
		AP Amp (µV)	34.30			
		SP/AP ratio (%)	40.82			

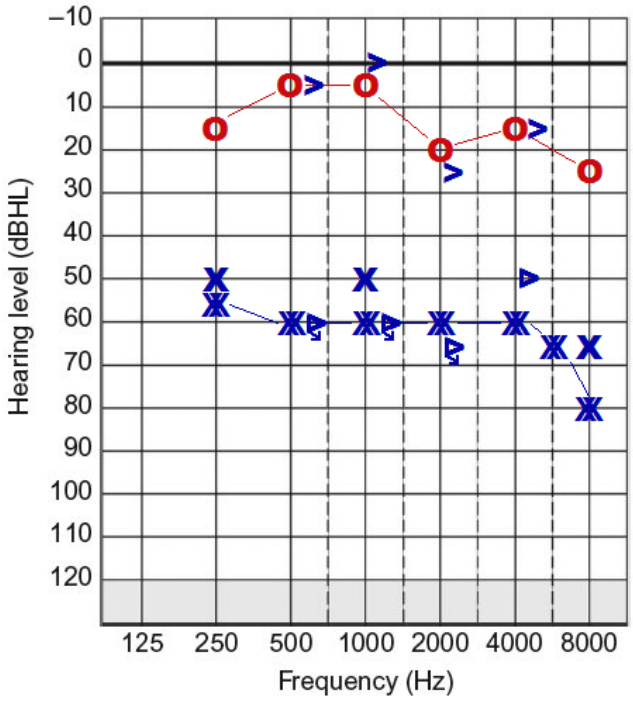

Figure 47: Participant Five's audiological results; right ear showing essentially normal hearing, the left ear indicating a moderate sloping to severe sensorineural hearing loss.

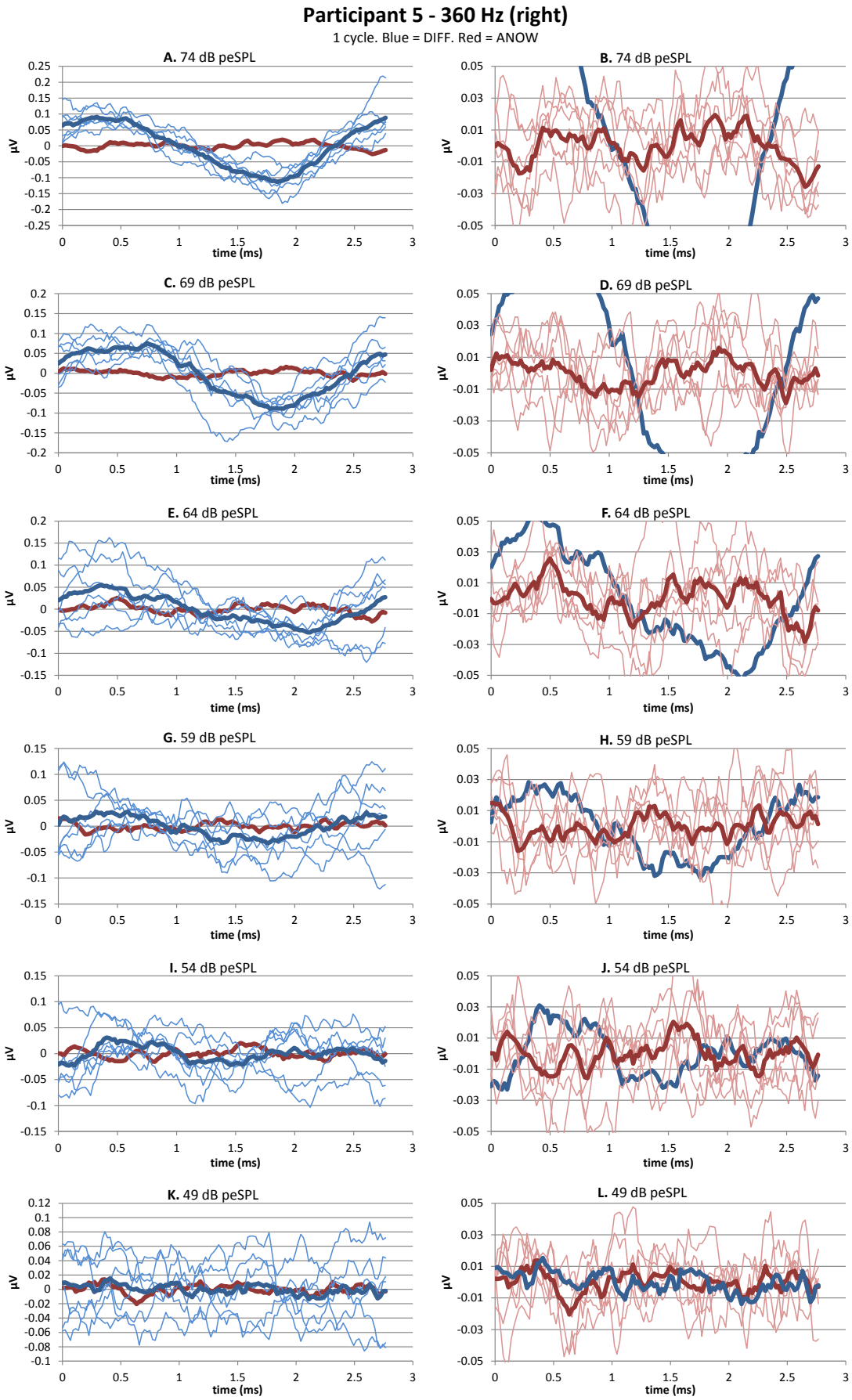

Figure 48: Participant 5's 360 Hz overlaid single-cycle DIFF (blue) and ANOW (red) waveforms elicited in the right ear at 49, 54, 59, 64, 69 and 74 dB peSPL. Plots B, D, F, H, J and L, represent zoomed-in versions of the waveforms in A, C, E, G, I and K respectively. The bold traces represent the mean overlaid waveform (n=2733) derived from 302 stimulus presentations. The light traces are the mean of 302 presentations.

Table 16: Mean (± standard deviation) RMS amplitudes for Participant 5's 360 Hz right-ear ANOW and DIFF waveforms at six intensity levels.

level (dB peSPL)	73.8	68.8	63.8	58.8	53.8	48.8
Mean ANOW amplitude (nV RMS)	22	20	22	19	21	17
StdDev ANOW amplitude (nV RMS)	± 4	± 4	± 7	± 3	± 5	± 3
Mean DIFF amplitude (nV RMS)	78	68	54	45	44	40
StdDev DIFF amplitude (nV RMS)	± 18	± 15	± 22	± 15	± 10	± 3
n (sub-averages)	22	20	22	19	21	17

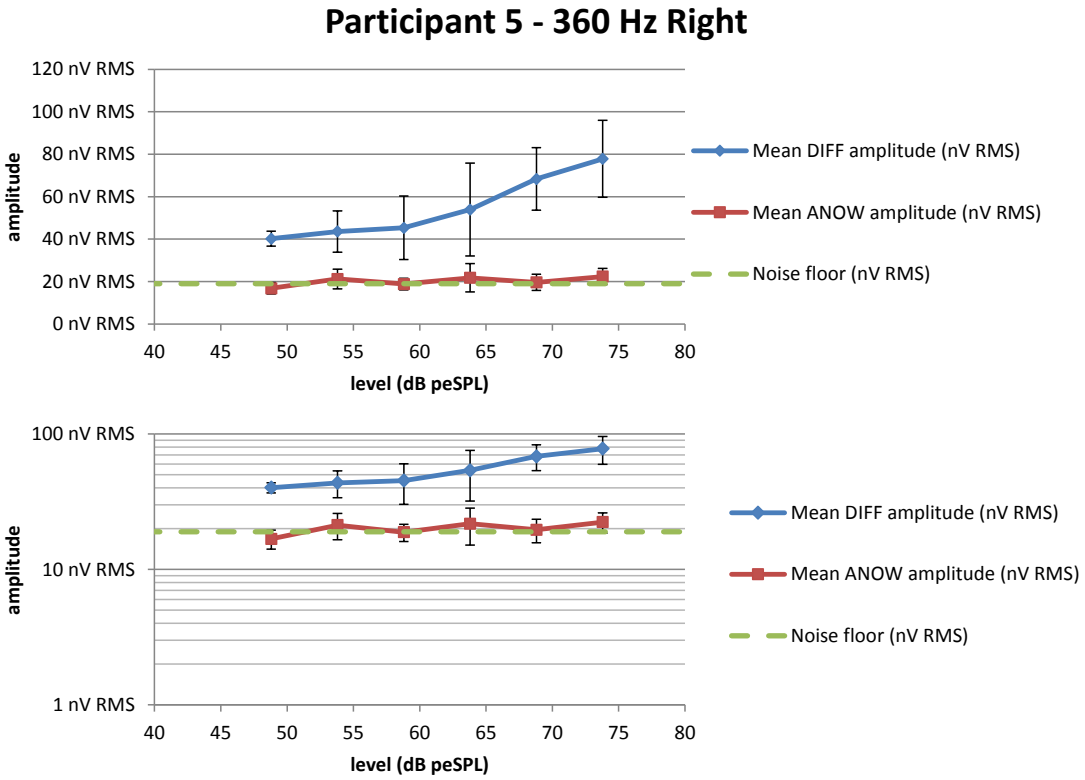

Figure 49: Input/output functions for Participant 5's 360 Hz right-ear DIFF (blue) and ANOW (red) waveforms respectively, shown on a linear amplitude scale (top) and a logarithmic one (bottom). The figure shows the ANOW waveform and the average noise floor 19 nV, which does not appear below 74 dB peSPL.

The data from participant Five indicated the ANOW was not present for 360 Hz in his right ear. Presence of the CM can be seen in all recorded cases in the DIFF waveform, seen in figure 48. At 360 Hz, the presence of the CM occurs from around 40 nV RMS, with increasing amplitude from 49 dB peSPL. The CM does not reduce to the level of the noise floor. At 360

Hz, the presence of the ANOW cannot be distinguished from the noise floor at 19 nV, as seen in figure 49.

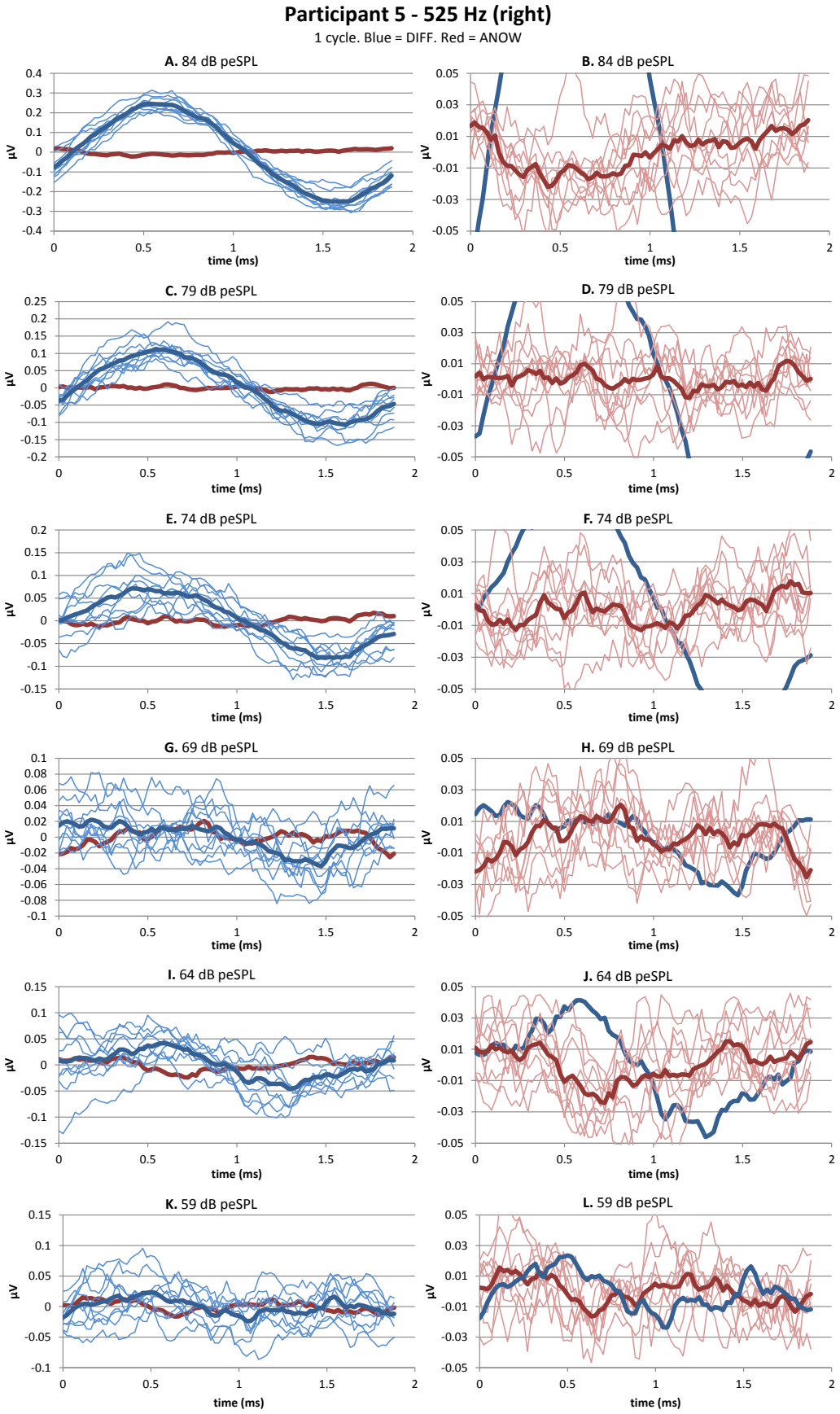

Figure 50: Participant 5's 725 Hz overlaid single-cycle DIFF (blue) and ANOW (red) waveforms elicited in the right ear at 45, 55, 65, 75 and 85 dB peSPL. Plots B, D, F, H, J and L, represent zoomed-in versions of the waveforms in A, C, E, G, I and K respectively. The bold traces represent the mean overlaid waveform (n=2733) derived from 302 stimulus presentations. The light traces are the mean of 302 presentations.

Table 17: Mean (± standard deviation) RMS amplitudes for Participant 5's 525 Hz right-ear ANOW and DIFF waveforms at six intensity levels.

level (dB peSPL)	84.4	79.4	74.4	69.4	64.4	59.4
Mean ANOW amplitude (nV RMS)	22	17	19	20	22	18
StdDev ANOW amplitude (nV RMS)	± 5	± 5	± 5	± 4	± 6	± 2
Mean DIFF amplitude (nV RMS)	174	78	66	30	40	30
StdDev DIFF amplitude (nV RMS)	± 28	± 22	± 18	± 12	± 13	± 10
n (sub-averages)	9	9	9	9	9	9

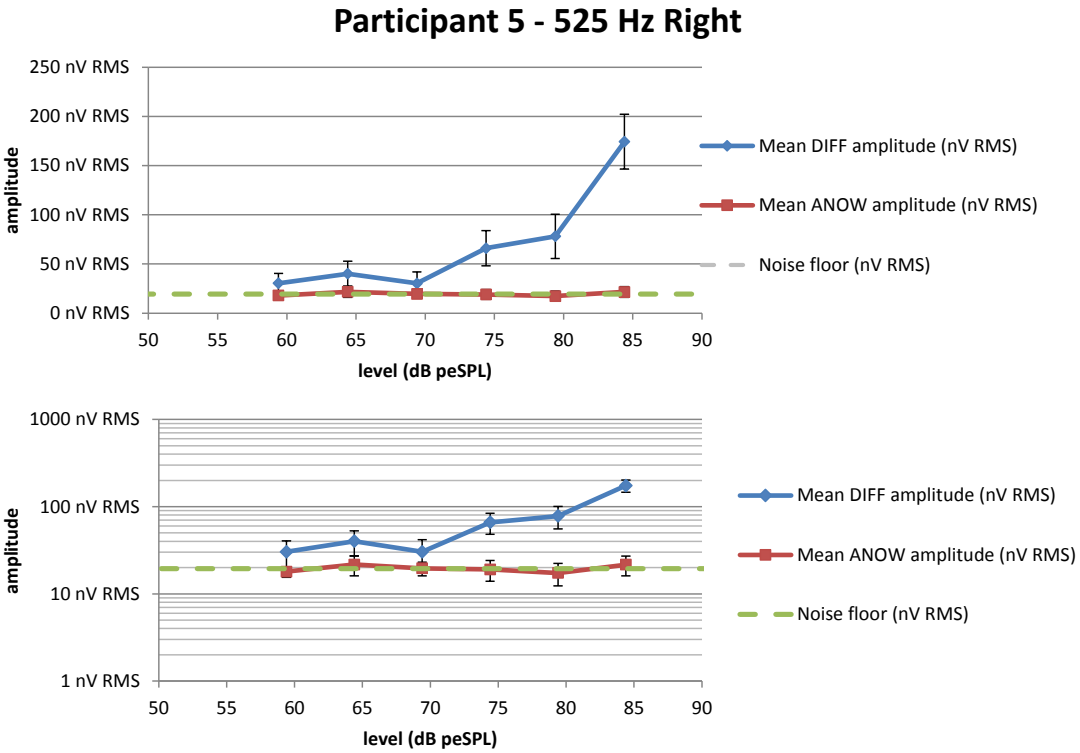

Figure 51: Input/output functions for Participant 5's 525 Hz right-ear DIFF (blue) and ANOW (red) waveforms respectively, shown on a linear amplitude scale (top) and a logarithmic one (bottom). The figure shows the ANOW waveform and the average noise floor 20 nV, which does not appear below 84 dB peSPL.

The data from participant Five indicated the ANOW was not present for 525 Hz in his right ear. Presence of the CM can be seen in the DIFF waveform, seen in figure 50. At 525 Hz, the presence of the CM can be seen emerging from the noise floor between 69 and 74 dB peSPL. At 525 Hz, the presence of the ANOW cannot be distinguished from the noise floor at 20 nV, as seen in figure 51.

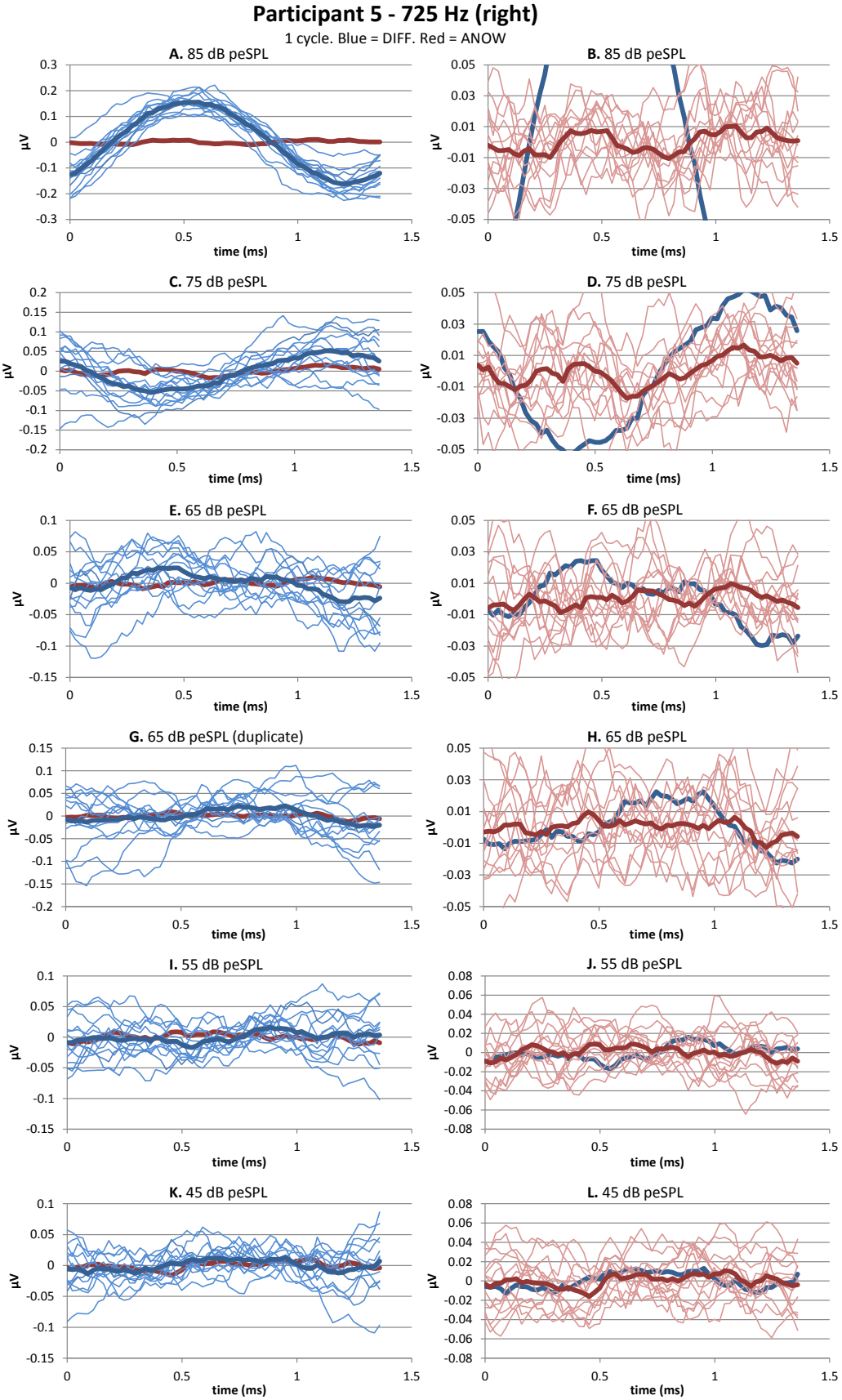

Figure 52: Participant 5's 525 Hz overlaid single-cycle DIFF (blue) and ANOW (red) waveforms elicited in the right ear at 49, 54, 59, 64, 69 and 74 dB peSPL. Plots B, D, F, H, J and L, represent zoomed-in versions of the waveforms in A, C, E, G, I and K respectively. The bold traces represent the mean overlaid waveform (n=2733) derived from 302 stimulus presentations. The light traces are the mean of 302 presentations.

Table 18: Mean (± standard deviation) RMS amplitudes for Participant 5's 725 Hz right-ear ANOW and DIFF waveforms at six intensity levels.

level (dB peSPL)	85.2	75.2	65.2	65.2	55.2	45.2
Mean ANOW amplitude (nV RMS)	20	21	19	23	20	24
StdDev ANOW amplitude (nV RMS)	± 3	± 7	± 4	± 3	± 4	± 5
Mean DIFF amplitude (nV RMS)	118	54	52	43	41	30
StdDev DIFF amplitude (nV RMS)	± 20	± 22	± 13	± 22	± 11	± 10
n (sub-averages)	13	13	13	13	13	13

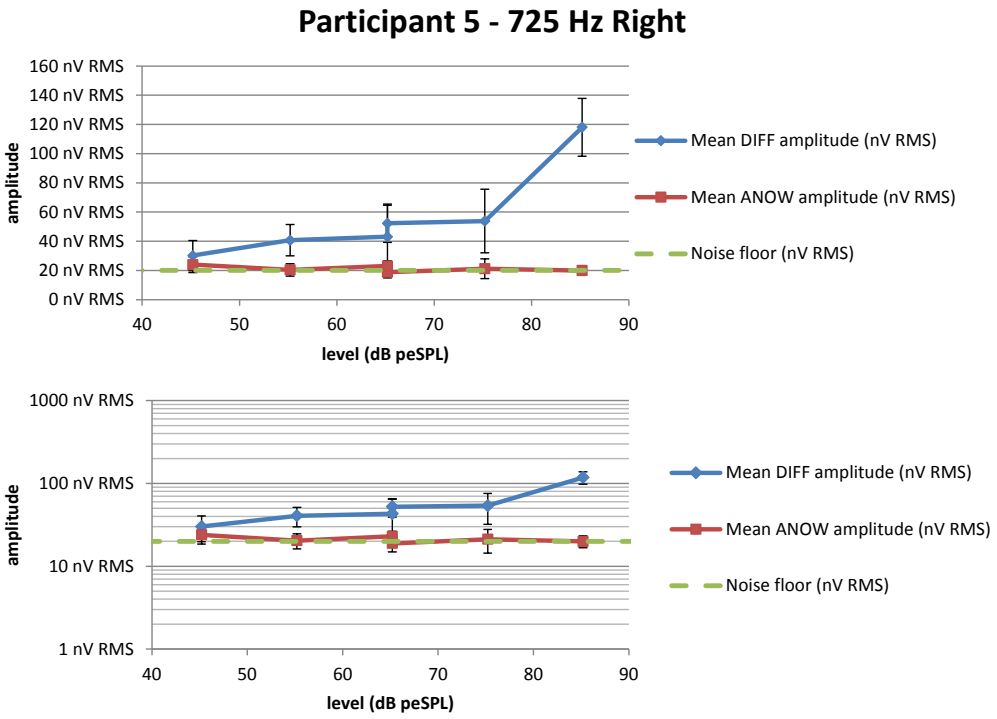

Figure 53: Input/output functions for Participant 5's 725 Hz right-ear DIFF (blue) and ANOW (red) waveforms respectively, shown on a linear amplitude scale (top) and a logarithmic one (bottom). The figure shows the ANOW waveform and average the noise floor 20 nV, which does not appear below 85 dB peSPL.

The data from participant Five indicated the ANOW was not present for 725 Hz in his right ear. Presence of the CM cannot be seen in all recorded cases in the DIFF waveform, seen in figure 52. At 725 Hz, the presence of the CM occurs from around 43 nV RMS at 65 dB peSPL.

At 725 Hz, the presence of the ANOW cannot be distinguished from the noise floor at 20 nV, as seen in figure 53.

The overall data from this participant indicated no ANOW presence above the noise floor for 360, 525, or 725 Hz in the right ear. The left ear was not tested due to participant time constraints. Presence of the CM can be seen in all recorded case in the DIFF waveform.

3.3 Comparison of ANOW processing strategies

All published accounts of the processing strategies used to extract the ANOW make reference to the use of both condensation (CON) and rarefaction (RAR) stimuli. In our implementation, this method makes use of long tone-bursts (approx. 30 ms in duration) delivered at approximately 18 stimuli/second. To generate an ANOW waveform by averaging responses to 300 CON and RAR stimuli therefore takes 33.3 seconds per frequency/intensity combination, or 10 minutes for three frequencies at six sound levels.

We hypothesised that if we were to consider the centre portion of the waveform, there would be a negligible difference between the first half-cycle of a DIFF waveform elicited by a condensation stimulus and the second half-cycle of a DIFF waveform elicited by a rarefaction stimulus. As long as there was no onset CAP present, the only difference between the two half-cycles would be a 180 degree phase shift. It could therefore be possible to halve the acquisition time for the ANOW by utilising waveforms evoked by only CON or RAR stimuli, not both.

To test this hypothesis, we compared DIFF and ANOW waveforms generated from CON and RAR stimuli (“CONRAR”), CON stimuli only (“CONshiftCON”), and RAR stimuli only (“RARshiftRAR”). For the CONshiftCON method, we replaced the RAR-evoked waveform with the CON-evoked waveform shifted by half a cycle. Similarly, the RARshiftRAR trace was

generated after replacing the CON-evoked waveform by the half-cycle-shifted RAR-evoked waveform.

As shown in Figure 54, there is very few differences visible between the responses recorded with the three different techniques, but the two shifted methods have the advantage of a 50% reduction in acquisition time. The measured RMS amplitudes of the DIFF

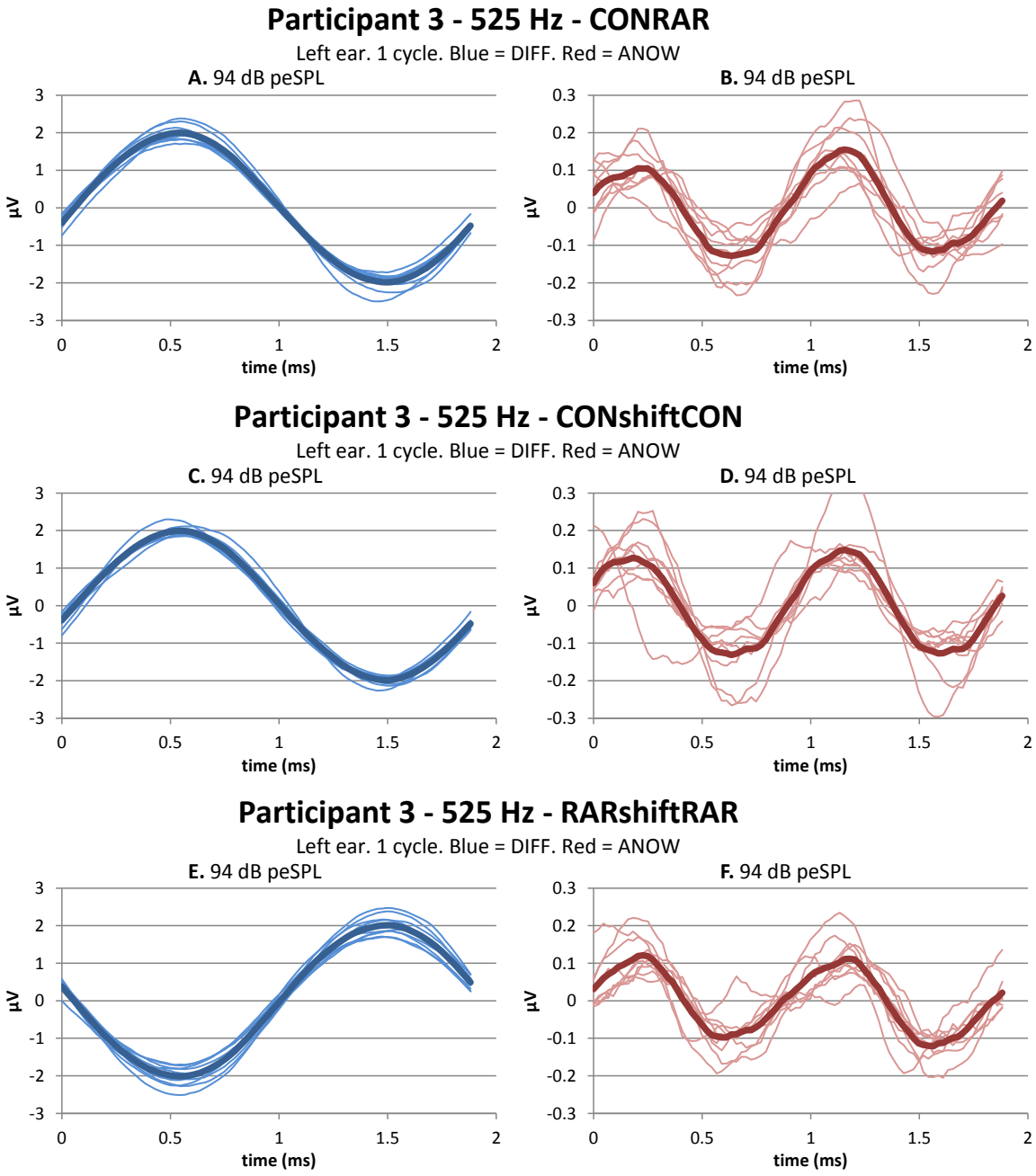

Figure 54: The comparisons of the different processes used to produce the ANOW

waveforms were 1398 ± 159 nV, 1393 ± 88 nV, and 1421 ± 200 nV for CONRAR, CONshiftCON and RARshiftRAR respectively. The measured RMS amplitudes of the ANOW waveforms were 102 ± 28 nV, 107 ± 43 nV, and 87 ± 30 nV for CONRAR, CONshiftCON and RARshiftRAR respectively, with respective noise floors of 29, 27, and 33 nV RMS.

3.4 Discussion

Overall, comparing the data analysed to the audiograms of the participants, we cannot conclude at this stage that the ANOW that we have measured is purely apical cochlea neural responses. Although we have not yet been able to convert the dB peSPL values calculated to dB HL, we can say that it is unlikely at this stage that the values represent the lower frequency hearing thresholds. For example, Participant Three, who has normal hearing between 360 and 725 Hz does not present with an ANOW until around 80 dB peSPL. This, when more accurately converted to dB HL, would more likely present as thresholds of her higher frequencies, approximately around 4000 Hz in her right ear. Similar findings can be seen with the Participant Four, with her ANOW responses closer in threshold response to around 4000 Hz, rather than representing her lower frequencies. Patuzzi, Yates, & Johnstone (1989) found that the CM for an intense low frequency tone came from the base, rather than the apex, of the guinea pig cochlea. Similar findings may be the case here, and further investigation needs to be undertaken, focusing on this area. From these results we can conclude that we are unable to show that the ANOW responses that we have recorded are purely apical cochlea responses in origin. To show this in the future, masking would be required to show frequency specificity and purely neural responses, with no interference from possible non-neural contributors, such as the OHCs.

Further calibrations need to be conducted to accurately convert dB peSPL to dB HL, for an accurate threshold comparison. Due to time constraints, this process was unable to be completed in time, but some conclusions could be made about the approximate threshold it would relate to, with an estimated 15 dB difference maximum between the dB peSPL and dB HL values. This allowed some conclusions to be drawn about the DIFF and ANOW responses in relation to participant threshold. At this stage of the research, lacking accurate threshold comparison from our given results, as well as the accuracy of the frequency selectivity, we cannot reliably draw conclusions in relation to the participant's ECochG and Ménière's results.

Latency and amplitude changes with increased stimulation can be seen for the CM responses throughout the data of the participants, such as in Figure 44 from Participant Four 725 Hz, right ear responses. This change (decrease in latency, increase in amplitude with increased stimulation), can be seen with many other neural responses, such as ABR and ECochG (Eggermont, 1974; Hecox & Galambos, 1974). Chertoff, Lichtenhan, & Willis (2010) also investigated into the amplitude and latency functions of human CAPs using different stimuli of clicks and chirps. They too found similar neural responses of the decrease in latency with increase in stimulus level, as well as increase in amplitude with increase in stimulus level. However the different compositions of the stimuli altered the significance of the latency and amplitude changes with stimulus. The chirp was found to have greater increase in amplitude compared to the click stimuli, which can be seen in figure 55. The chirp was also found to have a shallower latency than the click with increased stimulus, as seen in figure 56. They explain

this finding as being due to the nature of the chirp, causing greater neural firing in unison, as compared to the click stimulus (Chertoff, Lichtenhan, & Willis, 2010).

Latency and amplitude changes as seen with Participant Four's 725 Hz right ear DIFF

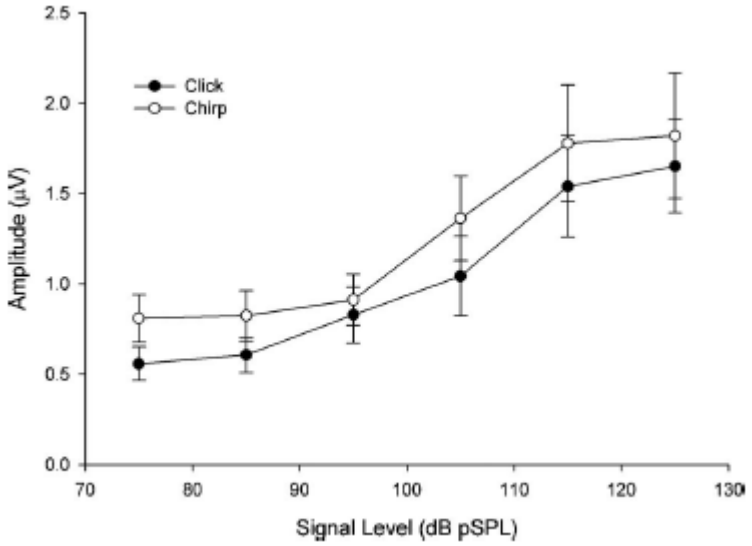

Figure 55: Amplitude of click (black) compared to chirp (white) stimuli on N1 (CAP) responses with change in signal level (Chertoff, Lichtenhan, & Willis, 2010).

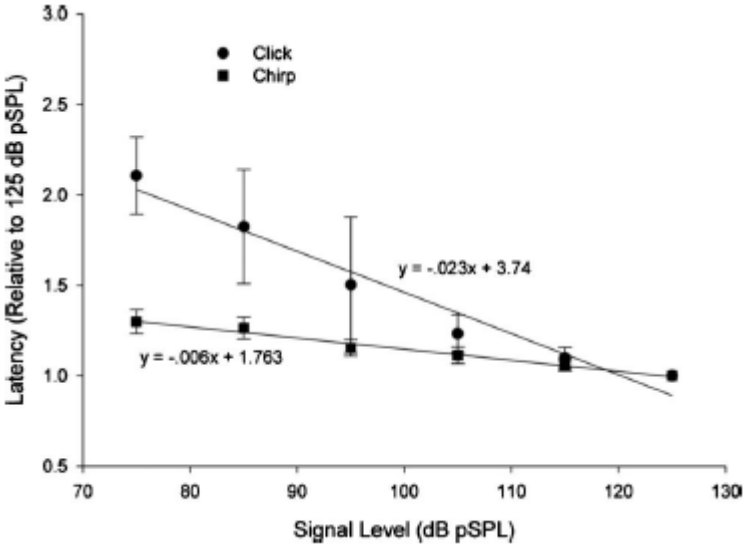

Figure 56: Latency of click (circle) compared to chirp (square) stimuli on N1 (CAP) responses with change in signal level (Chertoff, Lichtenhan, & Willis, 2010).

waveform in may be caused by neural similar neural effects as those discussed in Chertoff, Lichtenhan, & Willis (2010). As discussed in the results, the peak latencies for the DIFF waves (blue trace) decreased with increasing sound level, while the ANOW peak latencies (red trace)

increased with increasing sound level. This aspect of the latency trend of the ANOW was not expected, and does not fit with the evidence base seen around neural waveform latency trends. This result should take into consideration the large error bar at lower sound levels, which may be giving erroneous information regarding the latency trend seen. Further investigation into this area of the study will be required before any solid conclusions can be drawn. This also may help to explain the origin of the generators of the DIFF and ANOW waveforms. We cannot say with certainty the origins of the waveforms that we recorded, however the latency and amplitude changes observed may help to indicate possible generators, and in future research may show that the DIFF is produced solely from the OHCs, while the ANOW is truly neural in origin.

Chapter Four: Discussion

The current study aimed to develop the use of the ANOW in humans, specifically in those with Ménière's disease. We collected normative data from the participants with suspected Ménière's disease, which we used to compare to their subjective thresholds, and their ECochG responses. The findings, described in the previous chapter, do not fully support our hypothesis that the ANOW monitoring technique can accurately predict thresholds at lower frequencies. We also attempted to compare both neural and hair cell functioning through the comparison of the CM and the ANOW measured in the participants. These findings are promising, but do lead to further changes that need to be made to show frequency selectivity and evidence of purely neural responses from the ANOWs. From these findings we can begin to further develop a clinically viable low frequency monitoring technique through further research.

4.1 Limitations

The first point to be discussed about this study and its predominant findings, is that all the participants were suspected of having Ménière's disease, and at the very least had inner ear or vestibular system abnormalities requiring invasive ECochG testing. Taking this into account, our results cannot be used as normative data, as the subject ears cannot be defined as normal. The sample size of this study should also be taken into consideration. The sample size of five participants is a good starting point to further investigate the clinical usefulness of the ANOW, but the clinical implications from this data cannot be drawn. The case study data that we have collected has shown that the procedure can be done and produce viable results.

The second, more predominant limitation for this study is the idea that what we recorded was neural in origin. The ANOW has been discussed earlier, and has been proven in the Lichtenhan, Hartsock, Gill, Guinan Jr, and Salt (2014) to be neural in origin, by injecting

tetrodotoxin into the cochlea apex of guinea pigs, and measuring the hair cell (CM) and neural (ANOW) responses as the toxin took effect. This showed that ANOW was purely neural in origin. However it is impossible to conduct the same research as Lichtenhan et al. (2014) due to the nature of our participants (i.e. they were human). Lichtenhan et al. (2014) sought to disprove the "*alternate possibilities… …that ANOW originates from the excitation of low-frequency tails of high-characteristic frequency auditory nerve fibers or from distortion in the cochlear microphonic (CM).*" Our work has not been able to do this.

While Lichtenhan et al. (2014) concluded that the ANOW elicited with low-to-moderate level sounds (i.e. below 65 dB SPL) is a neural measure from the cochlear apex, they observed with regard to high-level sound that "*[the putative ANOW] from low-frequency high-level sounds originates, at least in part, from sources that are not neural action potentials"* which suggests that *"ANOW is not a suitable name for [the putative ANOW] at high sound levels*" because "*CM distortion can be an important origin of [the putative ANOW] from high-level sound*". However, it must be remembered that these limitations apply to the guinea pig, not humans.

We can however, in future studies, apply the use of stacked masking, to not only reduce the likelihood of non-neural high frequency interference, but also prove the select characteristic frequency of the ANOW being produced. Stacked masking noise can be used by producing high pass filtered noise at selected frequencies to eliminate contributing neural responses from the basal turn of the cochlea. This will result in a tone which is neural and specific. The stacked masking can be applied from previous other methods, as seen with the derived band measurement of the CAP and ABR.

The derived band ABR measurement comes from the paper developed by Don, Masuda, Nelson, and Brackmann (1997). Auditory brainstem responses and compound action

potentials have both been shown to be neural activity initiated in the brainstem by cochlear activation over time, and does not necessarily represent the specific placement along the cochlea that has been stimulated (Don & Eggermont, 1978; Eggermont & Don, 1980; Elberling, 1978). Don et al. (1997) developed the derived band ABR technique to specifically measure the response from a characteristic frequency using masking. The technique measures the ABR response using a high pass filtered masking noise to create ABR responses of a characteristic frequency. These characteristic frequency responses are the derived bands, which are created by successive subtraction of the responses obtained from the progressive high pass masking applied. See figure 57 for a pictorial representation of the derived band ABR measurement (Don et al., 1997). From this Don et al. (1997) found that by stacking the waveform, that the response is improved. This can be seen in figure 58. The idea of stacked derived band ABR measurement can be applied to the current study, where the use of high pass filtered masking can be applied to obtain an ANOW that is a specific characteristic frequency, but also shown to be neural in origin.

4.2 Directions for Future Research

Future endeavours of this study should include the addition of stacked derived ANOW masking, as well as a larger participant sample, as previously stated. Further sample selections should include participants with normal auditory system functioning. Sampling participants who do not require transtympanic ECochG may be problematic, and the method of electrode recording may have to change. Development of extratympanic recording would assist in this area. Preliminary trials that were conducted with the study did not have success with recording any auditory responses using Sanibel™ TM Electrode for ECochG electrodes. These

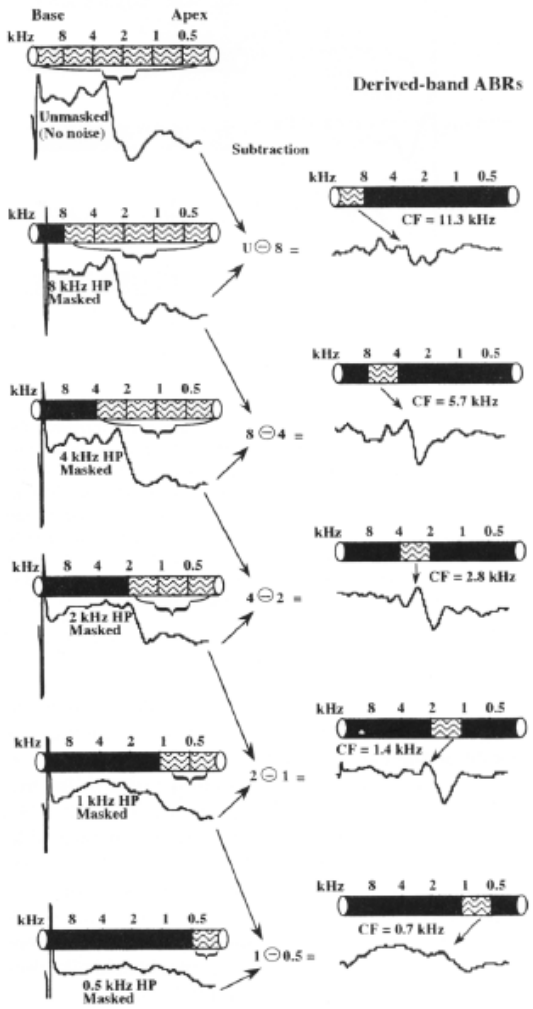

Figure 57: shows the derived band measurement for obtaining specific characteristic frequency ABRs. High pass masking is applied sequentially (left hand column), and subtracted from the previously acquired response to obtain the derived band measurement (right column). Taken from Don et al., (1997).

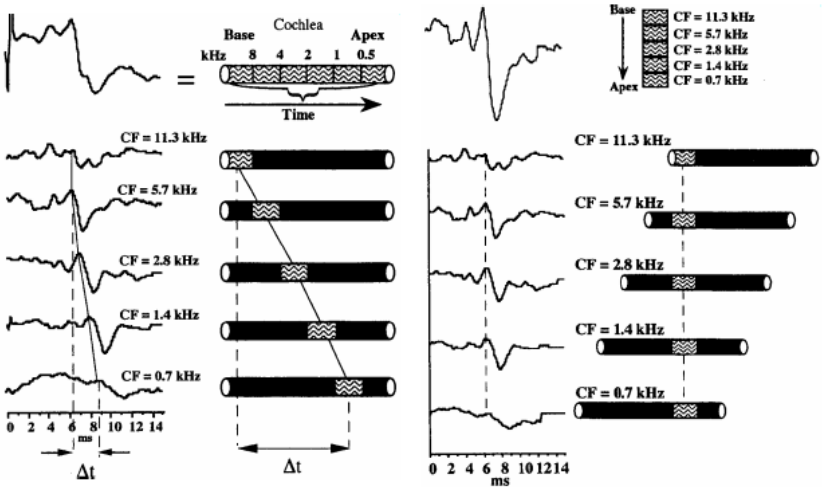

Figure 58: shows the derived band ABR measurement (left), and the stacked derived band ABR measurement (right) in comparison. Taken from Don et al., (1997).

recordings were attempted in a similar manner to how the transtympanic protocols were carried out, but using the researchers as participants. The results did not yield any measurable results, and was decided that this method, for the purposes of this study, was not viable. There is a vast amount of evidence to suggest that the extratympanic method of recording is feasible, practical, and a potential for future research endeavours (Bonucci & Hyppolito, 2009; Schoonhoven, Fabius, & Grote, 1995).

The other possibility of future research involves recording the ANOW in the electrically and acoustically challenging operating theatre environment. Previous attempts to record the ANOW during surgery within this study were also unsuccessful due to the difficulty of finding the source of electrical noise within the operating room. In the prior study, all attempts were taken to reduce the electrical noise but ultimately it was unsuccessful. Future research in this area, could include development of threshold seeking using the ANOW within the surgical environment.

4.3 Clinical Implications

The main clinical application that the ANOW now provides, is the ability to objectively measure low frequency thresholds, where no other method successfully does. The main concerns with ECochG components of the CAP and the SP, the ABR, and OAEs is that they do not monitor 500 Hz and below well, and in some cases even 1000 Hz and below (Gorga et al., 1993; Laureano, McGrady, & Campbell, 1995; Schoonhoven, Prijis, & Grote, 1996; Sininger, 2007). This new method of objectively monitoring hearing at low frequencies could allow for a more accurate audiometric threshold estimation in such situations as new born and young children hearing aid fittings, intraoperative monitoring during surgeries, and an added diagnosis of endolymphatic hydrops in the diagnosis of Ménière's disease.

This method of recording could add to the diagnoses of Ménière's disease. The current ECochG method lacks in accuracy in the lower frequencies (Laureano, McGrady, & Campbell, 1995; Schoonhoven, Prijis, & Grote, 1996; Spoor & Eggermont, 1976). Further investigation is required to determine if hydrops are more accurately estimated with the ANOW and CM, than with the current ECochG method. Testing of a normal hearing population would be required before the use of this data could determine hydrops or other inner ear disorder's effects on the ANOW recorded in this study.

The clinical use in operating theatres could be extended to a range of procedures. This could include vestibular schwannoma removal, cochlear implantation surgery, middle ear surgery, and in the diagnosis of Ménière's disease. Currently in vestibular schwannoma surgery, the main intraoperative auditory monitoring used is ABR, ECochG, or direct eighth nerve monitoring, the former of which does not give real time feedback during surgery, and the latter requires exposure of the eighth cranial nerve.

Choudhury et al. (2012) investigated the use of the ANN for low frequency hair cell and neural activity during cochlear implantation. They were able to measure some activity from what they assumed to be neural responses, as well as CM, CAP, and SP in several participants. They indicated that this could then be used to aid the cochlear implantation, and reduce the amount of damage caused to the cochlea and the patient's residual hearing. Combining the results from our study, and adding the stacked derived ANOW masking method, to ensure the results are frequency specific and neural in origin, this method could be used to assist intraoperatively in CI surgeries. Fitzpatrick et al. (2014) used the components of ECochG in patient's pre-CI, to see if cochlea responsiveness had an effect on post-CI speech outcomes. They measured the CAP, SP, CM, and ANN in this study, although again the ANN was not proven to be purely neural in response. They did find that the magnitude of the ECochG responses correlated to more positive speech outcomes in post lingual adults than other factors, such as degree of residual hearing or the period of deafness (Fitzpatrick et al., 2014). Many studies have found that the preservation of any residual hearing in adults, greatly improves sound quality and SNR for the patients (Fraysse et al., 2006; Gantz, Turner, Gfeller, & Lowder, 2005; James et al., 2005; Turner, Gantz, Vidal, Behrens, & Henry, 2004).

The rate of permanent postoperative inner ear damage following otologic surgery via reconstructive conductive mechanisms within the middle are low, recorded as 0 – 7%

(Häusler, 2004), when complications do occur, they can be severe and devastating (Guyot & Sakbani, 2007). Intraoperative monitoring during such procedures could accurately measure changes in auditory function if damage occurs. It can also be used to optimise the hearing outcome by assisting the surgeon as to the placement of any conductive prosthesis in the ossicular chain (Hsu, 2011; Wazen, Emerson, & Foyt, 1997). Reported feedback of intraoperative monitoring to the surgeons have been less studied in cochlear implantation and middle ear reconstructive surgeries, than for vestibular schwannoma removal; however all areas of intraoperative monitoring using the ANOW are still to be investigated (Danner, Mastrodimos, & Cueva, 2004; Hsu, 2011; Mandalà, Colletti, Tonoli, & Colletti, 2012).

It is well known that essentially normal hearing thresholds are important for auditory development in infants and young children (Boothroyd, 1997; Katz, 2009). For children with hearing impairment, this can mean the use of hearing devices such as hearing aids or cochlear implants for normal speech and language to develop. As discussed above, residual hearing with a cochlear implant assisted with hearing aids can be beneficial in adults. Children face greater difficulties than adults in this respect, as they do not have prior knowledge of language to assist them in discerning what they do hear, and need greater inputs of audibility than adults (Stelmachowicz, Pittman, Hoover, & Lewis, 2001). Added to this difficulty is the testing and measuring the hearing thresholds of young children. As previously mentioned, current methods of objectively measuring hearing thresholds do not always accurately measure low frequencies. This can have implications for child hearing aid fitting, as an optimal fitting means better acquisition of auditory sound for the child, and greater chance of normal speech and language development (McCreery, 2013). Identification of the correct threshold can impact on hearing aid fitting and therefore speech intelligibility. Thornton and Abbas (1980) found that those with a hearing impairment in the lower frequencies, compared to normal hearing

people, were worse at distinguishing speech when a high pass masker was applied to the speech stimulus, but better if a low pass masker was applied. Their findings suggest that those with a low frequency loss are able to make use of their remaining high frequency hearing just as well, if not better than those with normal hearing (Thornton & Abbas, 1980). Amplification of the low frequencies can improve sound quality for the client and give increased loudness (Punch & Beck, 1986). However over amplification may result in masking the mid and higher frequencies needed for speech clarity (Studebaker, Sherbecoe, McDaniel, & Gwaltney, 1999). Over or under amplification of lower frequencies can have an effect on speech perception, and therefore development, making the objective measurement of low frequency hearing thresholds important to develop further.

The methods of measurement of the ANOW from this study has allowed the observation of the responses from the OHCs by the CM, but also the neural response of the ANOW itself. This may lead to the development of using this method in the diagnosis of auditory neuropathy spectrum disorder (ANSD). ANSD is a dysfunction of the auditory nerve which has shown to affect temporal processing, resulting in poor speech perception (Berlin et al., 2010). The current methods of diagnosing ANSD involve DPOAEs, acoustic reflexes, and ABRs. The result for positive ANSD testing will show present DPOAEs (if normal hearing thresholds), absent acoustic reflexes, absent or abnormal ABRs, and also the presence of a CM (Berlin et al., 2010). These patients can present with normal hearing thresholds, but will struggle to understand speech in background noise. The methods used in this study could be developed as part of the test battery for diagnosing ANSD by the presence of the CM and the absence (or abnormality) of the ANOW in relation to the audiometric threshold. This would give an indication as to the site of dysfunction in one test, and also regardless of hearing threshold.

References

Aihara, N., Murakami, S., Watanabe, N., Takahashi, M., Inagaki, A., Tanikawa, M., & Yamada, K. (2009). Cochlear nerve action potential monitoring with the microdissector in vestibular schwannoma surgery. *Skull Base, 19*(5), 325.

American Speech-Language-Hearing Association. (1988). The short latency auditory evoked potentials: a tutorial paper by the working group on auditory evoked potential measurements of the committee on audiologic evaluation. *ASHA*, *9*.

Ashmore, J. (1987). A fast motile response in guinea-pig outer hair cells: the cellular basis of the cochlear amplifier. *The Journal of Physiology, 388*(1), 323-347.

Battista, R. A., Wiet, R. J., & Paauwe, L. (2000). Evaluation of three intraoperative auditory monitoring techniques in acoustic neuroma surgery. *Otology & Neurotology, 21*(2), 244-248.

Berezina, M. A., & Guinan, J. J. (2011). Suppression of Auditory-Nerve-Fiber Responses to Off-CF Tones. Paper presented at the WHAT FIRE IS IN MINE EARS: PROGRESS IN AUDITORY BIOMECHANICS: Proceedings of the 11th International Mechanics of Hearing Workshop.

Berlin, C. I., & Wenthold, R. (1997). Neurotransmission and Hearing Loss: Basic Science, Diagnosis, and Management: Proceedings of the Second Annual Kresge-Mirmelstein Symposium in Honor of Robert Wenthold, Held in New Orleans, September 29, 1995: Singular Publishing Group.

Berlin, C. I., Hood, L. J., Morlet, T., Wilensky, D., Li, L., Mattingly, K. R., Taylor-Jeanfreau, J., Keats, B. J., John, P. S., Montgomery, E. and Shallop, J. K. (2010). Multi-site diagnosis and management of 260 patients with Auditory Neuropathy/Dys-synchrony

(Auditory Neuropathy Spectrum Disorder*). *International journal of audiology*, *49*(1), 30-43

Bess, F. H., & Humes, L. (2008). *Audiology: The Fundamentals*: Lippincott Williams & Wilkins.

Billone, M., & Raynor, S. (1973). Transmission of radial shear forces to cochlear hair cells. *The Journal of the Acoustical Society of America*, *54*(5), 1143-1156.

Bonucci, A. S., & Hyppolito, M. A. (2009). Comparison of the use of tympanic and extratympanic electrodes for electrocochleography. *The Laryngoscope, 119*(3), 563-566.

Boothroyd, A. (1997). Auditory development of the hearing child. *Scandinavian Audiology-Supplement Only*, (46), 9-16.

Calloway, N. H., Fitzpatrick, D. C., Campbell, A. P., Iseli, C., Pulver, S., Buchman, C. A., & Adunka, O. F. (2014). Intracochlear electrocochleography during cochlear implantation. *Otology & Neurotology, 35*(8), 1451-1457.

Carpi, F., & Migliorini, S. (2009). Non-invasive wet electrocochleography. Biomedical Engineering, IEEE Transactions on, 56(11), 2744-2747.

Chertoff, M., Lichtenhan, J., & Willis, M. (2010). Click-and chirp-evoked human compound action potentials. *The Journal of the Acoustical Society of America*, *127*(5), 2992-2996.

Choi, C.-H., Chertoff, M. E., Bian, L., & Lerner, D. (2004). Constructing a cochlear transducer function from the summating potential using a low-frequency bias tone. *The Journal of the Acoustical Society of America, 116*(5), 2996-3007.

Choudhury, B., Fitzpatrick, D. C., Buchman, C. A., Wei, B. P., Dillon, M. T., He, S., & Adunka, O. F. (2012). Intraoperative round window recordings to acoustic stimuli from cochlear implant patients. *Otology & neurotology, 33*(9), 1507.

Coats, A. C. (1981). The summating potential and Meniere's disease: I. Summating potential amplitude in Meniere and non-Meniere ears. *Archives of Otolaryngology, 107*(4), 199-208.

Coats, A. C., & Martin, J. L. (1977). Human auditory nerve action potentials and brain stem evoked responses: effects of audiogram shape and lesion location. *Archives of otolaryngology, 103*(10), 605-622.

Cone-Wesson, B., Dowell, R. C., Tomlin, D., Rance, G., & Ming, W. J. (2002). The auditory steady-state response: comparisons with the auditory brainstem response. *Journal of the American Academy of Audiology*, *13*(4), 173-187.

Cosetti, M. K., Friedmann, D. R., Zhu, B. Z., Heman-Ackah, S. E., Fang, Y., Keller, R. G., Shapiro, W. H., Roland Jr, J. T., & Waltzman, S. B. (2013). The effects of residual hearing in traditional cochlear implant candidates after implantation with a conventional electrode. *Otology & Neurotology*, *34*(3), 516-521.

Cueva, R. A., Morris, G. F., & Prioleau, G. R. (1998). Direct cochlear nerve monitoring: first report on a new atraumatic, self-retaining electrode. *Otology & Neurotology, 19*(2), 202-207.

Cullen, J. K., Ellis, M., Berlin, C., & Lousteau, R. (1972). Human acoustic nerve action potential recordings from the tympanic membrane without anesthesia. *Acta oto-laryngologica, 74*(1-6), 15-22.

Dallos, P., & Cheatham, M. A. (1976). Production of cochlear potentials by inner and outer hair cells. *The Journal of the Acoustical Society of America, 60*(2), 510-512.

Dallos, P., & Wang, C.-Y. (1974). Bioelectric correlates of kanamycin intoxication. *International Journal of Audiology, 13*(4), 277-289.

Danner, C., Mastrodimos, B., & Cueva, R. A. (2004). A comparison of direct eighth nerve monitoring and auditory brainstem response in hearing preservation surgery for vestibular schwannoma. *Otology & Neurotology, 25*(5), 826-832.

Darrow, K. N., Maison, S. F., & Liberman, M. C. (2007). Selective removal of lateral olivocochlear efferents increases vulnerability to acute acoustic injury. *Journal of Neurophysiology, 97*(2), 1775-1785.

Davis, H., Deatherage, B. H., Eldredge, D. H., & Smith, C. A. (1958). Summating potentials of the cochlea. *American Journal of Physiology--Legacy Content, 195*(2), 251-261.

Davis, H., Derbyshire, A., Lurie, M., & Saul, L. (1934). The electric response of the cochlea. *American Journal of Physiology--Legacy Content, 107*(2), 311-332.

Deatherage, B. H., Eldredge, D. H., & Davis, H. (1959). Latency of action potentials in the cochlea of the guinea pig. *The Journal of the Acoustical Society of America, 31*(4), 479-486.

Digby, J., Purdy, S., & Kelly, A. (2014). Deafness Notification Report (2013): Notified cases of hearing loss (not remediable by grommets) among New Zealanders under the age of 19.

Digby, J., Purdy, S., & Kelly, A. (2015). Deafness Notification Report (2014) Hearing loss (not remediable by grommets) in New Zealanders under the age of 19. Accessable. Auckland, New Zealand.

Don, M., & Eggermont, J. (1978). Analysis of the click-evoked brainstem potentials in man using high-pass noise masking. *The journal of the acoustical society of America, 63*(4), 1084-1092.

Don, M., & Elberling, C. (1994). Evaluating residual background noise in human auditory brain-stem responses. *The Journal of the Acoustical Society of America, 96*(5), 2746-2757.

Don, M., Masuda, A., Nelson, R., & Brackmann, D. (1997). Successful detection of small acoustic tumors using the stacked derived-band auditory brain stem response amplitude. *Otology & Neurotology, 18*(5), 608-621.

Don, M., Ponton, C. W., Eggermont, J. J., & Kwong, B. (1998). The effects of sensory hearing loss on cochlear filter times estimated from auditory brainstem response latencies. *The Journal of the Acoustical Society of America, 104*(4), 2280-2289.

Durrant, J. D., Wang, J., Ding, D., & Salvi, R. J. (1998). Are inner or outer hair cells the source of summating potentials recorded from the round window? *The Journal of the Acoustical Society of America, 104*(1), 370-377.

Eggermont, J. J. (1974). Basic principles for electrocochleography. *Acta oto-laryngologica. Supplementum, 316*, 7.

Eggermont, J. J. (1979). Summating potentials in Meniere's disease. *Archives of oto-rhino-laryngology, 222*(1), 63-75.

Eggermont, J., & Don, M. (1980). Analysis of the click-evoked brainstem potentials in humans using high-pass noise masking. II. Effect of click intensity. *The Journal of the Acoustical Society of America, 68*(6), 1671-1675.

Eggermont, J., & Odenthal, D. (1974). Action potentials and summating potentials in the normal human cochlea. *Acta oto-laryngologica. Supplementum, 316*, 39.

Elberling, C. (1978). Compound impulse response for the brain stem derived through combinations of cochlear and brain stem recordings. *Scandinavian audiology, 7*(3), 147-157.

Exeter, D. J., Wu, B., Lee, A. C., & Searchfield, G. D. (2015). The projected burden of hearing loss in New Zealand (2011-2061) and the implications for the hearing health workforce. *The New Zealand medical journal, 128*(1418), 12.

Ferraro, J. A., & Ferguson, R. (1989). Tympanic ECochG and conventional ABR: a combined approach for the identification of wave I and the IV interwave interval. *Ear and hearing, 10*(3), 161-166.

Ferraro, J. A., Blackwell, W. L., Mediavilla, S., & Thedinger, B. (1994). Normal summating potential to tone bursts recorded from the tympanic membrane in humans. *The Journal of the American Academy of Audiology, 5*(1) 17-23.

Ferraro, J. A., Thedinger, B., Mediavilla, S., & Blackwell, W. (1994). Human summating potential to tone bursts: observations on tympanic membrane versus promontory recordings in the same patients. *The Journal of the American Academy of Audiology*, *5*(1), 24-29.

Fettiplace, R., & Hackney, C. M. (2006). The sensory and motor roles of auditory hair cells. *Nature reviews neuroscience, 7*(1), 19-29.

Fiscii, U. P., & Ruben, R. J. (1962). Electrical acoustical response to click stimulation after section of the eighth nerve. *Acta oto-laryngologica, 54*(1-6), 532-542.

Fitzpatrick, D. C., Campbell, A., Choudhury, B., Dillon, M., Forgues, M., Buchman, C. A., & Adunka, O. F. (2014). Round window electrocochleography just prior to cochlear implantation: relationship to word recognition outcomes in adults. *Otology & neurotology, 35*(1), 64.

Folsom, R. C. (1984). Frequency specificity of human auditory brainstem responses as revealed by pure-tone masking profiles. *The Journal of the Acoustical Society of America, 75*(3), 919-924.

Foundation, A. A. o. O.-H. a. N. S., Balkany, T. A., Gates, G. A., Goldenberg, R. A., Meyerhoff, W. L., & House, J. W. (1995). Committee on Hearing and Equilibrium guidelines for the diagnosis and evaluation of therapy in Meniere's disease*. *Otolaryngology-Head and Neck Surgery, 113*(3), 181-185.

Franklin, D. J., McCoy, M. J., Martin, G. K., & Lonsbury-Martin, B. L. (1992). Test/Retest Reliability of Distortion-Product: and Transiently Evoked Otoacoustic: Emissions. *Ear and hearing, 13*(6), 417-429.

Fraysse, B., Macías, Á.R., Sterkers, O., Burdo, S., Ramsden, R., Deguine, O., Klenzner, T., Lenarz, T., Rodriguez, M.M., Von Wallenberg, E., & James, C. (2006). Residual hearing conservation and electroacoustic stimulation with the nucleus 24 contour advance cochlear implant. *Otology & neurotology*, *27*(5), 624-633.

Fromm, B., Nylen, C., & Zotterman, Y. (1935). Studies in the mechanism of the Wever and Bray effect. *Acta Oto-Laryngologica, 22*(3), 477-486.

Galambos, R. (1956). Suppression of auditory nerve activity by stimulation of efferent fibers to cochlea. *Journal of Neurophysiology, 19*(5), 424-437.

Gantz, B. J., Dunn, C., Walker, E., Van Voorst, T., Gogel, S., & Hansen, M. (2016). Outcomes of Adolescents with a Short Electrode Cochlear Implant with Preserved Residual Hearing. *Otology & Neurotology, 37*(2), e118-e125.

Gantz, B. J., Turner, C., Gfeller, K. E., & Lowder, M. W. (2005). Preservation of hearing in cochlear implant surgery: advantages of combined electrical and acoustical speech processing. *The Laryngoscope*, *115*(5), 796-802.

Ghosh, S., Gupta, A. K., & Mann, S. S. (2002). Can electrocochleography in Meniere's disease be noninvasive? *The Journal of otolaryngology, 31*(6), 371-375.

Gibson, W. (1991). The 10-point score for the clinical diagnosis of Meniere's disease. Paper presented at the Proceedings of the Third International Inner Ear Symposium.

Gibson, W. P. (1993). The scope of intraoperative electrocochleography: Kugler Publications, Amsterdam.

Gibson, W. P. (2009). A comparison of two methods of using transtympanic electrocochleography for the diagnosis of Meniere's disease: click summating potential/action potential ratio measurements and tone burst summating potential measurements. *Acta Oto-Laryngologica, 129*(s560), 38-42.

Gibson, W., & Beagley, H. (1976). Electrocochleography in the diagnosis of acoustic neuroma. *The Journal of Laryngology & Otology, 90*(02), 127-139.

Gibson, W., Moffat, D., & Ramsden, R. (1977). Clinical electrocochleography in the diagnosis and management of Meniere's disorders. *International Journal of Audiology, 16*(5), 389-401.

Gibson, W., Prasher, D., & Kilkenny, G. (1983). Diagnostic significance of transtympanic electrocochleography in Meniere's disease. *Annals of Otology, Rhinology & Laryngology, 92*(2), 155-159.

Gillespie, P. G., & Walker, R. G. (2001). Molecular basis of mechanosensory transduction. *Nature, 413*(6852), 194-202.

Giraud, A. L., Garnier, S., Micheyl, C., Lina, G., Chays, A., & Chéry-Croze, S. (1997). Auditory efferents involved in speech-in-noise intelligibility. *Neuroreport, 8*(7), 1779-1783.

Google Books Ngram Viewer. http://books.google.com/ngrams. Based on research conducted from: Jean-Baptiste Michel*, Yuan Kui Shen, Aviva Presser Aiden, Adrian Veres, Matthew K. Gray, William Brockman, The Google Books Team, Joseph P. Pickett, Dale Hoiberg, Dan Clancy, Peter Norvig, Jon Orwant, Steven Pinker, Martin A.

Nowak, and Erez Lieberman Aiden*. *Quantitative Analysis of Culture Using Millions of Digitized Books*. **Science** (Published online ahead of print: 12/16/2010)

Gorga, M. P., Johnson, T. A., Kaminski, J. K., Beauchaine, K. L., Garner, C. A., & Neely, S. T. (2006). Using a combination of click-and toneburst-evoked auditory brainstem response measurements to estimate pure-tone thresholds. *Ear and hearing, 27*(1), 60.

Gorga, M. P., Neely, S. T., Bergman, B. M., Beauchaine, K. L., Kaminski, J. R., Peters, J., Schulte, L. and Jesteadt, W. (1993). A comparison of transient-evoked and distortion product otoacoustic emissions in normal-hearing and hearing-impaired subjects. *The Journal of the Acoustical Society of America, 94*(5), 2639-2648.

Guinan Jr, J. J. (2006). Olivocochlear efferents: anatomy, physiology, function, and the measurement of efferent effects in humans. *Ear and hearing, 27*(6), 589-607.

Guinan Jr, J. J., Lin, T., & Cheng, H. (2005). Medial-olivocochlear-efferent inhibition of the first peak of auditory-nerve responses: Evidence for a new motion within the cochlea. *The Journal of the Acoustical Society of America, 118*(4), 2421-2433.

Guinan, J. J., Warr, W. B., & Norris, B. E. (1983). Differential olivocochlear projections from lateral versus medial zones of the superior olivary complex. *Journal of Comparative Neurology, 221*(3), 358-370.

Guyot, J. P., & Sakbani, K. (2007). Patients' lives following stapedectomy complications. *Advances in Oto-Rhino-Laryngology*, *65*, 348-352

Hall, J. W. (2006). *New handbook of auditory evoked responses*. Boston, Massachusetts: Pearson.

Hallpike, C. S., & Cairns, H. (1938). Observations on the pathology of Meniere's syndrome. *The Journal of Laryngology & Otology, 53*(10), 625-655.

Harkrider, A. W., & Smith, S. B. (2005). Acceptable noise level, phoneme recognition in noise, and measures of auditory efferent activity. *Journal of the American Academy of Audiology, 16*(8), 530-545.

Häusler, R. (2004). Advances in surgery. In K. Jahnke (Ed.), *Middle Ear Surgery* (pp. 95-139. Stuttgart: Thieme.

Hecox, K., & Galambos, R. (1974). Brain stem auditory evoked responses in human infants and adults. *Archives of otolaryngology*, *99*(1), 30-33.

Henry, K. R. (1995). Auditory nerve neurophonic recorded from the round window of the Mongolian gerbil. *Hearing research, 90*(1), 176-184.

Heslop, Neil. (2014). Southern Cochlear Implant Programme. Retrieved from lecture given at University of Canterbury (8/10/2014).

Hood, L.J. (1998). *Clinical applications of the auditory brainstem response*. Singular Publishing Group, San Diego.

Hornibrook, J., Flook, E., Greig, S., Babbage, M., Goh, T., Coates, M., Care, R. and Bird, P. (2015). MRI Inner Ear Imaging and Tone Burst Electrocochleography in the Diagnosis of Ménière's Disease. *Otology & Neurotology*, *36*(6), 1109.

Hornibrook, J., Kalin, C., Lin, E., O'Beirne, G. A., & Gourley, J. (2012). Transtympanic Electrocochleography for the Diagnosis of Ménière's Disease. *International journal of otolaryngology*, 2012.

Hough, D., & Baker, R. S. (2004). Amplitude effects on electrocochleography outcomes. *The Laryngoscope, 114*(10), 1780-1784.

Hsu, G. S. (2011). Improving hearing in stapedectomy with intraoperative auditory brainstem responses. *Otolaryngology – Head and Neck Surgery, 144*(1), 60-63.

http://www.ncbi.nlm.nih.gov/pubmed/?term=auditory+brainstem+response – results by year, downloaded time line.

http://www.ncbi.nlm.nih.gov/pubmed?term=electrocochleography – results by year, downloaded time line.

Huffman, R. F., & Henson, O. (1990). The descending auditory pathway and acousticomotor systems: connections with the inferior colliculus. *Brain Research Reviews, 15*(3), 295-323.

Hughes, G. B., & Pensak, M. L. (2011). *Clinical Otology*: Thieme.

Humphries, K., Ashcroft, P., & Douek, E. (1977). Extra-tympanic electrocochleography. *Acta oto-laryngologica, 83*(1-6), 303-309.

Hurd, L., Hutson, K., & Morest, D. (1999). Cochlear nerve projections to the small cell shell of the cochlear nucleus: the neuroanatomy of extremely thin sensory axons. *Synapse, 33*(2), 83-117.

Hyde, M. L., Riko, K., & Malizia, K. (1990a). Audiometric accuracy of the click ABR in infants at risk for hearing loss. *Journal of the American Academy of Audiology, 1*(2), 59-66.

Jackson, L. E., & Roberson Jr, J. B. (2000). Acoustic neuroma surgery: use of cochlear nerve action potential monitoring for hearing preservation. *Otology & Neurotology, 21*(2), 249-259.

James, C., Albegger, K., Battmer, R., Burdo, S., Deggouj, N., Deguine, O., Dillier, N., Gersdorff, M., Laszig, R., Lenarz, T. and Rodriguez, M. M. (2005). Preservation of residual hearing with cochlear implantation: how and why. *Acta oto-laryngologica*, *125*(5), 481-491.

Jannetta, P. J., Møller, A. R., & Møller, M. (1984). Technique of hearing preservation in small acoustic neuromas. *Annals of surgery, 200*(4), 513.

Johnstone, B., Patuzzi, R., & Yates, G. (1986). Basilar membrane measurements and the travelling wave. *Hearing research, 22*(1), 147-153.

Johnstone, J., Alder, V., Johnstone, B., Robertson, D., & Yates, G. (1979). Cochlear action potential threshold and single unit thresholds. *The Journal of the Acoustical Society of America, 65*(1), 254-257.

Kaf, W. A., Abdelhakiem, M. K., Zahirsha, Z., & Lichtenhan, J. T. (2015). Ménière's Disease: Current and Potential New Objective Measures Using Electrocochleography. SIG 6 *Perspectives on Hearing and Hearing Disorders: Research and Diagnostics, 19*(2), 44-54.

Katz, J. (2009). *Handbook of Clinical Audiology* (6th Ed). Chapter 13 and 14.

Kemp, D. (1978). The evoked cochlear mechanical response and the auditory microstructure-evidence for a new element in cochlear mechanics. *Scandinavian audiology. Supplementum* (9), 35-47.

Kiefer, J., Gstoettner, W., Baumgartner, W., Pok, S. M., Tillein, J., Ye, Q., & Von Ilberg, C. (2004). Conservation of low-frequency hearing in cochlear implantation. *Acta oto-laryngologica, 124*(3), 272-280.

Kim, D. (1986). Active and nonlinear cochlear biomechanics and the role of outer-hair-cell subsystem in the mammalian auditory system. *Hearing research, 22*(1), 105-114.

Krueger, W. W., & Wagner, A. P. (1997). Needle placement with transtympanic electrocochleography. *The Laryngoscope, 107*(12), 1671-1673.

Kumagami, H., Nishida, H., & Baba, M. (1982). Electrocochleographic study of Meniere's disease. *Archives of Otolaryngology, 108*(5), 284-288.

Kumaragamage, C., Lithgow, B., & Moussavi, Z. (2015). A new low-noise signal acquisition protocol and electrode placement for electrocochleography (ECOG) recordings. *Medical & biological engineering & computing, 53*(6), 499-509.

Lacour, M., van de Heyning, P. H., Novotny, M., & Tighilet, B. (2007). Betahistine in the treatment of Ménière's disease. *Neuropsychiatric disease and treatment, 3*(4), 429.

Laureano, A. N., McGrady, M. D., & Campbell, K. C. (1995). Comparison of tympanic membrane-recorded electrocochleography and the auditory brainstem response in threshold determination. *Otology & Neurotology, 16*(2), 209-215.

Le Prell, C. G., Halsey, K., Hughes, L. F., Dolan, D. F., & Bledsoe Jr, S. C. (2005). Disruption of lateral olivocochlear neurons via a dopaminergic neurotoxin depresses sound-evoked auditory nerve activity. *Journal of the Association for Research in Otolaryngology, 6*(1), 48-62.

Le Prell, C. G., Shore, S. E., Hughes, L. F., & Bledsoe Jr, S. C. (2003). Disruption of lateral efferent pathways: functional changes in auditory evoked responses. *Journal of the Association for Research in Otolaryngology, 4*(2), 276-290.

Liberman, M. (1980). Efferent synapses in the inner hair cell area of the cat cochlea: an electron microscopic study of serial sections. *Hearing research, 3*(3), 189-204.

Lichtenhan, J. T., Cooper, N. P., & Guinan, J. J. (2013). A new auditory threshold estimation technique for low frequencies: proof of concept. *Ear and hearing, 34*(1), 42.

Lichtenhan, J., Hartsock, J., Gill, R., Guinan Jr, J., & Salt, A. (2014). The Auditory Nerve overlapped Waveform (ANOW) originates in the cochlear Apex. *Journal of the Association for Research in Otolaryngology, 15*(3), 395-411.

Maloff, E. S., & Hood, L. J. (2014). A Comparison of Auditory Brain Stem Responses Elicited by Click and Chirp Stimuli in Adults with Normal Hearing and Sensory Hearing Loss. *Ear and hearing*, *35*(2), 271-282.

Mandalà, M., Colletti, L., Tonoli, G., & Colletti, V. (2012). Electrocochleography during cochlear implantation for hearing preservation. *Otolaryngology – Head and Neck Surgery, 146*(5), 774-781.

Margolis, R. H., Rieks, D., Fournier, E. M., & Levine, S. E. (1995). Tympanic electrocochleography for diagnosis of Meniere's disease. *Archives of Otolaryngology – Head & Neck Surgery, 121*(1), 44-55.

Marx, M., James, C., Foxton, J., Capber, A., Fraysse, B., Barone, P., & Deguine, O. (2015). Speech Prosody Perception in Cochlear Implant Users With and Without Residual Hearing. *Ear and hearing, 36*(2), 239-248.

Mason, J. A., & Herrmann, K. R. (1998). Universal infant hearing screening by automated auditory brainstem response measurement. *Pediatrics*, *101*(2), 221-228.

Mason, S., Singh, C., & Brown, P. (1980). Assessment of non-invasive electrocochleography. *The Journal of Laryngology & Otology, 94*(07), 707-718.

McCreery, R. (2013). Building Blocks: Speech Intelligibility Index: No Magic Number, but a Reasonable Solution. *The Hearing Journal*, *66*(4), 8-10.

McGee, T. J., & Clemis, J. D. (1981). Effects of conductive hearing loss on auditory brainstem response. *The Annals of otology, rhinology, and laryngology*, *91*(3 Pt 1), 304-309.

Mekjavic, I. B., Rogelj, K., Radobuljac, M., & Eiken, O. (2002). Inhalation of warm and cold air does not influence brain stem or core temperature in normothermic humans. Journal of applied physiology, 93(1), 65-69.

Møller, A. R., & Jannetta, P. J. (1983). Monitoring auditory functions during cranial nerve microvascular decompression operations by direct recording from the eighth nerve. *Journal of neurosurgery, 59*(3), 493-499.

Møller, A., & Jannetta, P. (1985). Neural generators of the auditory brainstem response. *The auditory brainstem response*, 13-31.

Moore, E. J. (1971). Human cochlear microphonics and auditory nerve action potentials from surface electrodes. ProQuest Information & Learning.

Mori, N., Matsunaga, T., & Asai, H. (1981). Intertest reliability in non-invasive electrocochleography. *International Journal of Audiology, 20*(4), 290-299.

Musiek, F. E., & Baran, J. A. (2007). *The Auditory System, Anatomy, Physiology and Clinical Correlates*. Boston, Massachusetts: Allyn & Bacon.

Nam, H., & Guinan Jr, J. J. (2011). Auditory-Nerve Responses to Clicks at Low Levels, and the Initial Peak at High Levels, are Suppressed at Opposite Bias-Tone Phases. Paper presented at the WHAT FIRE IS IN MINE EARS: PROGRESS IN AUDITORY BIOMECHANICS: Proceedings of the 11th International Mechanics of Hearing Workshop.

Naunton, R., & Zerlin, S. (1976). Human whole-nerve response to clicks of various frequency. *International Journal of Audiology, 15*(1), 1-9.

Nayagam, B. A., Muniak, M. A., & Ryugo, D. K. (2011). The spiral ganglion: connecting the peripheral and central auditory systems. *Hearing research, 278*(1), 2-20.

Ng, M., Sriredd y, S., Horlbeck, D. M., & Niparko, J. K. (2001). Safety and patient experience with transtympanic electrocochleography. *The Laryngoscope, 111*(5), 792-795.

Nieder, P., and Nieder, I. (1970). Antimasking effect of crossed olivocochlear bundle stimulation with loud clicks in guinea pig. *Exp. Neurol., 28,* 179-188.

O'Beirne, G. A. (2014). The Auditory Brainstem Response. CMDS 656, advanced diagnostic audiological evaluation, University of Canterbury.

O'Beirne, G.A., & Bird, P.A. (2015). Development of an intraoperative monitoring system for middle-ear, vestibular schwannoma, and cochlear implant surgery. Te Pihareinga. Celebration and Showcase of Hearing and Vestibular Research in New Zealand, Auckland, 11 September 2015.

Oghalai, J. S. (2004). The cochlear amplifier: augmentation of the traveling wave within the inner ear. *Current opinion in otolaryngology & head and neck surgery*, *12*(5), 431.

Palmer, A., & Russell, I. (1986). Phase-locking in the cochlear nerve of the guinea-pig and its relation to the receptor potential of inner hair-cells. *Hearing research, 24*(1), 1-15.

Patuzzi, R. (1996). Cochlear micromechanics and macromechanics. *The cochlea* (pp. 186-257). Springer New York.

Patuzzi, R. B., Yates, G. K., & Johnstone, B. M. (1989). The origin of the low-frequency microphonic in the first cochlear turn of guinea-pig. *Hearing research, 39*(1), 177-188.

Pickles, J. O. (2012). *An introduction to the physiology of hearing* (4th ed.). Bingley, United Kingdom: Emerald Group Publishing.

Prieve, B. A., Gorga, M. P., Schmidt, A., Neely, S., Peters, J., Schultes, L., & Jesteadt, W. (1993). Analysis of transient-evoked otoacoustic emissions in normal-hearing and hearing-impaired ears. *The Journal of the Acoustical Society of America, 93*(6), 3308-3319.

Probst, R., Coats, A., Martin, G., & Lonsbury-Martin, B. (1986). Spontaneous, click-, and toneburst-evoked otoacoustic emissions from normal ears. *Hearing research, 21*(3), 261-275.

Punch, J. L., & Beck, L. B. (1986). Relative effects of low-frequency amplification on syllable recognition and speech quality. *Ear and hearing*, *7*(2), 57-62.

Radeloff, A., Shehata-Dieler, W., Scherzed, A., Rak, K., Harnisch, W., Hagen, R., & Mlynski, R. (2012). Intraoperative monitoring using cochlear microphonics in cochlear implant patients with residual hearing. *Otology & Neurotology, 33*(3), 348-354.

Rask-Andersen, H., Liu, W., Erixon, E., Kinnefors, A., Pfaller, K., Schrott-Fischer, A, & Glueckert, R. (2012). Human cochlea: anatomical characteristics and their relevance for cochlear implantation. *The Anatomical Record, 295*(11), 1791-1811.

Riedel, H., & Kollmeier, B. (2002). Comparison of binaural auditory brainstem responses and the binaural difference potential evoked by chirps and clicks. *Hearing research*, *169*(1), 85-96.

Roberson, J., Senne, A., Brackmann, D., Hitselberger, W. E., & Saunders, J. (1996). Direct cochlear nerve action potentials as an aid to hearing preservation in middle fossa acoustic neuroma resection. *Otology & Neurotology, 17*(4), 653-657.

Rogers, A. R., Burke, S. R., Kopun, J. G., Tan, H., Neely, S. T., & Gorga, M. P. (2010). Influence of Calibration Method on DPOAE Measurements: II. Threshold Prediction. *Ear and hearing, 31*(4), 546.

Ruckenstein, M. J. (2010). Ménière's Disease: Evidence and Outcomes: Plural Pub.

Ruckenstein, M. J., Cueva, R. A., & Prioleau, G. R. (1997). Advantages of a new, atraumatic, self-retaining electrode for direct cochlear nerve monitoring. *Skull base surgery, 7*(2), 69.

Ruckenstein, M. J., Rutka, J. A., & Hawke, M. (1991). How I do it otology and neurotology a specific issue and its solution the treatment of Meniere's disease: Torok revisited. *The Laryngoscope, 101*(2), 211-218.

Russell, I. J., Kossl, M. (1992). Sensory transduction and frequency selectivity in the basal turn of the guinea-pig cochlea (Review). *Phil. Trans. R. Soc. Lond. B: BioI. Sci. 336*, 317-324.

Ruth, R. A., Lambert, P. R., & Ferraro, J. A. (1988). Electrocochleography: methods and clinical applications. *Otology & Neurotology, 9*, 1-11.

Ruth, R., & Lambert, P. (1989). Comparison of tympanic membrane to promontory electrode recordings of electrocochleographic responses in patients with Meniere's disease. *Otolaryngology - Head and neck surgery, 100*(6), 546-552.

Salamy, A., McKean, C. M., & Buda, F. B. (1975). Maturational changes in auditory transmission as reflected in human brain stem potentials. *Brain research*, *96*(2), 361-366.

Sanders, M., Houghton, N., Dewes, O., McCool, J., & Thorne, P. R. (2015). Estimated prevalence of hearing loss and provision of hearing services in Pacific Island nations. J Prim Health Care, 7(1), 5-15.

Santos-Sacchi, J., & Dilger, J. (1988). Whole cell currents and mechanical responses of isolated outer hair cells. *Hearing research, 35*(2), 143-150.

Schoonhoven, R., Fabius, M. A., & Grote, J. J. (1995). Input/output curves to tone bursts and clicks in extratympanic and transtympanic electrocochleography. *Ear and hearing, 16*(6), 619-630.

Schoonhoven, R., Prijs, V. F., & Grote, J. J. (1996). Response thresholds in electrocochleography and their relation to the pure tone audiogram. *Ear and hearing, 17*(3), 266-275.

Shera, C. A., & Guinan Jr, J. J. (2008). Mechanisms of mammalian otoacoustic emission Active Processes and Otoacoustic Emissions in Hearing (pp. 305-342): Springer.

Siegel, A., & Sapru, H. N. (2006). Essential Neuroscience: Lippincott Williams & Wilkins.

Sininger, Y. (2007). The use of auditory brainstem response in screening for hearing loss and threshold prediction. Burkard RF, Don M, Eggermont JJ. Auditory Evoked Potentials Baltimore: Lippincot Williams&Wilkins, 254, 74.

Sininger, Y. S., Abdala, C., & Cone-Wesson, B. (1997). Auditory threshold sensitivity of the human neonate as measured by the auditory brainstem response. *Hearing research, 104*(1), 27-38.

Sohmer, H., & Feinmesser, M. (1967). Cochlear action potentials recorded from the external ear in man. *The Annals of otology, rhinology, and laryngology, 76*(2), 427-435.

Spoendlin, H., & Baumgartner, H. (1977). Electrocochleography and cochlear pathology. *Acta oto-laryngologica, 83*(1-6), 130-135.

Spoendlin, H., & Schrott, A. (1989). Analysis of the human auditory nerve. *Hearing research, 43*(1), 25-38.

Spoor, A., & Eggermont, J. (1976). Electrocochleography as a method for objective audiogram determination Hearing and Davis: Essays honoring Hallowell Davis (pp. 411-418): Washington University Press New York.

Stapells, D. R. (2000). Threshold estimation by the tone-evoked auditory brainstem response: a literature meta-analysis. *Journal of Speech Language Pathology and Audiology, 24*(2), 74-83.

Stapells, D., & Oates, P. (1997). Estimation of the pure-tone audiogram by the auditory brainstem response: a review. *Audiology and Neurotology, 2*(5), 257-280.

Starr, A., & Achor, L. J. (1975). Auditory brain stem responses in neurological disease. *Archives of Neurology*, *32*(11), 761-768.

Starr, A., Amlie, R. N., Martin, W. H., & Sanders, S. (1977). Development of auditory function in newborn infants revealed by auditory brainstem potentials. *Pediatrics*, *60*(6), 831-839.

Stelmachowicz, P. G., Pittman, A. L., Hoover, B. M., & Lewis, D. E. (2001). Effect of stimulus bandwidth on the perception of/s/in normal-and hearing-impaired children and adults. *The Journal of the Acoustical Society of America*, *110*(4), 2183-2190.

Studebaker, G. A., Sherbecoe, R. L., McDaniel, D. M., & Gwaltney, C. A. (1999). Monosyllabic word recognition at higher-than-normal speech and noise levels. *The Journal of the Acoustical Society of America*, *105*(4), 2431-2444.

Thompson, G. C., & Thompson, A. M. (1986). Olivocochlear neurons in the squirrel monkey brainstem. *Journal of Comparative Neurology, 254*(2), 246-258.

Thornton, A. R., & Abbas, P. J. (1980). Low-frequency hearing loss: Perception of filtered speech, psychophysical tuning curves, and masking. *The Journal of the Acoustical Society of America*, *67*(2), 638-643.

Turner, C. W., Gantz, B. J., Vidal, C., Behrens, A., & Henry, B. A. (2004). Speech recognition in noise for cochlear implant listeners: benefits of residual acoustic hearing. *The Journal of the Acoustical Society of America*, *115*(4), 1729-1735.

Van Deelen, G., & Smoorenburg, G. (1986). Electrocochleography for different electrode positions in guinea pig. *Acta oto-laryngologica, 101*(3-4), 207-216.

Von Békésy, G., & Wever, E. G. (1960). *Experiments in hearing*. New York: McGraw-Hill.

Wangemann, P. (2006). Supporting sensory transduction: cochlear fluid homeostasis and the endocochlear potential. *The Journal of physiology, 576*(1), 11-21.

Warr, W. B., & Guinan, J. J. (1979). Efferent innervation of the organ of Corti: two separate systems. *Brain research, 173*(1), 152-155.

Warr, W. B., Boche, J. B., & Neely, S. T. (1997). Efferent innervation of the inner hair cell region: origins and terminations of two lateral olivocochlear systems. *Hearing research, 108*(1), 89-111.

Wazen, J., Emerson, R., & Foyt, D. (1997). Intra-operative electrocochleography in stapedectomy and ossicular reconstruction. *The American Journal of Otology, 18*, 707-713.

Wersinger, E., & Fuchs, P. A. (2011). Modulation of hair cell efferents. *Hearing research, 279*(1), 1-12.

Wilson, J., Henson, M., & Henson, O. (1991). Course and distribution of efferent fibers in the cochlea of the mouse. *Hearing research, 55*(1), 98-108.

World Health Organisation. (2015). http://www.who.int/mediacentre/factsheets/fs300/en/

Yamakawa, K. (1938). Über die pathologische Veränderung bei einem Meniere-Kranken. *J Otorhinolaryngol Soc Jpn*, 44, 2310-2312.

Yoshie, N., Ohashi, T., & Suzuki, T. (1967). Non-surgical recording of auditory nerve action potentials in man. *The Laryngoscope, 77*(1), 76-85.

Zheng, J., Shen, W., He, D. Z., Long, K. B., Madison, L. D., & Dallos, P. (2000). Prestin is the motor protein of cochlear outer hair cells. *Nature, 405*(6783), 149-155.

Zheng, X.-Y., Ding, D.-L., McFadden, S. L., & Henderson, D. (1997). Evidence that inner hair cells are the major source of cochlear summating potentials. *Hearing research, 113*(1), 76-88.

Appendix A: Patient Information and Consent Forms

Canterbury DHB
District Health Board
Te Poari Hauora ō Waitaha

Information Sheet

A new method for investigating hearing in Ménière's Disease

You are invited to take part in a study looking at hearing and the presence of Ménière's Disease.

The results may provide important information regarding low-frequency hearing thresholds and the presence or absence of Ménière's.

Such information may make it possible to diagnose Ménière's in the future and the techniques developed during this study may also be used to monitor low-frequency hearing during cochlear implant surgery.

What is required of me if I choose to take part?

All that will be different for you is that some extra sounds will be presented to you during your Electrocochleography assessment with Mr Hornibrook.

This is expected to add no more than 30 minutes to your appointment.

In addition to this you will complete a hearing assessment.

What's involved in each part of the hearing assessment?

Otoscopy: The audiologist will have a look in your ears using a special ear-torch called an "otoscope". This will tell us if your ears have any significant wax or debris in the ear canals and if your eardrum looks healthy.

Pure-tone audiometry: You will be played a series of (mostly very quiet) tones (or 'beeps'), and will be asked to tell the audiologist whenever you have heard a sound. This helps us to find the softest sounds you can hear, and let us know about your hearing.

Is there any risk to me by being involved in this study?

The study will in no way affect your assessment with Mr Hornibrook. You can pull out of the study at any time and this will have no effect on your care.

Will my GP be told I am in the study?

It is up to you whether you would like your GP to know that you are taking part in this study. For us to tell your GP, you must first give us your written permission.

If I need an interpreter, can one be provided?

Yes, we can organise an interpreter to help you. You will be asked if you need an interpreter if you choose to sign the consent form.

Important information

If you take part in the study your privacy and confidentiality will be protected and there will be no information shown to people outside the medical study staff that could be identified to you. No material that could personally identify you will be used in any reports on this study.

If you have any queries or concerns regarding your rights as a participant in this study, you may wish to contact an independent health and disability advocate:
Free phone: 0800 555 050
Email: advocacy@hdc.org.nz

This study has received ethical approval from the Upper South B Regional Ethics Committee (13/STH/49), and the University of Canterbury Human Ethics Committee (HEC 2012/94).

Where can I get more information about the study?

Please feel free to contact the researchers at any stage if you have any queries about this study (details listed below).

If you would like to take part in the study, you will be given a consent form during your assessment with Mr Hornibrook.

Researchers:

Greg O'Beirne, PhD

Associate Professor in Audiology

Department of Communication Disorders

University of Canterbury

Private Bag 4800

Christchurch 8140

Tel: +64 3 364 2987 ext. 7085
Fax: +64 3 364 2760

Email: gregory.obeirne@canterbury.ac.nz

Miss Ashleigh Allsop

MAud student

Department of Communication Disorders

University of Canterbury

Private Bag 4800

Christchurch 8140

Email : ashleigh.allsop@pg.canterbury.ac.nz

Canterbury DHB
District Health Board
Te Poari Hauora ō Waitaha

Consent Form

A new method for investigating hearing in Ménière's Disease

English	I wish to have an interpreter.	Yes	No
Maori	E hiahia ana ahau ki tetahi kaiwhakamaori/kaiwhaka pakeha korero.	Ae	Kao
Cook Island	Ka inangaro au i tetai tangata uri reo.	Ae	Kare
Fijian	Au gadreva me dua e vakadewa vosa vei au	Io	Sega
Niuean	Fia manako au ke fakaaoga e taha tagata fakahokohoko kupu.	E	Nakai
Samoan	Ou te mana'o ia i ai se fa'amatala upu.	Ioe	Leai
Tokelaun	Ko au e fofou ki he tino ke fakaliliu te gagana Peletania ki na gagana o na motu o te Pahefika	Ioe	Leai
Tongan	Oku ou fiema'u ha fakatonulea.	Io	Ikai

1. I have read and I understand the information sheet for volunteers taking part in the above-named study. I have had the opportunity to discuss this study and have had any questions answered satisfactorily.

2. I have had the opportunity to use whanau support or a friend to help me ask questions and understand the study.

3. I have had this project explained to me by one of the investigators.

4. I understand the aims of the study and what is required of me to participate.

5. I understand that taking part in this study is voluntary (my choice) and that I may withdraw from the study at any time without having to give a reason, including the withdrawal of any information I have provided. This will in no way affect my future/continuing health care.

6. I understand that my participation in this study is confidential and that no material which could identify me will be used in any reports in this study.

7. I understand that the results collected in this study will be kept in a secure location for a period of up to 10 years.

8. I understand that a suitable interpreter will be provided if necessary.

9. I know who to contact if I have any questions about the study.

10. I have had time to consider whether or not to participate in the study

11. I would like a copy of the summarised results at the completion of the study — Yes / No

12. I agree to my GP or other current provider being informed of my participation in this study — Yes / No

Participant to sign:

I …… (full name)

hereby consent to take part in this study to investigate a new method for investigating hearing in Ménière's Disease

Signature..... Date.....

Researcher to sign:

I..... (full name) believe that consent was given freely by the participant and have witnessed the signing of the consent form above

Signature..... Date.....